Retrospective Theses and Dissertations

Iowa State University Capstones, Theses and Dissertations

1999

Atom transfer and rearrangement reactions catalyzed by methyltrioxorhenium, MTO

Josemon Jacob
Iowa State University

INFORMATION TO USERS

Atom transfer and rearrangement reactions catalyzed
by methyltrioxorhenium, MTO

by

Josemon Jacob

A dissertation submitted to the graduate faculty

in partial fulfillment of the requirements for the degree of

DOCTOR OF PHILOSOPHY

Major: Organic Chemistry

Major Professor: James H. Espenson

Iowa State University

Ames, Iowa

1999

UMI Number: 9940210

UMI
300 North Zeeb Road
Ann Arbor, MI 48103

Graduate College

Iowa State University

This is to certify that the Doctoral dissertation of

Josemon Jacob

has met the dissertation requirements of Iowa State University

.

Signature was redacted for privacy.

Major Professor

Signature was redacted for privacy.

For the Major Program

Signature was redacted for privacy.

For the Graduate College

TABLE OF CONTENTS

iv

GENERAL INTRODUCTION

Introduction

Organometallic chemistry, a discipline that combines aspects of both inorganic and organic chemistry, has revolutionized research and development in the past 50 years. Homogeneous catalysis, an important application following the explosive growth in organometallic chemistry, offers higher selectivity, milder reaction conditions and high atom economy.[1] Many industrial processes are now available where stereospecific synthesis using transition metal catalysts play an indispensable role. The chemistry and reactivities of transition metal-oxo complexes have attracted extensive attention in the past decade due to their application in catalysis.[2] In my graduate research, I explored the utility of the high valent organorhenium oxide, methylrhenium trioxide (MTO) in catalytic atom transfer and rearrangement reactions.

Although MTO was first reported by Beattie and Jones in 1979,[3] its catalytic properties were not recognized till the early 90's.[4] Herrmann and coworkers who recognized the ability of MTO to activate hydrogen peroxide came up with a very facile synthesis in 1991(eqn 1).[5] The spectroscopic features of MTO are summarized in Table 1. Attractive features of MTO include its ease of synthesis and purification, stability in air, solubility in water and in most organic solvents and its effectiveness as a homogeneous catalyst.

$$Re_2O_7 + 2\,SnMe_4 + \text{[structure]} \longrightarrow 2\,\text{MTO} + CF_3(CF_2CO_2SnMe_3)_2$$

MTO

(1)
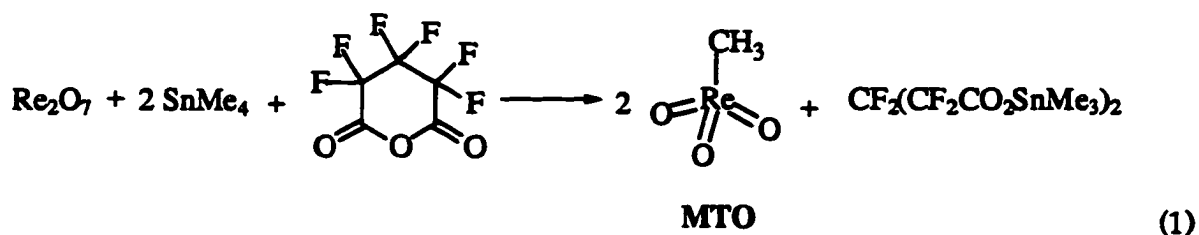
Table 1. Spectroscopic features of MTO

Spectroscopy	signals
IR in CH_2Cl_2	1000(w) 967 (vs) cm^{-1}
^1H NMR in $CDCl_3$	δ 2.63 (s) ppm
^{13}C NMR in $CDCl_3$	δ 19.03 ppm
UV-Vis in H_2O	239 nm(ϵ 1900 L $mol^{-1}cm^{-1}$)
	270nm (ϵ 1300 L $mol^{-1}cm^{-1}$)

Sulfur Atom Transfer Reactions

Metal centered oxygen atom transfer reactions are interesting because of their relevance to hydroxylase enzymes in biological systems and their potential in catalytic oxidation processes.[6,7] Previous work in our lab has shown that MTO catalyzes O-atom transfer reactions from various organic and inorganic oxidants through a catalytic cycle involving a Re(V) species as shown in Scheme 1.[8,9] The mechanisms of these atom transfer reactions have been studied in detail.
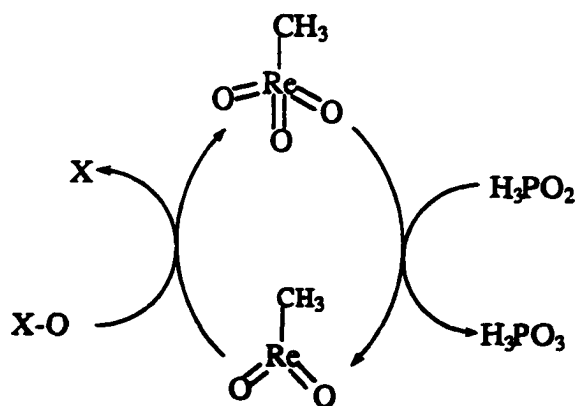
$X-O$ = epoxides, sulfoxides, ClO_4^-, BrO_4^- etc.

Scheme 1. catalytic cycle for O atom transfer reactions with MTO

In this work, I report the extension of the chemistry to sulfur atom transfer reactions. Triphenylphosphine was used as the sulfur acceptor from episulfides in this study. The reactions were carried out in CD_3CN or C_6D_6 at room temperature with 2% MTO as the catalyst. Preliminary experiments showed that the reaction was characterized by a long induction period which could be accounted for. Mechanistic considerations suggested that the induction period could be averted by replacing the oxygen atoms on rhenium by sulfur. This was achieved by the addition of H_2S which eliminated the induction period completely.

Chart 1

D   M-L
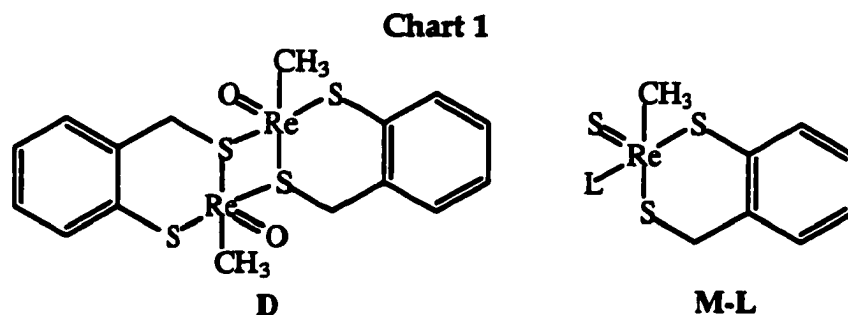
Since characterization of the catalyst obtained on reaction of MTO with hydrogen sulfide proved to be difficult, we turned to model systems. Several complexes based on 2-mercaptomethylthiophenol as a ligand were synthesized and crystallographically characterized (of general formula D and M-L in Chart 1). ^1H NMR or UV-Vis spectroscopy were used in the kinetic studies. A new method for the conversion of metal-oxo to sulfido compounds was developed. These results and further investigations with these complexes are discussed in chapters I, II, III and IV.

Rearrangement Reactions

Lewis acids play a vital role in catalyzing numerous organic reactions.[10] MTO, with rhenium in its highest oxidation state of +7, is a powerful Lewis acid.

In this study, the utility of MTO in effecting a 1,3-transposition of hydroxyl groups in allylic and propargylic alcohols were investigated (eqns 2 and 3).

$$\text{(2)}$$

$$\text{(3)}$$
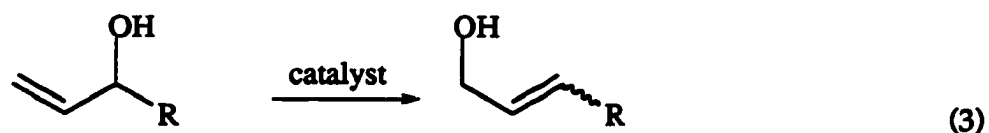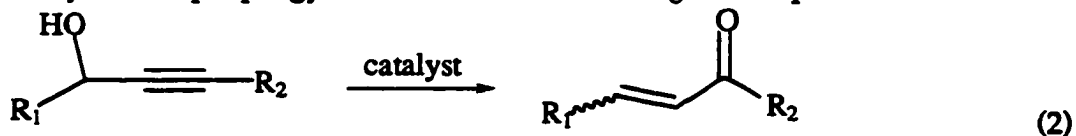
Propargylic alcohols on rearrangement give α,β-unsaturated aldehydes or ketones which are valuable as Michael acceptors in synthesis. In this study, the rearrangement of a variety of aliphatic and aromatic propargylic alcohols were studied in the presence of catalytic amounts of MTO. The reactions are characterized by a long induction period which was poorly understood. The same chemistry was extended to allylic alcohols and the more stable product predominates at equilibrium. Kinetic, equilibrium and labeling studies (deuterium and ^{18}O) were carried out to determine the mechanism of isomerization. In collaboration with Prof. Mark Gordon's group at ISU, we carried out theoretical studies on model systems to predict the direction of equilibrium in these systems. The results of these investigations are summarized in chapters V and VI.

Oxidation of Arenes to p-Quinones

Selective C-H bond activation of readily available chemical feedstocks poses a great scientific challenge in that the first formed products are generally more reactive than the starting materials. Hence selectivity is a major challenge to anyone working in this field. In fact, great advances have been made in the

selective functionalization of CH₄ to CH₃OH in recent years. Hydrogen peroxide is considered one of the best sources of oxygen atom in oxidation reactions since the product after oxidation is water and hence no problems arise in terms of
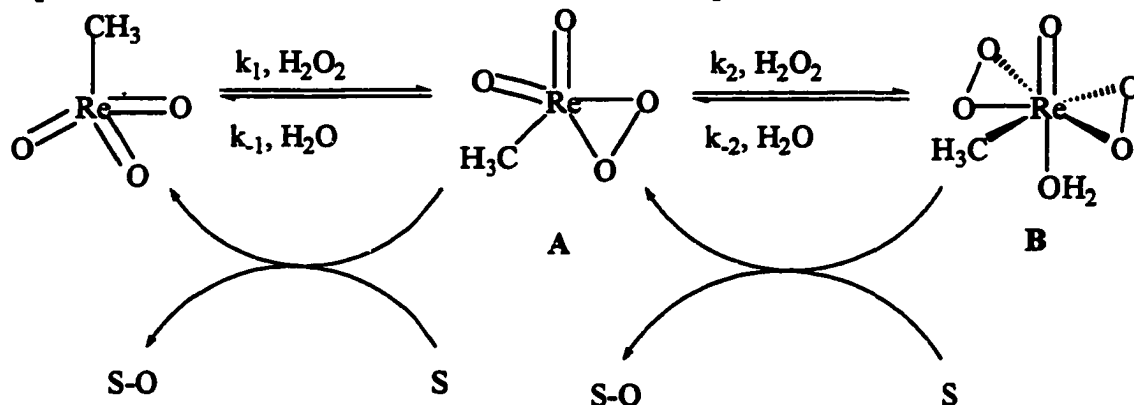
Scheme 2. Catalytic cycle for oxidations with MTO and H_2O_2

waste disposal. Although hydrogen peroxide reactions by themselves are slow, MTO activates hydrogen peroxide to form a monoperoxocomplex, A and a bisperoxo complex, B. Both these complexes are capable of transferring oxygen atoms to various oxidants in a catalytic cycle as shown in Scheme 2. Previous work in our lab has shown that the MTO/H_2O_2 system can oxidize a range of substrates and the kinetics and mechanisms of these reactions have been studied in detail.[11-15] In this study, the direct oxidation of substituted arenes to p-quinones by hydrogen peroxide catalyzed by MTO was investigated. The reactions were studied in acetic acid at 60°C with 8 mol% catalyst and was monitored by GC-MS. The results of this investigation are summarized in Chapter VI.

Dissertation Organization

The dissertation consists of seven chapters. Chapter I corresponds to a manuscript submitted to *Chemical Communications*. Chapter II corresponds to a manuscript published in *Inorganic Chemistry*. Chapters III and IV have been submitted as communications to *Inorganic Chemistry*. Chapter V has been published in *Organometallics* and Chapter VII in *Inorganica Chimica Acta*. We

decided not to publish the work described in Chapter VI. Each chapter is self-contained with its own equations, figures, tables and references. Following the last manuscript is general conclusions. Except for the theoretical studies described in Chapter V and the X-ray structural analysis, all the work in this dissertation was performed by the author of this thesis, Josemon Jacob.

References

1) Herrmann, W. A.; Cornils, B. *Applied Homogeneous Catalysis with Organometallic Compounds*; VCH: New York, 1996; Vol. 1-2.

2) Casey, C. P. *Science* **1993**, *259*, 1552.

3) Beattie, I. R.; Jones, P. J. *Inorg. Chem.* **1979**, *18*, 2318.

4) Herrmann, W. A.; Fischer, R. W.; Marz, D. W. *Angew. Chem. Int. Ed. Engl.* **1991**, *30*, 1638.

5) Herrmann, W. A.; Kuhn, F. E.; Fischer, R. W.; Thiel, R. W.; Ramao, C. C. *Inorg. Chem.* **1992**, *31*, 4431.

6) Chinn, L. J. *Selection of Oxidants in Synthesis*; Marcel Dekker: New York, 1971.

7) Conghlan, M. P. *Molybdenum and Molybdenum-containing Enzymes*; Pergamon: New York, 1980.

8) Abu-Omar, M. M.; Appelman, E. H.; Espenson, J. H. *Inorg. Chem.* **1996**, *35*, 7751.

9) Abu-Omar, M. M.; Espenson, J. H. *Inorg. Chem.* **1995**, *34*, 6239-40.

10) Trost, B. M. *Comprehensive Organic Synthesis*; Pergamon press:, 1991; Vol. 5.

11) Vassell, K. A.; Espenson, J. H. *Inorg. Chem.* **1994**, *33*, 5491-98.

12) Zhu, Z.; Espenson, J. H. *J. Org. Chem.* **1995**, *1995*, 1326-32.

13) Zauche, T. H.; Espenson, J. H. *Inorg. Chem.* **1997**, *36*, 5257-61.

14) Stankovic, S.; Espenson, J. H. *J. Org. Chem.* **1998**, *63*, 4129-30.

15) Al-Ajlouni, A.; Espenson, J. H. *J. Org. Chem.* **1996**, *61*, 3969-76.

CHAPTER I. STEREOSPECIFIC RHENIUM CATALYZED DESULFURIZATION OF THIIRANES

A communication accepted for publication in Chemical Communications

Josemon Jacob and James H. Espenson*

Abstract

Methylrhenium trioxide (MTO) acts as a catalyst in the desulfurization of thiiranes by triphenylphosphine at room temperature. An enormous enhancement in rate is observed when MTO is pretreated with hydrogen sulfide prior to the reaction. Using 2-mercaptomethylthiophenol as a ligand, we synthesized a dimeric Re(V) model complex to study the mechanism of this reaction. We were able to show that a Re(V) species is the active form of the catalyst in the system. The reaction works efficiently for both aromatic and aliphatic substrates and proceeds with complete retention of stereochemistry and is very tolerant to functional groups.

Introduction

Desulfurization of thiiranes is known to occur thermally,[1] photochemically[2] and by a wide variety of reagents. These reagents include trivalent phosphorous compounds,[3,4] aminium salts,[5] iron[6] and rhodium carbonyl complexes,[7] peculiar selinium derivatives,[8] atomic carbon[9,10] and by phenyl radicals.[11] One of the most widely used reactions of thiiranes (also called episulfides) is the stereospecific desulfurization by trivalent phosphorous compounds to give an alkene and a sulfur-phosphorous derivative. Triphenylphosphine is the most common reagent and the mechanism of desulfurization has been studied by Denney et al.[4] These are very slow reactions, the rate constant for the reaction of triphenyl phosphine and 1-butenesulfide being $(0.9\text{-}1.8) \times 10^{-5}$ $M^{-1}s^{-1}$ at 40°C in different solvents. Our group's

interest in this area stems from our recent studies on catalytic oxygen atom transfer reactions using organorhenium oxides.[12-14] We were interested in extending our studies to sulfur atom transfer reactions and herein we report the results of our investigation.

$$Ph_3P \quad + \quad \underset{S}{\triangle\!\!\!\!\diagup} \quad \xrightarrow[\text{r. t.}]{\underset{CD_3CN}{\text{cat. MTO/H}_2S}} \quad S=PPh_3 \quad + \quad \diagup\!\!\!=\!\!\!\diagup$$

$$(1)$$
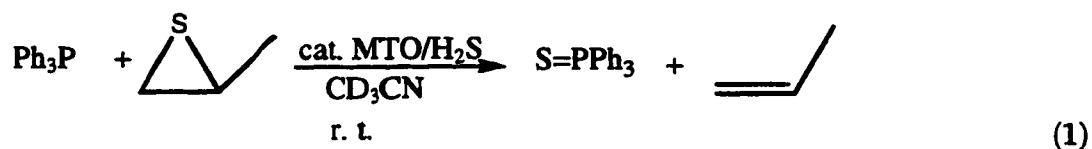
Results and Discussion

Propylene sulfide was the substrate of choice in our initial experiments. The addition of catalytic amounts of methylrheniumtrioxide, (MTO) shows formation of the olefin although the reaction is still quite slow (see **Fig 1**). As seen in the graph, the reaction is characterized by a long induction period. Independent studies in our lab have shown that the formation of Re(V) from MTO by reaction with Ph$_3$P is characterized by an induction period very close to that observed in this reaction.[15] **Scheme 1** shows a plausible mechanism.

Scheme 1. Suggested mechanism for MTO catalyzed desulfurization of thiiranes with Ph$_3$P.
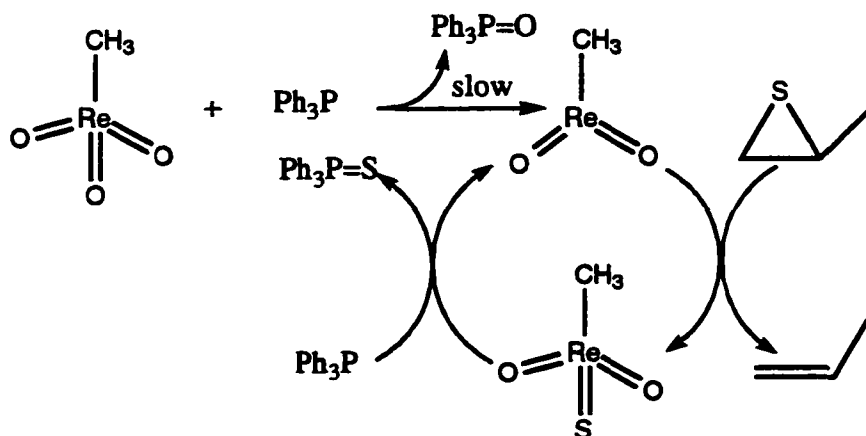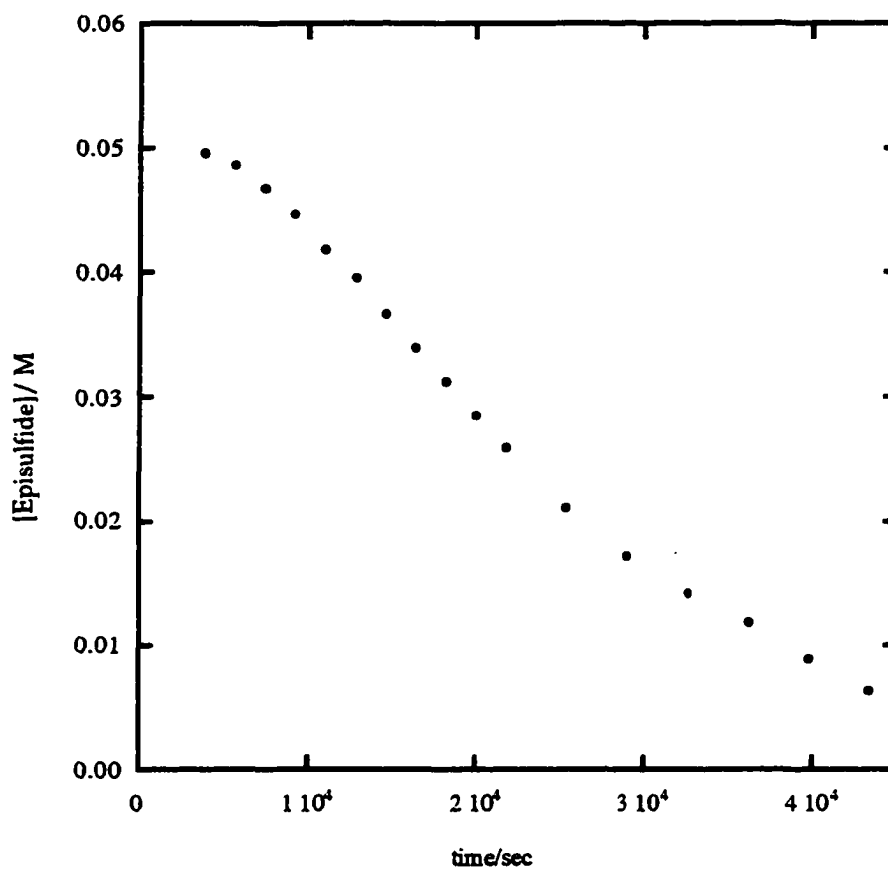
Figure 1. Kinetics of the reaction of propylene sulfide with Ph3P in the presence of MTO as followed by ^{1}H NMR. Conditions: MTO = 20mM; propylene sulfide = 50mM; Ph3P = 200mM.

Analogous to the mechanism of catalytic oxygen atom transfer reactions, Re(V) is proposed to be the active catalyst species in this reaction, suggestive in part from the observed induction period.[16] The mechanistic scheme suggests that the induction period can be eliminated if one substitutes one or more of the oxygen atoms on MTO by sulfur (Re(VII) transfers a sulfur atom to a phosphine much faster than an oxygen). Using ^{18}O labeled water, we have shown that MTO can exchange its oxygens with water resulting in ^{18}O labeled MTO.[17] This led us to the idea that it might be possible to use H_2S to exchange one or more of the oxygen atoms on MTO with sulfur. In a test reaction, H_2S was bubbled through MTO in CD_3CN first and then the reaction was repeated (eqn 1). As predicted, we found significant enhancement in rate in the desulfurization reaction of propylene sulfide (Fig 2). Removal of H_2S by bubbling argon through the reaction prior to the addition of the phosphine and episulfide did not alter the result at all. Furthur investigation showed that the reaction is very general with episulfides and occurs very efficiently at room temperature for a variety of substrates. The results are shown in **Table 1**.

As evident from **Table 1**, the reaction works very efficiently for a range of substrates and is very tolerant to functional groups. It works well for both aliphatic and aromatic substrates and when both epoxy and episulfido groups are present (entry 10), only the episulfide undergoes this atom transfer reaction in the time scale indicated. The reaction proceeds with complete retention of stereochemistry as indicated by entries 12 and 13 where the stereochemistry in the episulfide is preserved in the olefin.

Reaction Mechanism

So what happens in the presence of H_2S? A likely mechanism in the absence of H_2S was discussed earlier (**Scheme 1**). In the presence of H_2S, we anticipated the following exchange to happen (eqn 2). Literature reports the preparation of Re_2S_7
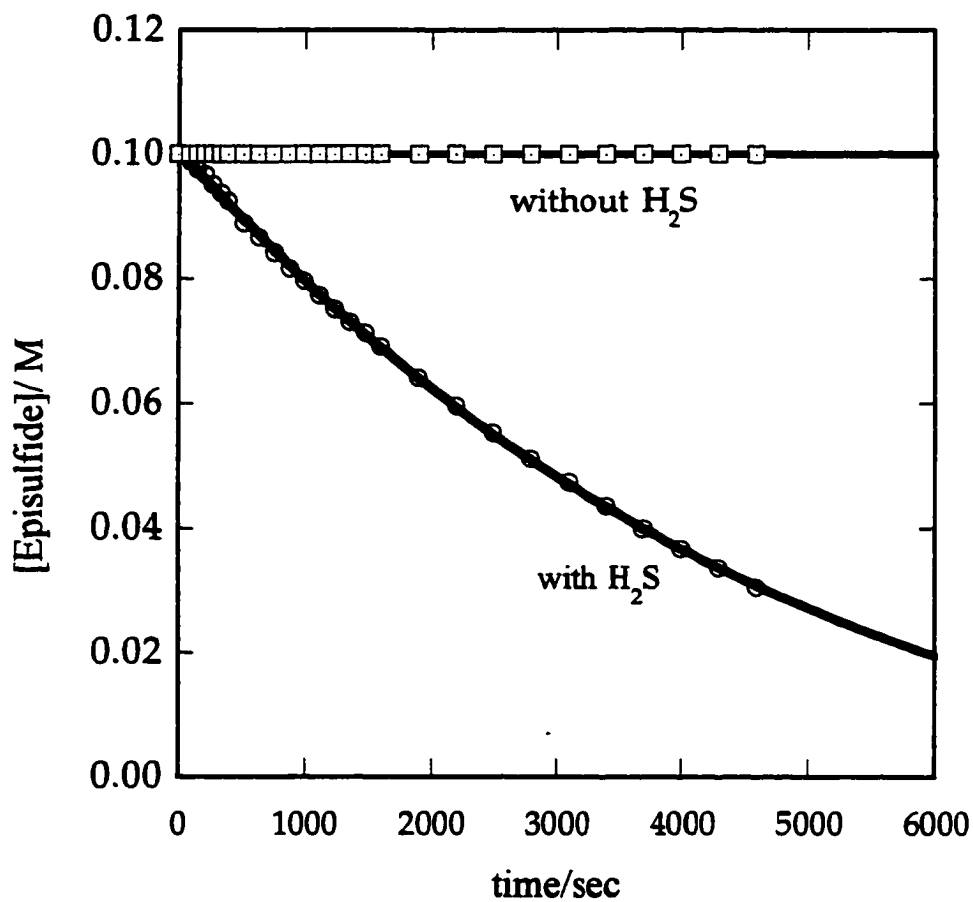
Figure 2. Kinetics of the reaction of propylene sulfide with triphenylphosphine in the presence of MTO and H_2S. Conditions: MTO = 2mM; propylene sulfide = 100mM; Ph_3P = 125mM.

from $KReO_4$ and MoS_3 form $(NH_4)_2MoO_4$ by direct reaction with H_2S.[18] Also the Re(V) and Mo(IV) sulfides were prepared from the same starting materials by reaction with H_2S at elevated temperatures (>450°C).[19]

$$(2)$$
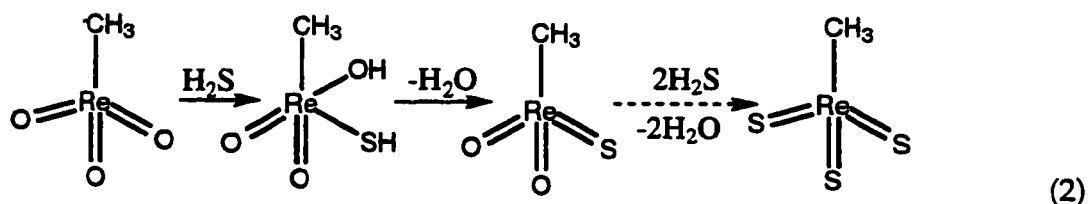
On bubbling H_2S through a solution of MTO in CD_3CN, a black solid separates out within a few minutes. The product so obtained was found to be insoluble in all organic solvents and in water. This made characterization of the catalyst rhenium species quite difficult. One alternative is to use known oxidation chemistry of MTO with hydrogen peroxide. Addition of excess hydrogen peroxide dissolved the black solid product obtained on reaction of MTO with H_2S, but the chemical shift of the new species observed by ^{1}H NMR did not match with the bisperoxocomplex of MTO. Our next approach was to suitably complex MTO to generate model systems inorder to establish the mechanism. Nitrogen based ligands were the initial choice since such complexes of MTO are well characterized and well documented in literature.[14] Although phenanthroline, bipyridine and 8-hydroxyquinoline complexes of MTO were synthesized, all of them failed to react with H_2S. We then turned our focus on to sulfur based ligands. Any sulfur based MTO complex will provide a system closer to the one obtained by reaction of MTO with H_2S. We chose 2-mercaptomethylthiophenol as the ligand and on reaction with MTO, it forms a new dimeric yellow Re(V) complex, D (eqn. 3).[20,21] The complex D on reaction with triphenylphosphine forms the green mononuclear complex, M-L (eqn. 4). The synthesis and characterization of these complexes were reported earlier.[22]

$$4 \text{ (o-benzene di(CH}_2\text{SH)} + 2 \underset{\overset{O}{\underset{O}{}}}{CH_3\text{-}Re\text{=}O} \xrightarrow{-4H_2O} 2 \text{ (benzo-dithiole)} + D$$

D

(3)

$$D + 2Ph_3P \longrightarrow 2 \ PPh_3\text{—Re—S} \quad \text{(M-L)}$$

M-L

(4)
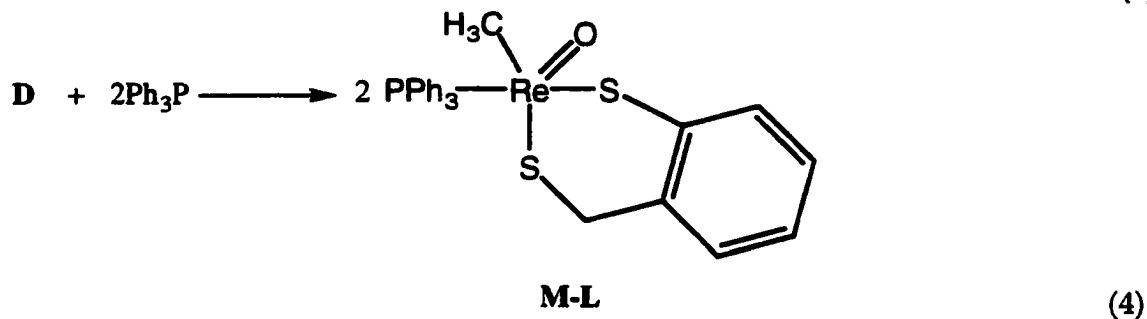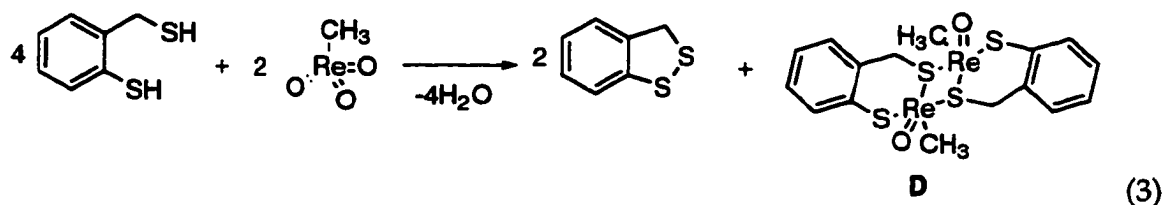
With the Re(V) dimer, **D** in hand, we tested the proposed mechanism in **Scheme 1**. According to the mechanism, the active catalyst is a Re(V) species. If this were true, this dimer should be able to desulfurize two equivalents of episulfide in the absence of phosphine. **Fig. 3** shows the kinetics of an experiment with a four fold excess of propylene sulfide. Clearly, **D** reacts with two equivalents of the thiirane establishing that the active catalyst is a Re(V) species. Also, the reaction can be made catalytic by the addition of triphenylphosphine although the reaction is slower than the MTO/H_2S system. But almost the same rate of desulfurization is achieved if H_2S is bubbled through the dimer solution before the addition of the episulfide and phosphine (**Fig. 4**). On reaction with H_2S, the color of the solution changes from yellow to pink. Although, this suggests atleast partial conversion of Re=O in **D** to Re=S, we were not able to isolate such a species. We also checked whether **M-L** is a catalyst in the desulfurization reaction since under the reaction conditions, **M-L** is slowly formed in the reaction. With concentrations and conditions remaining the same as in **Fig. 4**, we found only <10% desulfurization in 3 hours. This is not
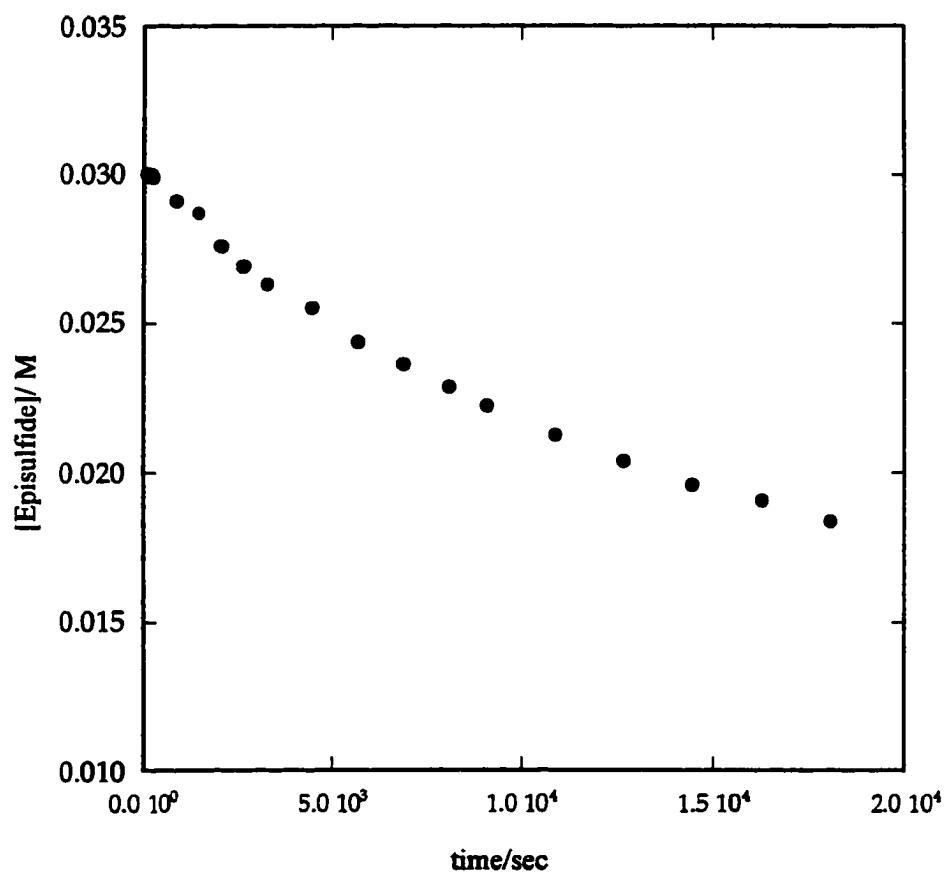
Figure 3. Kinetics of the reaction of **D** (7.5mM) with propylene sulfide (30mM) in C_6D_6 as followed ^1H NMR at room temperature.

surprising since **D** (or its monomer) is coordinatively unsaturated and sterically less hindered than **M-L** although both are Re(V) complexes.

Returning the discussion to the original MTO/H$_2$S system, the question sill remains about whether or not a sulfur analogue of MTO is formed in the reaction or whether some Re(V) is also formed along with Re(VII) in the system. We believe that the black solid obtained on reaction of MTO with H$_2$S is an oligomeric form of alkylrhenium sulfides. Transition metal sulfides including high oxidation state rhenium sulfides are known to oligomerize and some of them have been characterized as well.[23] When the black solid obtained on reaction with H$_2$S was treated with propylene sulfide, 4% desulfurization was observed in 2 hours (starting with 5mM MTO) suggesting the formation of some Re(V) also in the system. In another set of experiments, H$_2$S was bubbled through 20mM MTO in CD$_3$CN till all of MTO had reacted (as observed by ^{1}H NMR). The excess hydrogen sulfide was removed by bubbling argon and then the reaction of this rhenium product with Ph$_3$P was monitored by ^{31}P NMR. It is clear from our experiments that a Re(VII) sulfide easily transfers a sulfur atom to a phosphine to generate Re(V) and the phosphine sulfide. 5mM Ph$_3$P was added at a time and monitored by ^{31}P NMR. Only Ph$_3$P=S was observed on addition of 15mM and an addition of another 5mM showed very small amounts of Ph$_3$P. Addition of more phosphine did not lead to more of Ph$_3$P=S. This experiment also clearly suggests that most of MTO exists as Re(VII) on reaction with H$_2$S.

Conclusions

In conclusion, we have reported here a novel catalytic system to effect the desulfurization of episulfides at ambient temperature and pressure. The reaction is completely stereospecific and very tolerant to functional groups. Efforts are now
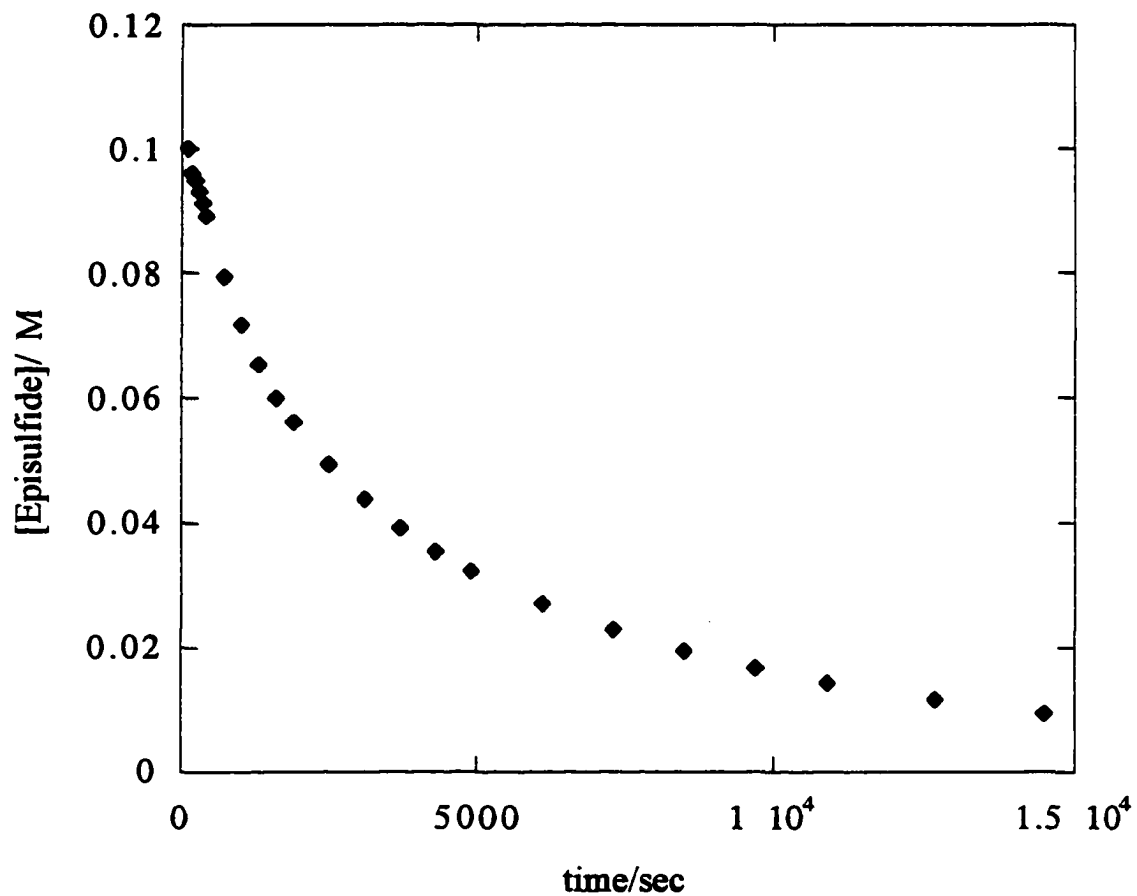
Figure 4. Kinetics of the reaction between propylene sulfide and triphenylphosphine in the presence of D and H_2S at room temperature. Conditions: D = 2mM, Ph_3P = 125mM, propylene sulfide = 100mM

underway to synthesize a sulfur analogue of D which, we believe, will show enhanced reactivity.

Experimental Section

Materials

Propylene sulfide, cyclohexene sulfide and MTO were purchased from commercial sources. All other episulfides were synthesized from the corresponding epoxides in a one or two step procedure using Bordwell's method.[24,25] The NMR spectra were recorded either on a varian VXR 300MHz or a Bruker 400MHz spectrometer. The chemical shifts were referenced to the solvent peaks (7.15 for C_6D_6 and 1.93 for CD_3CN). In the kinetic experiments, Ph_3CH was used as an internal standard.

General Procedure

In a typical experiment, H_2S was bubbled through 2mM MTO in CD_3CN for about five minutes when a black solid separates out from solution. The excess H_2S is removed by bubbling argon through the system and then Ph_3P and the episulfide are added. The reaction is monitored by NMR and the yields reported are based on proton integration relative to solvent or Ph_3CH. The chemical shifts of the product olefins agreed very well with literature.[26,27]

References

1) Dittmer, D. C. *Thiiranes and Thiirenes*; Pergamon press:, 1984; Vol. 7.

2) Torres, M.; Lown, E. M.; Gunning, H. E.; Strausz, O. P. *Pure & Appl. Chem.* **1980**, *52*, 1623-43.

3) Dybowski, P.; Skowronska, A. *Synthesis* **1991**, 1134-36.

4) Denney, D. B.; Boskin, M. J. *J. Am. Chem. Soc.* **1960**, *82*, 4736-38.

5) Calo, V.; Lopez, L.; Nacci, A.; Mele, G. *Tetrahedron* **1995**, *51*, 8935-40.

6) Trost, B. M.; Ziman, S. D. *J. Org. Chem*. **1973**, *38*, 932-36.

7) Calet, S.; Alper, H. *Tetrahedron Lett* . **1986**, *27*, 3573-76.

8) Calo, V.; Lopez, L.; Mincuzzi, A.; Pesce, G. *Synthesis* **1976**, 200-1.

9) Skell, P. S.; Klabunde, K. J.; Plonka, J. H.; Roberts, J. S.; Williams-Smith, D. L. *J. Am. Chem. Soc.* **1973**, *95*, 1547-52.

10) Klabunde, K. J.; Skell, P. S. *J. Am. Chem. Soc.* **1971**, *93*, 3807-8.

11) Weseman, J. K.; Williamson, R.; J. L. Green, J.; Shevlin, P. B. *J. Chem. Soc. Chem. Comm.* **1973**, 901-2.

12) Espenson, J. H.; Abu-Omar, M. M. *Adv. Chem. Ser.* **1997**, *253*, 99-134.

13) Espenson, J. H. *Chem. Comm.* **1999**, 479-88.

14) Ramao, C. C.; Kuhn, F. E.; Herrmann, W. A. *Chem. Rev.* **1997**, *97*, 3197-3246.

15) Eager, M. D.; Espenson, J. H. **1999**, *in press.*

16) Abu-Omar, M. M.; Appelman, E. H.; Espenson, J. H. *Inorg. Chem.* **1996**, *35*, 7751-57.

17) Abu-Omar, M. M.; Hansen, P. J.; Espenson, J. H. *J. Am. Chem. Soc.* **1996**, *118*, 4966-74.

18) Broadbent, H. S.; Slaugh, L. H.; Jarvis, N. L. *J. Am. Chem. Soc* . **1954**, *76*, 1519.

19) Weisser, O.; Landa, S. *Sulphide Catalysts, Their Properties and Applications;* Pergamon press: New York, **1973**.

20) Klingsberg, E.; Schreiber, A. M. *J. Am. Chem. Soc.* **1962**, *84*, 2941-44.

21) Hortman, A. G.; Aron, A. J.; Bhattacharya, A. K. *J. Org. Chem* **1978**, *43*, 3374-78.

22) Jacob, J.; Guzei, I. A.; Espenson, J. H. *Inorg. Chem.* **1999**, *38*, 1040-41.

23) Goodman, J. T.; Rauchfuss, T. B. *Inorg. Chem.* **1998**, *37*, 5040-41.

24) Bordwell, F. G.; Anderson, H. M. *J. Am. Chem. Soc.* **1954**, *75*, 4959-62.

25) Sander, M. *Chem. Rev.* **1966**, *66*, 297.

26) Pouchert, J. C.; Behnke, J. *The Aldrich Library of 13C and 1H FT NMR Spectra,* **1993**; Vol. 1.

27) Silverstein, R. M.; Bassler, G. C.; Morril, T. C. *Spectrometric Identification of Organic Compounds*; 5th ed.; John Wiley & Sons:, 1971.

Table 1. Yields obtained in the MTO catalyzed desulfurization of different thiiranes at room temperature.[a]
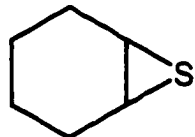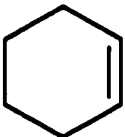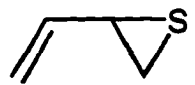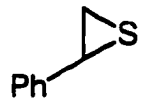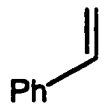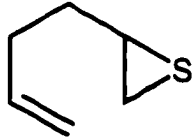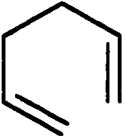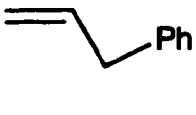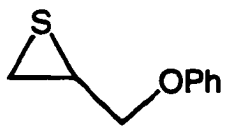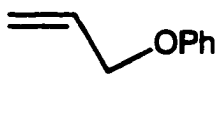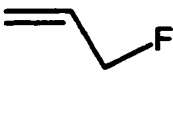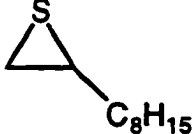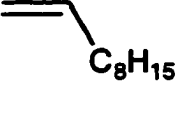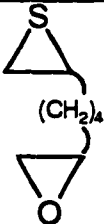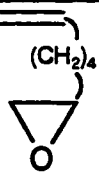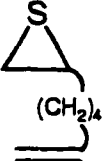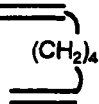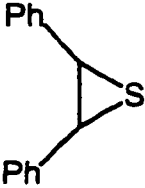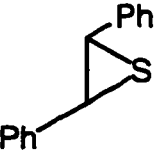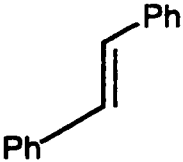
Entry	Substrate	Product	time	% yield
1			3h	100
2			5 min	100
3			5min	96
4			5 min	100
5			1h	100
6			4h	89
7			6h	100
8			9h	50
9			1h	9h

Table 1 continued

Entry	Substrate	Product	Time	%Yield
10			2h	100
11			1h	100
12			30 min	100
13			30 min	100

a. In a typical experiment, H_2S is bubbled through 2mM soln of MTO in CD_3CN for 5 minutes first, the excess H_2S then removed by bubbling argon through the solution. To this Ph_3P (125mM) is added followed by the thiirane (100mM) and the reaction followed by ^{1}H NMR at 25°C. The reaction also worked very well on a 2gm scale.

Supporting Information

^{1}H and ^{13}C NMR data for the episulfides

Substrate	^{1}H NMR	^{13}C NMR
vinylthiirane	δ 5.44(m, 2H) 5.15(m, 1H) 3.41(m, 1H) 2.63(dd, 1H, J=6.3, 1.5Hz) 2.31 (dd, 1H, J=5.4, 1.5Hz) ppm	δ 139.44, 117.60, 36.75, 25.33 ppm.
styrene sulfide	δ 7.31-7.24(m, 5H) 3.95(dd, 1H, J=6.0, 6.8Hz) 2.87(dd, 1H, J=6.8, 1.6Hz) 2.71(dd, 1H, J=6.0, 1.6Hz) ppm.	δ 140.81, 129.94, 128.93, 128.08, 37.04, 28.05 ppm
but-3-enyl-thiirane (entry 5 on table)	δ 5.88(m, 1H) 5.10-4.99(m, 2H) 2.90(m, 1H) 2.49(m, 1H) 2.21(m, 3H) 1.91(m, 1H) 1.48(m, 1H) ppm.	δ 139.34, 115.98, 37.07, 36.52, 34.56, 26.75 ppm.
3-phenoxypropene sulfide	δ 7.30(m, 2H) 6.94(m, 3H) 4.05(m, 2H) 3.28(m, 1H) 2.59(dd, 1H, J=8.4, 1.2H) 2.35(dd, 1H, J=7.2, 1.2H) ppm.	δ 159.90, 130.95, 122.40, 115.93, 73.79, 32.93, 24.38 ppm.
3-phenylpropene sulfide	δ 7.35-7.22(m, 5H) 3.10(m, 1H) 3.03(m, 1H) 2.81(m, 1H) 2.54(dd, 1H, J=5.2, 0.8Hz) 2.32(dd, 1H, J=5.2, 0.8Hz) ppm	δ 141.17, 130.00, 129.82, 127.91, 43.39, 37.19, 26.69 ppm.

3- fluoropropene sulfide	δ 3.33(m, 2H) 3.09(dd, 1H, J=9.2, 6.8Hz) 2.67(m, 1H) 2.43(dd, 1H, J=6.8, 1.5Hz) ppm.	δ 40.67, 34.12, 26.41 ppm.
1-decene sulfide	δ 2.85-2.82(m, 2H) 2.64(dd, 1H, J=5.2, 4.4Hz) 2.37(dd, 1H, J=5.2, 1.8Hz) 1.45-1.28(m, 14H) 0.87(t, 3H, J=6.8Hz) ppm.	δ 53.12, 47.66, 33.62, 32.99, 30.63, 30.57, 30.37, 27.11, 23.77, 14.77 ppm.
2-(4-Oxiranyl-butyl)-thiirane (entry 10)	δ 2.87(m, 2H) 2.73(dd, 1H, J=4.8, 4.2Hz) 2.45(m, 2H) 2.12(d, 1H, J=5.7Hz) 1.83(m, 1H) 1.52(m, 7H) ppm.	δ 52.17, 47.05, 36.44, 35.76, 32.37, 29.13, 25.84, 25.58 ppm.
hex-5-enylthiirane (entry 11)	δ 5.75(m, 1H 4.98(m, 2H) 2.85(m, 1H) 2.47(dd, 1H, J=8.4, 1.2Hzz) 2.12(dd, 1H, J=7.6, 1.2Hzz) 2.05(m, 2H) 1.82(m, 1H) 1.45(m, 5H) ppm.	δ 138.74, 114.57, 36.47, 35.97, 33.68, 28.85, 28.51, 25.96 ppm.
trans- Stilbene sulfide	δ 7.41-7.27(m, 10H) 4.17 (s, 2H) ppm	δ 140.14, 129.97, 129.14, 128.33, 45.92 ppm.
cis- Stilbene sulfide	δ 7.28-7.11(m, 10H) 4.46(s, 2H) ppm.	δ 136.65, 130.67, 129.01, 128.51, 45.30 ppm

CHAPTER II. SYNTHESIS, STRUCTURE AND REACTIVITY OF NOVEL DITHIOLATO Re(V) COMPLEXES

A paper published in Inorganic Chemistry[1]

Josemon Jacob, Ilia A. Guzei, and James H. Espenson*

Abstract

Treatment of methyltrioxorhenium(VII), MTO, with the dithiol o-HSC$_6$H$_4$CH$_2$SH results in a dimeric rhenium(V) chelate, [CH$_3$Re(O)(S$_2$^{L})]$_2$, where S$_2$^{L} is the dithiolate ligand present as a chelate. The dimer is created through two S$\rightarrow$Re interactions, this sulfur being one coordinated to the other rhenium atom. The central Re$_2$S$_2$ core is nearly a planar trapezoid, the dihedral angle between the two {Re, S, S} planes being 19.2(2)°. The Re-Re distance of 3.14A° precludes the existance of any metal-metal bond. The coordination sphere of rhenium can be viewed as a distorted square pyramidal with three sulfur atoms and a carbon atom in the basal plane and an oxygen atom at the apex. The dimer is monomerized upon reaction with triphenylphosphine, giving the intensely green CH$_3$(Ph$_3$P)Re(O)(S$_2$^{L}). Both dimer and monomer were fully characterized crystallographically and spectroscopically (^{1}H and ^{13}C NMR and by elemental analysis). The dimer reverts to MTO upon treatment with certain oxygen donors XO, such as Me$_3$NO, pyridine-NO, Ph$_3$AsO, Me$_2$SO, and Ph$_3$SbO. These reactions also produce X and the organic persulfide.

[1]Jacob, J.; Guzei, I. A.; Espenson, J. H.; *Inorg. Chem.* **1999**, *38*, 1040-1041.

Introduction

Oxygen atom transfer catalyzed by transition metal complexes holds great interest owing to its chemical and biological relevance.[1-8] The intriguing mechanisms of certain of these reactions catalyzed by organorhenium oxides have been revealed.[9,10] As we became involved in certain sulfur atom transfer reactions, it became important to synthesize stable thiolato complexes derived from methyltrioxorhenium (CH_3ReO_3 or MTO), in that they are related to important catalytic intermediates. A tetrathiophenylato complex, unstable above 15°C, has been reported,[11] as have anionic dithiolato complexes of rhenium(V)sulfides.[12] Prompted by these reports, we sought to prepare new, thermally stable thiolato complexes derived from MTO.

Results and Discussion

The reaction of MTO (0.8 mmol, 200 mg) with a two-fold excess of the dithiol[13,14] was carried out at 0 °C in toluene (10 mL); after 15 min., 5 mL hexane was added and the mixture kept in a freezer overnight. The product was a dimeric dithiolato-dirhenium complex, **D**, that forms fine needles, isolated in 88% yield. Its structure was determined from spectrosocopic[15] and X-ray data,[16,17] as shown in eq 1 and **Figure 1**.

$$(1)$$
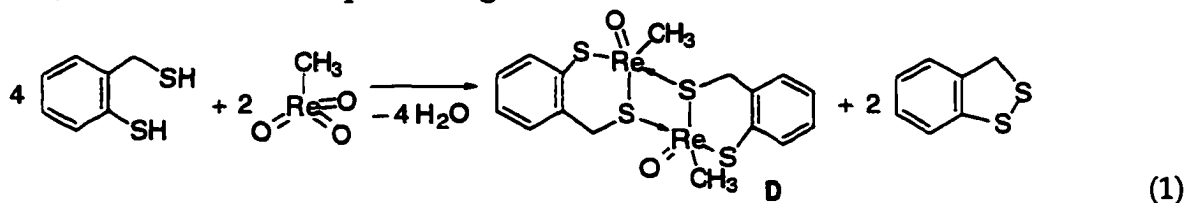
As depicted, **D** is a dinuclear compound held together with coordinate bonds from the sulfur of one ligand to the other rhenium. A dithiolate ligand chelates Re(V), which is also coordinated by single oxo and methyl groups.
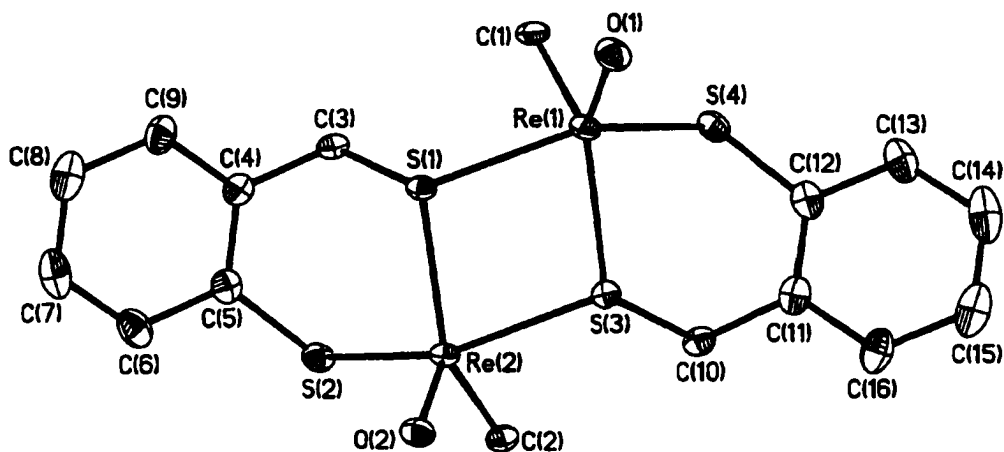
Figure 1: Perspective view of the dinuclear rhenium(V) compound **D** with thermal ellipsoids at the 30% probability level. Selected bond lengths (Å) and angles (°): Re(1)–S(1) 2.386; Re(1)–S(3) 2.362; Re(1)–S(4) 2.299; Re(1)–O(1) 1.670; Re(1)–C(1) 2.120; S(3)–Re(1)–S(1) 75.2; S(3)–Re(1)–S(4) 90.8; S(4)–Re(1)–S(1) 146.2; S(3)–Re(1)–O(1) 112.7; S(3)–Re(1)–C(1) 143.2; O(1)–Re(1)–C(1) 103.8.

Accompanying this product is the cyclic organic disulfide, required to balance the reduction of Re(VII) to Re(V). D contains a four-membered heteroatomic ring comprised of two rhenium and two sulfur atoms. The two {Re, S, S} planes within the central Re_2S_2 core define a dihedral angle of 19.2(2)°. The rhenium atoms exist in a severely distorted trigonal bipyramid: two sulfur atoms lie in apical positions, at an average angle of 148(2)°, considerably off linearity. Sulfur, oxygen, and carbon atoms are found in the equatorial plane. The distortions are such that, alternatively, the coordination sphere of the rhenium atoms can be described as distorted square pyramidal with a carbon and three sulfur atoms in the basal plane and an oxygen atom at the apex. One set of three sulfur atoms and carbon is coplanar within 0.01(1) Å; the second within 0.09(1) Å. The rhenium-oxo vectors are almost normal to those planes, at angles of 84.5(1)° and 83.9(1)°. Although the rhenium-sulfur distance between the monomeric units (av. 2.373(11) Å) exceeds that found within each monomer (av. 2.294(8) Å), it falls well within similar rhenium-sulfur bond lengths.[12,18] Mixed sulfido-oxo complexes of rhenium[18] and molybdenum[19] have been reported.

Most likely, a first-formed mononuclear Re(VII) chelate then undergoes reductive elimination. Further ligand coordination and dimerization yields the Re(V) dithiolato complex D. Although excess dithiol was used in the synthesis, it did not monomerize D and remained unreacted. A tetrathiophenolatocomplex of MTO,[11] stable at low temperatures, undergoes reductive elimination at higher temperature. In our study, low temperature NMR experiments did not detect any intermediary Re(VII) species. However, the reactivity of D towards various two electron oxidants (vide infra) suggests the intermediacy of a Re(VII) species.

Given the dimeric structure, it seemed possible that a Re(V) monomer might be formed by coordination of an exogenous Lewis base, L. The addition of

two equivalents of Ph_3P to the yellow dimer resulted in the quantitative formation of the intensely green mononuclear dithiolato complex (ε_{606} = 1.9 × 10^2 L mol⁻¹ cm⁻¹), eq 2.

$$(2)$$
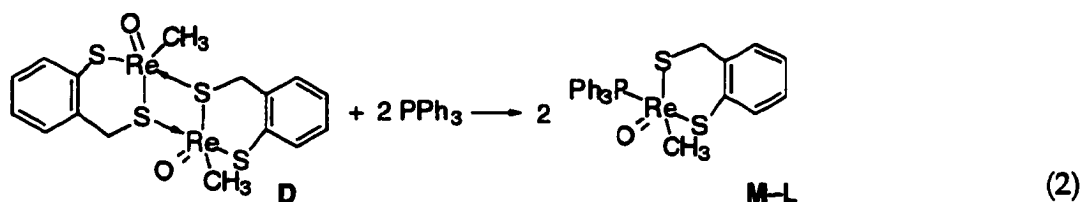
The rhenium(V) phosphine compound M–L was characterized by ^1H and ^{13}C NMR spectroscopy, elemental analysis and (despite quite small crystals grown by the slow diffusion of hexane into a toluene solution) single crystal X-ray analysis.[17,20,21] Its molecular structure, presented in **Figure 2**, shows two independent molecules with virtually identical parameters in the asymmetric unit; only one is shown. In the following discussion the structural parameters have been averaged between two molecules. As in the case of **D**, the molecular geometry of M–L can be viewed as highly distorted trigonal bipyramidal with one sulfur and one phosphorus atom in the apical positions (av. P–Re–S angle is 149.4(4)°). Sulfur, carbon, and oxygen atoms lie in the equatorial plane. Alternatively, the rhenium atom is in a distorted square pyramidal environment with a phosphorus, carbon, and two sulfur atoms in the basal plane (planarity within 0.14(1) Å) and an oxygen atom at the vertex. The oxygen-rhenium vector intersected the basal plane at 84.6(1)°. The bond distances to rhenium fall in the usual ranges. The similar structural features of both complexes are noteworthy because the one is a dimer, the other a monomer.

Since complexes of methyldioxorhenium is known to abstract oxygen from various oxidants to form MTO,[9,22] we investigated the reactivity of **D**
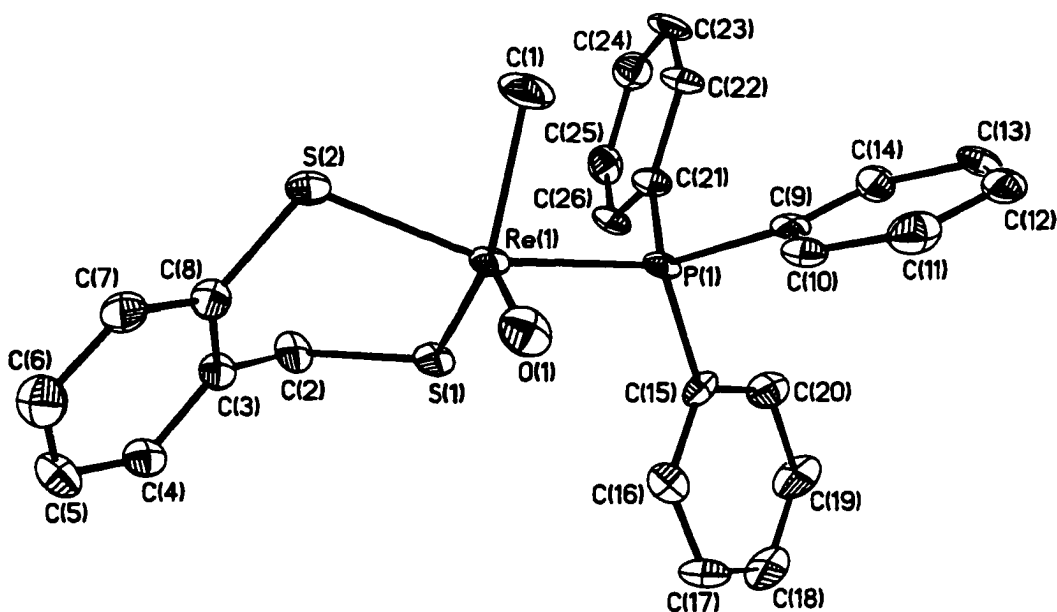
Figure 2: Perspective view of **M–L** with thermal ellipsoids at the 30% probability level. Selected bond lengths (Å) and angles (°) (corresponding parameters for the second molecule in parentheses): Re(1)–S(1) 2.283 (2.275); Re(1)–S(2) 2.329 (2.340); Re(1)–P(1) 2.452 (2.447); Re(1)–O(1) 1.677 (1.696); Re(1)–C(1) 2.125 (2.131); S(2)–Re(1)–S(1) 91.0 (90.6); S(2)–Re(1)–C(1) 78.6 (78.8); S(2)–Re(1)–O(1) 108.9 (109.1); C(1)–Re(1)–P(1) 83.3 (83.0).

towards various oxygen donors, XO. Addition of 4 equiv. XO in benzene solution caused both the rhenium and its dithiolate ligand to be oxidized:[23,24]

$$+ \; 4\,X\text{-O} \longrightarrow 2\,CH_3ReO_3 \; + 4\,X \; + 2 \; \text{(disulfide)}$$

(3)
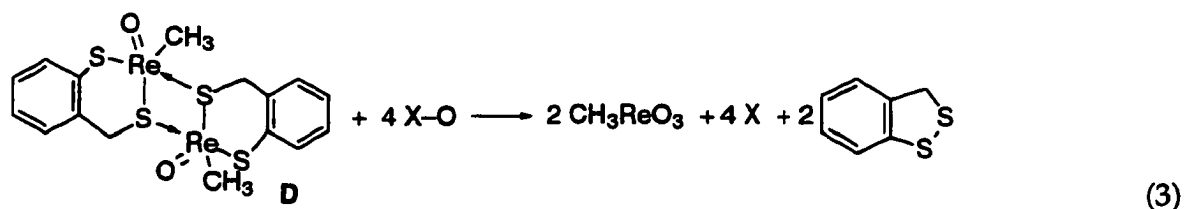
The reactions were monitored by ^1H NMR.[25] With XO = pyridine-N-oxide, Me_3NO or Ph_3AsO, complete reaction occurred within 5 min. Me_2SO required 1.5 d for 81% conversion, whereas Ph_3SbO gave only 50% reaction in 3 days. The disulfide isolated from this reaction and from eq 1 showed ^1H and ^{13}C NMR spectra identical to those of a sample prepared independently.[26] Perhaps inital O-transfer to form the Re(VII) thiolato is rate controlling; detailed studies are now underway to define the differences in reactivity of various oxidants.

Conclusions

In summary, we have synthesized, analyzed and characterized new oxorhenium(V) complexes containing a dithiolato ligand. The dinuclear version of this complex is monomerized upon reaction with triphenylphosphine. The dimer readily reacts with several O-atom donors, undergoing oxidation both at the metal and the ligand. We are currently investigating the scope and mechanism of this reaction and further studying the reactivity of this binuclear complex.

References

1) Holm, R. H. *Chem. Rev.* **1987**, *87*, 1401.

2) Espenson, J. H.; Abu-Omar, M. M. *Adv. Chem. Ser.* **1997**, *253*, 99-134.

3) Sheldon, R. A.; Kochi, J. K. *Metal-Catalyzed Oxidations of Organic Compounds*; Academic Press: New York, 1981.

4) Abrams, M. J.; Davison, A.; Jones, A. G. *Inorg. Chim. Acta* **1984**, *82*, 125.

5) Begnan, I. A.; Behm, J.; Cook, M. R.; Herrmann, W. A. *Inorg. Chem.* **1991**, *30*, 2165.

6) Conry, R. R.; Mayer, J. M. *Inorg. Chem.* **1990**, *29*, 4862-4867.

7) Schultz, B. E.; Gheller, S. F.; Muetterties, M. C.; Scott, M. J.; Holm, R. H. *J. Am. Chem. Soc.* **1993**, *115*, 2714.

8) Moyer, B. A.; Sipe, B. K.; Meyer, T. J. *Inorg. Chem.* **1981**, *20*, 1475.

9) Abu-Omar, M. M.; Appleman, E. H.; Espenson, J. H. *Inorg. Chem.* **1996**, *35*, 7751-7757.

10) Abu-Omar, M. M.; Espenson, J. H. *Inorg. Chem.* **1995**, *34*, 6239-6240.

11) Takacs, J.; Cook, M. R.; Kiprof, P.; Kuchler, J. G.; Herrmann, W. A. *Organometallics* **1991**, *10*, 316.

12) Goodman, J. T.; Rauchfuss, T. B. *Inorg. Chem.* **1998**, *37*, 5040-5041.

13) Klingsberg, E.; Schreiber, A. M. *J. Am. Chem. Soc.* **1962**, *84*, 2941-2944.

14) Hortmann, A. G.; Aron, A. J.; Bhattacharya, A. K. *J. Org. Chem.* **1978**, *43*, 3374-3378.

15) Spectroscopic data for the dinuclear compound D are as follows: ^{1}H NMR δ 7.52 (d, 2H, J = 8Hz), 7.03 (m, 2H), 6.91(m, 4H), 4.05 (d, 2H, J = 10.8 Hz), 3.53 (d, 2H, J = 10.8 Hz), and 2.91 (s, 6H) ppm. ^{13}C NMR: δ 141.94, 135.81, 130.62, 130.56, 130.18, 127.87, 36.91, 17.10 ppm. Elemental analysis: Calcd: C 25.85, H 2.44, S 17.27; Found: C 26.68, H 2.53, S 17.33.

16) X-ray crystal data for $C_{16}H_{18}O_2Re_2S_4 \cdot C_7H_8$: monoclinic, $P2_1/c$, a = 14.6264(8) Å, b = 18.7219(10) Å, c = 9.3664(5) Å, β = 93.393(1)°, V = 2560.3(2) Å^3, Z = 4, T = 163(2) K, D_{calcd} = 2.166 Mg/m^3, R(F) = 1.98% for 4407 independently observed (I $\geq$ 2σ (I)) reflections (4 $\leq$ 2θ $\leq$ 53°).

17) All atoms other than hydrogen were refined with anisotropic displacement coefficients. All hydrogen atoms were included in the structure factor calculation at idealized positions and were allowed to ride on the neighboring atoms with relative isotropic displacement coefficients. The software and sources of the scattering factors are contained in the SHELXTL (version 5.1) program library (G. Sheldrick, Bruker Analytical X-Ray Systems, Madison, WI). Absorption corrections were carried out by programs SADABS (Blessing, R. H. *Acta Cryst.* **1995**, *A51*, 33-38), for D) and DIFABS (Walker, N.; Stuart, D. *Acta Cryst.* **1983**, *A39*, 158, for M-L).

18) Tisato, F.; Bolzati, C.; Duatti, A.; Bandoli, G.; Refosco, F. *Inorg. Chem.* **1993**, *32*, 2042-2048.

19) Tanner, L. D.; Haltiwanger, R. C.; DuBois, M. R. *Inorg. Chem.* **1988**, *27*, 1741-1746.

20) ^{1}H NMR δ 7.84 (d, 1H, J = 7.6 Hz), 7.67 (m, 6H), 7.11(t, 1H, J = 7.6 Hz), 7.04 (d, 1H, J=7.6 Hz), 6.90 (m, 10H), 4.80 (d, 1H, J=10.6 Hz), 3.25 (d, 1H, J = 10.6 Hz), 2.97(d, 3H, J = 8.4 Hz) ppm. ^{13}C NMR δ142.66, 140.37, 137.84 (d, J = 9.2 Hz), 134.62 (d, J = 7.7Hz), 133.99 (d, J = 14.7Hz), 131.14 (d, J = 1.7Hz), 130.98, 130.47, 129.29, 126.29, 42.54 (d, J = 7.1Hz,) 15.45 (d, J = 3Hz) ppm. ^{31}P NMR δ 27.82 ppm. Elemental analysis: Calcd: C 49.25 H 3.82 S 10.12; Found: C 49.25, H 3.60, S 9.78.

21) X-ray crystal data for $C_{26}H_{24}O_2PReS_2$: triclinic, $P\bar{1}$, a = 11.7741(5) Å, b = 13.9288(6) Å, c = 14.7608(7) Å, α = 83.860(1)°, β= 84.093(1)°, γ = 81.878(1)°, V = 2373.23(18) Å^3, Z = 4, T = 163(2) K, D_{calcd} = 1.774 Mg/m^3, R(F) = 5.01% for 7178 independent observed (I ≥ 2σ(I)) reflections (4 ≤ 2θ ≤ 56°).

22) Zhu, Z.; Espenson, J. H. *J. Mol. Catal.* **1995**, *103*, 87.

23) Arterburn, J. B.; Perry, M. C.; Nelson, S. L.; Dible, B. R.; Holguin, M. S. *J. Am. Chem. Soc.*, **1997**, *119*, 9309.

24) Abu-Omar, M. M.; Khan, S. I. *Inorg. Chem.* **1998**, *37*, 4979.

25) In the case of Me_3NO, the reaction proceeds with decomposition of the product, MTO. Although free MTO has δ 1.20 ppm in C_6D_6, in all these cases the MTO formed in the reaction showed a chemical shift $1.50 \leq δ \leq 1.70$ ppm due to the coordination of X formed in the reaction. See also: Wang, W-D, Espenson, J. H. *J. Am. Chem. Soc.*, **1998**, *120*, 11335.

26) Wallace, T. J. *J. Org. Chem.* **1966**, *31*, 1217-1221.

SUPPORTING INFORMATION

General Considerations

Spectroscopic procedures:

The ^{1}H, ^{13}C and ^{31}P NMR spectra were recorded on either a Varian VXR-300 or Bruker DRX-400 spectrometers. C_6D_6 was used as the reference in ^{1}H and ^{13}C NMR experiments and 85% H_3PO_4 for ^{31}P NMR. All chemicals except the dithiol ligand was purchased from commercial sources.

Spectroscopic and analytical data for the ligand and the two complexes

2-mercaptomethylthiophenol(1):

a) Synthesis of 4,5-Benzo-1,2-dithiole-3-thione

Twenty grams of 2,2'-dithiobenzoic acid (0.065 mol) and 20 gms of phosphorous pentasulfide were refluxed for 45 minutes in 150 mL of pyridine, cooled and diluted with water. Filtration and subsequent washing with cold alcohol gave an 80-90% yield of orange product. Recrystallization from cyclohexane gave short orange needle like crystals. m. p. 94°C

^{1}H NMR: δ 8.14-7.91 (m, 2H) 7.78-7.75 (m, 2H) ppm

^{13}C NMR: δ 219.13, 154.58, 142.07, 134.62, 129.13, 127.14, 26.22 ppm

b) Synthesis of 2-mercaptomethylthiophenol

A solution of 4,5-Benzo-1,2-dithiole-3-thione (15 gm, 0.08 mol) in 125mL of anhydrous Et_2O-THF (1:1) was added dropwise during one hour to a stirred solution of 6.7 gms of $LiAlH_4$ in 125 mL of ether under argon. The reaction

mixture was stirred for 16h at room temperature. Unreacted $LiAlH_4$ was decomposed by addition of 2-propanol (50 mL). The mixture was acidified with 150 mL of 10% H_2SO_4 solution, and the product was extracted into ether. After washing with brine, the combined extracts were dried over $MgSO_4$ and concentrated. The yellow 2-mercaptomethylthiophenol, isolated in 70% yield, was purified by distillation.

^{1}H NMR: δ 7.35 (m, 1H), 7.29 (m, 1H) 7.14 (m, 2H) 4.01 (s, 1H) 3.77 (d, 2H, J = 7.5 Hz) 2.14 (t, 1H, J = 7.5Hz) ppm.

^{13}C NMR: δ 140.95, 132.61, 131.85, 130.86, 129.25, 127.87, 28.70 ppm.

Synthesis of the dimer D:

3.2mmol (0.5mL) of 2-mercaptomethylthiophenol was added dropwise to 0.8mmol (200mg) MTO dissolved in 10mL of toluene at 0°C in an Erlenmeyer flask. After 15 min, 5mL of hexane was added and the reaction mixture kept in a freezer overnight. D forms fine needle like crystals which if filtered, washed with cold hexane and dried. Yield = 259mg (88%).

Spectroscopic data for D:

^{1}H NMR: δ 7.52 (d, 2H, J = 8Hz), 7.03 (m, 2H) 6.91 (m, 4H), 4.05 (d, 2H, J =10.8Hz) 3.53 (d, 2H, J = 10.8Hz), 2.91 (s, 6H) ppm.

^{13}C NMR: δ 141.94, 135.81, 130.62, 130.56, 130.18, 127.87, 36.91, 17.10 ppm

Elemental analysis: Calcd: C 25.85, H 2.44, S 17.27; Found: C 26.58, H 2.53, S 17.33.

The monomeric complex M-L:

Single cystals were grown by slow diffusion of hexane to a toluene solution of M-L.

^{1}H NMR: δ 7.84 (d, 1H, J = 7.6Hz), 7.67 (m, 6H), 7.11 (t, 1H, J = 7.6Hz) 7.04 (d, 1H, J = 7.6Hz), 6.90 (m, 10H), 4.80 (d, 1H, J = 10.6Hz) 3.25 (d, 1H, J = 10.6Hz), 2.97 (d, 3H, J = 8.4Hz) ppm.

^{13}C NMR: δ142.66, 140.37, 137.84 (d, J = 9.2Hz) 134.62 (d, J = 7.7 Hz) 133.99 (d, J = 14.7Hz), 131.14 (d, J = 1.7Hz), 130.98, 130.47, 129.29, 126.29, 42.54 (d, J = 7.1Hz), 15.45 (d, J = 3Hz) ppm.

Elemental analysis: Calcd: C 49.25, H 3.82, S 10.12; Found: C 49.25, H 3.60, S 9.78.

3H-benzo-1,2-dithiole: ^{1}H NMR: δ 6.86 (m, 1H) 6.64 (m, 3H) 3.75 (s, 2H) ppm.

^{13}C NMR: δ 142.26, 139.53, 127.44, 125.21, 124.66, 122.74, 43.37 ppm.

Table S-1. Crystal data and structure refinement for dimer D

Empirical formula	$C_{23}H_{26}O_2Re_2S_4$
Formula weight	835.08
Temperature	163(2)K
Wavelength	0.71073 A°
Crystal system	Monoclinic
Space group	P21/c
Unit cell dimensions	$a = 14.6264$ (8) A° $\alpha = 90°$
	$b = 18.7219(10)$ A° $\beta = 93.393(1)°$
	$c = 9.3664(5)$ A° $\gamma = 90°$
Volume	2560.3 (2) A°^{3}
Z	4
Density (calculated)	2.166 Mg/m^3
Absorption coefficient	9.791 mm^{-1}
F(000)	1576
Crystal size	$0.46 \times 0.35 \times 0.10$ mm^3
Theta range for data collection	2.43 to 26.37°.
Index ranges	$-18 \leq h \leq 18, 0 \leq k \leq 23, 0 \leq l \leq 11$
Reflections collected	30405
Independent reflections	5226 [R(int) = 0.0522]
Completeness to theta = 26.37°	99.7%
Absorption correction	Empirical
Max. and min. transmission	0.4410 and 0.0935
Refinement method	Full-matrix least-squares on F^2
Data / restraints / parameters	5226 / 0 / 283
Goodness-of-fit on F2	1.016
Final R indices [I>2sigma(I)]	R1 = 0.0198, wR2 = 0.0423
R indices (all data)	R1 = 0.0277, wR2 = 0.0438
Largest diff. peak and hole	1.014 and –0.809 e.Å^{-3}

Table S–2. Atomic coordinates ($\times 10^4$) and equivalent isotropic displacement parameters ($\text{Å}^2 \times 10^3$) for **D**. U(eq) is defined as one third of the trace of the orthogonalized U^{ij} tensor.

	x	y	z	U(Eq)
Re(1)	5817(1)	-981(1)	-1155(1)	24(1)
Re(2)	4697(1)	-2604(1)	188(1)	22(1)
S(1)	4441(1)	-1366(1)	-145(1)	22(1)
S(2)	3234(1)	-2852(1)	-670(1)	32(1)
S(3)	6167(1)	-2122(1)	-191(1)	24(1)
S(4)	6819(1)	-1156(1)	-2924(1)	33(1)
O(1)	6234(2)	-318(1)	-118(3)	35(1)
O(2)	4792(2)	-2874(1)	1900(3)	29(1)
C(1)	5028(3)	-449(2)	-2810(4)	31(1)
C(2)	5000(3)	-3505(2)	-1064(4)	30(1)
C(3)	3344(3)	-1211(2)	-1165(4)	27(1)
C(4)	2600(3)	-1459(2)	-266(4)	31(1)
C(5)	2511(3)	-2189(2)	29(4)	32(1)
C(6)	1830(3)	-2407(3)	926(5)	42(1)
C(7)	1265(3)	-1909(3)	1509(5)	53(1)
C(8)	1368(3)	-1198(3)	1228(5)	54(1)
C(9)	2034(3)	-972(2)	359(5)	40(1)
C(10)	6907(3)	-2647(2)	-1309(4)	28(1)
C(11)	7787(3)	-2264(2)	-1480(4)	34(1)
C(12)	7812(3)	-1615(2)	-2212(4)	35(1)
C(13)	8659(3)	-1296(3)	-2404(5)	48(1)
C(14)	9464(4)	-1611(3)	-1860(6)	63(2)
C(15)	9434(4)	-2234(3)	-1113(5)	58(1)
C(16)	8609(3)	-2562(3)	-913(5)	44(1)
C(17)	8509(6)	-932(3)	1479(6)	99(3)
C(18)	8388(5)	-439(3)	2634(6)	62(2)
C(19)	7547(4)	-381(3)	3219(6)	60(2)
C(20)	7440(5)	101(4)	4339(7)	84(2)
C(21)	8151(6)	503(4)	4883(7)	88(2)
C(22)	8962(5)	444(4)	4282(8)	93(2)
C(23)	9092(4)	-22(3)	3172(7)	73(2)

Table S–3. Bond lengths [Å] and angles [°] for D.

Re(1)-O(1)	1.670(2)
Re(1)-C(1)	2.126(4)
Re(1)-S(4)	2.2992(11)
Re(1)-S(3)	2.3624(9)
Re(1)-S(1)	2.3859(10)
Re(2)-O(2)	1.679(2)
Re(2)-C(2)	2.117(4)
Re(2)-S(2)	2.2883(11)
Re(2)-S(1)	2.3650(9)
Re(2)-S(3)	2.3782(10)
S(1)-C(3)	1.841(4)
S(2)-C(5)	1.781(4)
S(3)-C(10)	1.836(4)
S(4)-C(12)	1.783(5)
C(3)-C(4)	1.489(6)
C(4)-C(9)	1.384(6)
C(4)-C(5)	1.402(5)
C(5)-C(6)	1.400(6)
C(6)-C(7)	1.380(7)
C(7)-C(8)	1.367(7)
C(8)-C(9)	1.373(6)
C(10)-C(11)	1.490(6)
C(11)-C(12)	1.396(6)
C(11)-C(16)	1.401(6)
C(12)-C(13)	1.396(6)
C(13)-C(14)	1.388(7)
C(14)-C(15)	1.362(7)
C(15)-C(16)	1.376(7)
C(17)-C(18)	1.441(7)
C(18)-C(23)	1.365(8)
C(18)-C(19)	1.381(8)
C(19)-C(20)	1.400(8)
C(20)-C(21)	1.358(9)
C(21)-C(22)	1.347(10)
C(22)-C(23)	1.380(8)

Table S-3 continued.

O(1)-Re(1)-C(1)	103.80(14)
O(1)-Re(1)-S(4)	107.41(10)
C(1)-Re(1)-S(4)	83.29(11)
O(1)-Re(1)-S(3)	112.75(10)
C(1)-Re(1)-S(3)	143.02(11)
S(4)-Re(1)-S(3)	90.83(3)
O(1)-Re(1)-S(1)	106.31(10)
C(1)-Re(1)-S(1)	89.76(12)
S(4)-Re(1)-S(1)	146.26(3)
S(3)-Re(1)-S(1)	75.18(3)
O(2)-Re(2)-C(2)	106.28(13)
O(2)-Re(2)-S(2)	107.27(10)
C(2)-Re(2)-S(2)	82.28(12)
O(2)-Re(2)-S(1)	115.14(9)
C(2)-Re(2)-S(1)	138.13(10)
S(2)-Re(2)-S(1)	90.89(3)
O(2)-Re(2)-S(3)	103.43(10)
C(2)-Re(2)-S(3)	89.93(12)
S(2)-Re(2)-S(3)	149.29(3)
S(1)-Re(2)-S(3)	75.28(3)
C(3)-S(1)-Re(2)	110.44(12)
C(3)-S(1)-Re(1)	118.46(12)
Re(2)-S(1)-Re(1)	102.56(4)
C(5)-S(2)-Re(2)	107.00(13)
C(10)-S(3)-Re(1)	112.79(13)
C(10)-S(3)-Re(2)	116.78(13)
Re(1)-S(3)-Re(2)	102.88(4)
C(12)-S(4)-Re(1)	109.77(13)
C(4)-C(3)-S(1)	107.5(3)
C(9)-C(4)-C(5)	119.6(4)
C(9)-C(4)-C(3)	120.6(4)
C(5)-C(4)-C(3)	119.7(4)
C(6)-C(5)-C(4)	118.7(4)
C(6)-C(5)-S(2)	118.4(3)
C(4)-C(5)-S(2)	122.9(3)
C(7)-C(6)-C(5)	120.3(4)

Table S-3 continued

C(8)-C(7)-C(6)	120.4(5)
C(7)-C(8)-C(9)	120.3(5)
C(8)-C(9)-C(4)	120.8(4)
C(11)-C(10)-S(3)	110.2(3)
C(12)-C(11)-C(16)	119.0(4)
C(12)-C(11)-C(10)	121.3(4)
C(16)-C(11)-C(10)	119.6(4)
C(11)-C(12)-C(13)	119.0(4)
C(11)-C(12)-S(4)	124.0(3)
C(13)-C(12)-S(4)	117.0(4)
C(14)-C(13)-C(12)	120.8(5)
C(15)-C(14)-C(13)	120.0(5)
C(14)-C(15)-C(16)	120.5(5)
C(15)-C(16)-C(11)	120.7(5)
C(23)-C(18)-C(19)	118.6(6)
C(23)-C(18)-C(17)	121.4(7)
C(19)-C(18)-C(17)	120.0(6)
C(18)-C(19)-C(20)	119.3(6)
C(21)-C(20)-C(19)	121.5(7)
C(22)-C(21)-C(20)	118.1(7)
C(21)-C(22)-C(23)	122.0(7)
C(18)-C(23)-C(22)	120.4(6)

Symmetry transformations used to generate equivalent atoms:

Table S-4. Anisotropic displacement parameters ($A°2 \times 103$) for D. The anisotropic displacement factor exponent takes the form: $-2\pi^2[\ h^2\ a^{*2}U^{11} +$ .....$+2hka^*b^*U^{12}\ ]$

	U^{11}	U^{22}	U^{33}	U^{23}	U^{13}	U^{12}
Re(1)	30(1)	19(1)	23(1)	-2(1)	3(1)	-5(1)
Re(2)	28(1)	17(1)	21(1)	1(1)	0(1)	-1(1)
S(1)	28(1)	18(1)	21(1)	-1(1)	1(1)	-1(1)
S(2)	33(1)	25(1)	38(1)	-1(1)	-3(1)	-7(1)
S(3)	27(1)	24(1)	20(1)	-1(1)	1(1)	1(1)
S(4)	38(1)	34(1)	27(1)	2(1)	7(1)	-7(1)
O(1)	37(2)	28(2)	40(2)	-7(1)	2(1)	-9(1)
O(2)	37(2)	25(1)	24(1)	3(1)	3(1)	-1(1)
C(1)	42(3)	19(2)	33(2)	4(2)	6(2)	4(2)
C(2)	36(3)	22(2)	31(2)	-3(2)	-1(2)	3(2)
C(3)	33(2)	21(2)	26(2)	-1(2)	-3(2)	2(2)
C(4)	30(2)	34(2)	28(2)	-3(2)	-3(2)	1(2)
C(5)	26(2)	41(2)	27(2)	-2(2)	-7(2)	-3(2)
C(6)	32(3)	52(3)	42(3)	3(2)	-2(2)	-13(2)
C(7)	34(3)	82(4)	43(3)	0(3)	8(2)	-9(3)
C(8)	37(3)	73(4)	54(3)	-16(3)	6(2)	6(3)
C(9)	25(2)	47(3)	49(3)	-6(2)	0(2)	4(2)
C(10)	35(3)	27(2)	23(2)	-4(2)	3(2)	5(2)
C(11)	32(3)	47(3)	22(2)	-11(2)	2(2)	3(2)
C(12)	32(3)	45(3)	27(2)	-11(2)	5(2)	-7(2)
C(13)	39(3)	62(3)	46(3)	-9(2)	13(2)	-14(3)
C(14)	33(3)	99(5)	58(3)	-21(3)	9(3)	-12(3)
C(15)	36(3)	89(4)	48(3)	-18(3)	-2(2)	13(3)
C(16)	33(3)	63(3)	36(2)	-9(2)	2(2)	10(2)
C(17)	155(8)	71(4)	66(4)	-9(3)	-21(4)	34(4)
C(18)	82(5)	48(3)	54(3)	8(3)	-6(3)	13(3)
C(19)	46(4)	56(3)	79(4)	40(3)	10(3)	10(3)
C(20)	86(6)	95(5)	72(4)	53(4)	16(4)	33(4)
C(21)	118(7)	81(5)	63(4)	-5(3)	-10(4)	58(5)
C(22)	78(6)	81(5)	116(6)	-12(4)	-13(5)	19(4)
C(23)	51(4)	75(4)	91(5)	-17(4)	2(3)	-6(3)

Table S–5. Hydrogen coordinates ($\times 10^4$) and isotropic displacement parameters ($\text{Å}^2 \times 10^3$) for D.

	x	y	z	U(eq)
H(1A)	4688	-55	-2400	47
H(1B)	4595	-786	-3280	47
H(1C)	5435	-259	-3512	47
H(2A)	5492	-3783	-570	45
H(2B)	5198	-3347	-1994	45
H(2C)	4452	-3804	-1206	45
H(3A)	3269	-697	-1387	32
H(3B)	3326	-1480	-2076	32
H(6)	1758	-2899	1133	51
H(7)	801	-2062	2109	63
H(8)	976	-859	1636	65
H(9)	2108	-476	186	48
H(10A)	7032	-3119	-861	34
H(10B)	6592	-2727	-2260	34
H(13)	8683	-859	-2913	58
H(14)	10037	-1393	-2008	76
H(15)	9986	-2445	-728	69
H(16)	8596	-2994	-385	53
H(17A)	8889	-710	774	148
H(17B)	7910	-1056	1020	148
H(17C)	8810	-1367	1855	148
H(19)	7045	-666	2865	72
H(20)	6858	148	4727	101
H(21)	8078	817	5665	106
H(22)	9460	733	4635	111
H(23)	9675	-53	2779	87

Table S–6. Crystal data and structure refinement for the monomeric phosphine, M-L

Empirical formula	$C_{26} H_{24} O P Re S_2$
Formula weight	633.74
Temperature	163(2) K
Wavelength	0.71073 Å
Crystal system	Triclinic
Space group	P1$^-$
Unit cell dimensions	a = 11.7741(5) Å α =83.860(1)°
	b = 13.9288(6) Å β = 84.093(1)°
	c = 14.7608(7) Å γ = 81.878(1)°
Volume	2373.23(18) Å^3
Z	4
Density (calculated)	1.774 Mg/m3
Absorption coefficient	5.380 mm^{-1}
F(000)	1240
Crystal size	0.16 ×0.14× 0.10 mm^3
Theta range for data collection	1.39 to 28.28°
Index ranges	$-15 \le h \le 15, -18 \le k \le 18, 0 \le l \le 19$
Reflections collected	28807
Independent reflections	11505 [R(int) = 0.0847]
Completeness to theta = 28.28∞	97.7 %
Absorption correction	Empirical
Max. and min. transmission	1.000 / 0.535
Refinement method	Full-matrix least-squares on F^2
Data / restraints / parameters	11505 / 88 / 559
Goodness-of-fit on F^2	0.940
Final R indices [I>2σ(I)]	R1 = 0.0501, wR2 = 0.1085
R indices (all data)	R1 = 0.0951, wR2 = 0.1232
Largest diff. peak and hole	2.389 and −2.787 e.Å^{-3}

Table S–7. Atomic coordinates (× 10⁴) and equivalent isotropic displacement parameters ($\text{Å}^2 \times 10^3$) for **M–L**. U(eq) is defined as one third of the trace of the orthogonalized Uij tensor.

	x	y	z	U(eq)
Re(1)	2096(1)	2716(1)	235(1)	19(1)
S(1)	1411(2)	1808(1)	-734(1)	21(1)
S(2)	227(2)	3287(2)	795(1)	27(1)
P(1)	3666(2)	2774(1)	-988(1)	18(1)
O(1)	2793(5)	2101(4)	1097(4)	32(1)
C(1)	2169(8)	4238(6)	171(7)	41(2)
C(2)	-158(6)	1819(6)	-548(5)	23(2)
C(3)	-622(6)	1622(5)	421(5)	20(2)
C(4)	-1186(6)	805(6)	698(5)	23(2)
C(5)	-1694(7)	667(6)	1574(5)	30(2)
C(6)	-1663(7)	1337(6)	2201(5)	33(2)
C(7)	-1065(7)	2118(6)	1930(5)	28(2)
C(8)	-543(6)	2269(5)	1064(5)	22(2)
C(9)	4975(6)	3150(5)	-632(5)	21(2)
C(10)	5250(6)	2884(5)	253(5)	21(2)
C(11)	6298(7)	3061(6)	519(6)	31(2)
C(12)	7056(7)	3516(6)	-117(6)	27(2)
C(13)	6772(7)	3796(6)	-989(6)	31(2)
C(14)	5728(6)	3600(6)	-1257(5)	24(2)
C(15)	4231(6)	1637(5)	-1479(5)	20(2)
C(16)	4142(7)	750(6)	-967(6)	33(2)
C(17)	4651(8)	-102(6)	-1321(7)	48(3)
C(18)	5230(8)	-99(6)	-2178(7)	43(3)
C(19)	5342(8)	780(6)	-2680(6)	35(2)
C(20)	4868(7)	1643(6)	-2323(5)	26(2)
C(21)	3220(6)	3620(5)	-1950(5)	19(2)
C(22)	3357(7)	4614(5)	-2014(5)	26(2)
C(23)	2975(7)	5233(6)	-2760(6)	31(2)
C(24)	2485(7)	4880(6)	-3433(6)	29(2)
C(25)	2357(7)	3898(6)	-3376(6)	28(2)
C(26)	2700(6)	3275(5)	-2639(5)	21(2)

Table S-7 continued

Re(1A)	-2104(1)	2260(1)	4876(1)	17(1)
S(1A)	-3364(2)	3220(1)	5779(1)	21(1)
S(2A)	-3631(2)	1647(1)	4336(1)	23(1)
P(1A)	-826(2)	2275(1)	6080(1)	16(1)
O(1A)	-1369(5)	2846(4)	3987(3)	27(1)
C(1A)	-1531(8)	735(5)	5014(6)	31(2)
C(2A)	-4871(6)	3223(6)	5545(5)	25(2)
C(3A)	-5093(6)	3372(5)	4569(5)	21(2)
C(4A)	-5815(7)	4179(6)	4213(5)	27(2)
C(5A)	-6079(7)	4270(6)	3329(6)	34(2)
C(6A)	-5624(8)	3556(6)	2759(6)	36(2)
C(7A)	-4885(7)	2777(6)	3085(5)	28(2)
C(8A)	-4607(6)	2673(5)	3970(5)	21(2)
C(9A)	681(6)	1857(5)	5737(5)	21(2)
C(10A)	1118(7)	2035(6)	4833(5)	29(2)
C(11A)	2289(8)	1814(7)	4578(7)	41(2)
C(12A)	3027(7)	1415(6)	5233(7)	39(2)
C(13A)	2600(7)	1214(6)	6125(6)	32(2)
C(14A)	1428(7)	1464(6)	6384(5)	27(2)
C(15A)	-751(6)	3446(5)	6500(5)	22(2)
C(16A)	-961(7)	4297(5)	5931(5)	24(2)
C(17A)	-872(8)	5196(6)	6219(7)	37(2)
C(18A)	-554(7)	5242(6)	7086(6)	34(2)
C(19A)	-321(7)	4414(6)	7657(6)	35(2)
C(20A)	-400(7)	3511(5)	7359(5)	25(2)
C(21A)	-1257(6)	1474(5)	7074(5)	17(2)
C(22A)	-837(7)	480(5)	7173(5)	29(2)
C(23A)	-1269(7)	-126(6)	7905(6)	31(2)
C(24A)	-2114(7)	261(6)	8529(5)	30(2)
C(25A)	-2525(7)	1238(6)	8440(5)	25(2)
C(26A)	-2114(6)	1849(5)	7722(5)	20(2)

Table S–8. Bond lengths [Å] and angles [°] for M–L

Re(1)-O(1)	1.677(5)
Re(1)-C(1)	2.125(8)
Re(1)-S(1)	2.2830(18)
Re(1)-S(2)	2.329(2)
Re(1)-P(1)	2.452(2)
S(1)-C(2)	1.837(7)
S(2)-C(8)	1.778(7)
P(1)-C(21)	1.816(6)
P(1)-C(15)	1.823(7)
P(1)-C(9)	1.839(7)
C(2)-C(3)	1.488(9)
C(3)-C(8)	1.395(9)
C(3)-C(4)	1.401(9)
C(4)-C(5)	1.374(10)
C(5)-C(6)	1.389(10)
C(6)-C(7)	1.379(10)
C(7)-C(8)	1.369(9)
C(9)-C(14)	1.376(10)
C(9)-C(10)	1.378(9)
C(10)-C(11)	1.393(10)
C(11)-C(12)	1.393(11)
C(12)-C(13)	1.365(11)
C(13)-C(14)	1.400(10)
C(15)-C(16)	1.390(10)
C(15)-C(20)	1.386(10)
C(16)-C(17)	1.381(11)
C(17)-C(18)	1.373(12)
C(18)-C(19)	1.378(11)
C(19)-C(20)	1.385(10)
C(21)-C(26)	1.399(9)
C(21)-C(22)	1.409(9)
C(22)-C(23)	1.396(9)
C(23)-C(24)	1.366(11)
C(24)-C(25)	1.390(10)
C(25)-C(26)	1.373(9)

Table S-8 continued

Re(1A)-O(1A)	1.696(5)
Re(1A)-C(1A)	2.131(7)
Re(1A)-S(1A)	2.2754(19)
Re(1A)-S(2A)	2.340(2)
Re(1A)-P(1A)	2.4468(19)
S(1A)-C(2A)	1.841(7)
S(2A)-C(8A)	1.776(7)
P(1A)-C(21A)	1.820(7)
P(1A)-C(15A)	1.823(7)
P(1A)-C(9A)	1.824(7)
C(2A)-C(3A)	1.478(9)
C(3A)-C(4A)	1.400(9)
C(3A)-C(8A)	1.407(9)
C(4A)-C(5A)	1.362(10)
C(5A)-C(6A)	1.386(11)
C(6A)-C(7A)	1.369(10)
C(7A)-C(8A)	1.366(9)
C(9A)-C(10A)	1.390(10)
C(9A)-C(14A)	1.382(9)
C(10A)-C(11A)	1.391(10)
C(11A)-C(12A)	1.385(11)
C(12A)-C(13A)	1.374(12)
C(13A)-C(14A)	1.399(10)
C(15A)-C(16A)	1.385(9)
C(15A)-C(20A)	1.389(9)
C(16A)-C(17A)	1.386(10)
C(17A)-C(18A)	1.380(11)
C(18A)-C(19A)	1.366(11)
C(19A)-C(20A)	1.394(10)
C(21A)-C(22A)	1.400(9)
C(21A)-C(26A)	1.403(9)
C(22A)-C(23A)	1.397(10)
C(23A)-C(24A)	1.377(11)
C(24A)-C(25A)	1.375(10)
C(25A)-C(26A)	1.378(9)

Table S-8 continued

O(1)-Re(1)-C(1)	111.9(3)
O(1)-Re(1)-S(1)	116.6(2)
C(1)-Re(1)-S(1)	131.1(3)
O(1)-Re(1)-S(2)	108.9(2)
C(1)-Re(1)-S(2)	78.6(3)
S(1)-Re(1)-S(2)	90.97(7)
O(1)-Re(1)-P(1)	101.2(2)
C(1)-Re(1)-P(1)	83.3(3)
S(1)-Re(1)-P(1)	82.17(7)
S(2)-Re(1)-P(1)	148.96(7)
C(2)-S(1)-Re(1)	112.6(2)
C(8)-S(2)-Re(1)	107.9(3)
C(21)-P(1)-C(15)	105.2(3)
C(21)-P(1)-C(9)	107.2(3)
C(15)-P(1)-C(9)	101.9(3)
C(21)-P(1)-Re(1)	110.7(3)
C(15)-P(1)-Re(1)	117.2(3)
C(9)-P(1)-Re(1)	113.7(2)
C(3)-C(2)-S(1)	115.5(5)
C(8)-C(3)-C(4)	118.6(6)
C(8)-C(3)-C(2)	120.6(6)
C(4)-C(3)-C(2)	120.8(6)
C(5)-C(4)-C(3)	120.6(7)
C(4)-C(5)-C(6)	120.6(7)
C(7)-C(6)-C(5)	118.1(7)
C(8)-C(7)-C(6)	122.4(7)
C(7)-C(8)-C(3)	119.5(7)
C(7)-C(8)-S(2)	118.6(6)
C(3)-C(8)-S(2)	121.9(5)
C(14)-C(9)-C(10)	120.2(6)
C(14)-C(9)-P(1)	120.8(5)
C(10)-C(9)-P(1)	118.6(5)
C(9)-C(10)-C(11)	120.2(7)
C(12)-C(11)-C(10)	119.3(7)
C(13)-C(12)-C(11)	120.5(7)
C(12)-C(13)-C(14)	120.0(8)

Table S-8 continued

C(9)-C(14)-C(13)	119.8(7)
C(16)-C(15)-C(20)	118.7(7)
C(16)-C(15)-P(1)	120.2(6)
C(20)-C(15)-P(1)	120.7(6)
C(17)-C(16)-C(15)	119.6(8)
C(16)-C(17)-C(18)	121.7(8)
C(17)-C(18)-C(19)	118.9(8)
C(18)-C(19)-C(20)	120.1(8)
C(15)-C(20)-C(19)	120.9(8)
C(26)-C(21)-C(22)	119.0(6)
C(26)-C(21)-P(1)	118.8(5)
C(22)-C(21)-P(1)	122.2(5)
C(23)-C(22)-C(21)	119.6(7)
C(24)-C(23)-C(22)	120.5(7)
C(23)-C(24)-C(25)	120.0(7)
C(26)-C(25)-C(24)	120.8(7)
C(25)-C(26)-C(21)	120.0(7)

O(1A)-Re(1A)-C(1A)	112.1(3)
O(1A)-Re(1A)-S(1A)	116.14(19)
C(1A)-Re(1A)-S(1A)	131.5(2)
O(1A)-Re(1A)-S(2A)	109.06(19)
C(1A)-Re(1A)-S(2A)	78.8(2)
S(1A)-Re(1A)-S(2A)	90.60(7)
O(1A)-Re(1A)-P(1A)	100.13(18)
C(1A)-Re(1A)-P(1A)	83.0(2)
S(1A)-Re(1A)-P(1A)	83.49(7)
S(2A)-Re(1A)-P(1A)	149.72(7)
C(2A)-S(1A)-Re(1A)	112.5(3)
C(8A)-S(2A)-Re(1A)	106.4(3)
C(21A)-P(1A)-C(15A)	106.2(3)
C(21A)-P(1A)-C(9A)	107.0(3)
C(15A)-P(1A)-C(9A)	102.6(3)
C(21A)-P(1A)-Re(1A)	109.8(2)
C(15A)-P(1A)-Re(1A)	117.2(2)

Table S-8 continued

C(9A)-P(1A)-Re(1A)	113.4(2)
C(3A)-C(2A)-S(1A)	115.5(5)
C(4A)-C(3A)-C(8A)	117.7(7)
C(4A)-C(3A)-C(2A)	122.1(7)
C(8A)-C(3A)-C(2A)	120.2(6)
C(5A)-C(4A)-C(3A)	121.4(8)
C(4A)-C(5A)-C(6A)	119.9(7)
C(7A)-C(6A)-C(5A)	119.5(8)
C(6A)-C(7A)-C(8A)	121.5(7)
C(7A)-C(8A)-C(3A)	119.9(6)
C(7A)-C(8A)-S(2A)	118.7(6)
C(3A)-C(8A)-S(2A)	121.4(5)
C(10A)-C(9A)-C(14A)	119.1(7)
C(10A)-C(9A)-P(1A)	119.9(6)
C(14A)-C(9A)-P(1A)	120.6(6)
C(9A)-C(10A)-C(11A)	120.6(8)
C(12A)-C(11A)-C(10A)	119.7(8)
C(13A)-C(12A)-C(11A)	120.2(8)
C(12A)-C(13A)-C(14A)	120.0(8)
C(16A)-C(15A)-C(20A)	118.3(7)
C(16A)-C(15A)-P(1A)	119.8(6)
C(20A)-C(15A)-P(1A)	121.7(6)
C(17A)-C(16A)-C(15A)	121.2(7)
C(16A)-C(17A)-C(18A)	119.3(8)
C(19A)-C(18A)-C(17A)	120.8(8)
C(18A)-C(19A)-C(20A)	119.7(8)
C(15A)-C(20A)-C(19A)	120.7(7)
C(22A)-C(21A)-C(26A)	118.9(6)
C(22A)-C(21A)-P(1A)	122.3(6)
C(26A)-C(21A)-P(1A)	118.6(5)
C(23A)-C(22A)-C(21A)	120.4(8)
C(24A)-C(23A)-C(22A)	119.5(7)
C(25A)-C(24A)-C(23A)	120.4(7)
C(24A)-C(25A)-C(26A)	121.1(8)
C(25A)-C(26A)-C(21A)	119.7(7)

Table S–9. Anisotropic displacement parameters $(\approx \text{Å}^2 \times 10^3)$ for **M–L**. The anisotropic displacement factor exponent takes the form: $-2\pi^2[\ h^2\ a^{*2}U^{11}\ +...+\ 2\ h\ k\ a^*b^*U^{12}\ ]$

	U^{11}	U^{22}	U^{33}	U^{23}	U^{13}	U^{12}
Re(1)	25(1)	13(1)	22(1)	-9(1)	-3(1)	-6(1)
S(1)	27(1)	18(1)	22(1)	-12(1)	-2(1)	-9(1)
S(2)	31(1)	19(1)	34(1)	-17(1)	2(1)	-7(1)
P(1)	24(1)	12(1)	21(1)	-6(1)	-5(1)	-7(1)
O(1)	35(3)	34(4)	31(3)	-5(3)	-13(3)	-11(3)
C(1)	54(6)	22(5)	51(6)	-19(4)	14(5)	-18(4)
C(2)	24(4)	29(5)	21(4)	-13(3)	-5(3)	-13(3)
C(3)	21(4)	22(4)	22(4)	-11(3)	-2(3)	-7(3)
C(4)	26(4)	22(4)	25(4)	-6(3)	-8(3)	-7(3)
C(5)	36(5)	29(5)	25(4)	2(4)	-1(4)	-13(4)
C(6)	39(5)	38(6)	22(4)	-2(4)	1(4)	-6(4)
C(7)	31(5)	22(5)	32(5)	-14(4)	1(4)	-4(4)
C(8)	22(4)	24(4)	21(4)	-8(3)	-4(3)	-5(3)
C(9)	23(4)	11(4)	32(4)	-12(3)	-10(3)	-2(3)
C(10)	31(4)	12(4)	19(4)	-4(3)	-1(3)	-3(3)
C(11)	36(5)	25(5)	33(5)	-5(4)	-16(4)	2(4)
C(12)	26(5)	18(4)	39(5)	-11(4)	-12(4)	-2(4)
C(13)	33(5)	16(4)	50(6)	-17(4)	-5(4)	-9(4)
C(14)	24(4)	22(4)	30(4)	-8(3)	-6(3)	-5(3)
C(15)	14(4)	22(4)	29(4)	-18(3)	-12(3)	4(3)
C(16)	29(5)	26(5)	45(5)	-2(4)	1(4)	-9(4)
C(17)	43(6)	13(5)	86(8)	1(5)	-3(6)	-3(4)
C(18)	29(5)	28(5)	79(8)	-41(5)	-14(5)	3(4)
C(19)	39(5)	34(6)	35(5)	-28(4)	-5(4)	9(4)
C(20)	29(4)	24(5)	28(4)	-9(3)	-10(3)	-1(4)
C(21)	28(4)	15(4)	16(4)	-2(3)	-4(3)	-5(3)
C(22)	33(5)	11(4)	35(5)	-4(3)	-3(4)	-7(3)
C(23)	38(5)	10(4)	47(5)	4(4)	-7(4)	-10(4)
C(24)	32(5)	27(5)	28(4)	3(4)	-4(4)	-2(4)
C(25)	20(4)	33(5)	34(5)	-7(4)	-10(3)	-7(4)
C(26)	28(4)	15(4)	22(4)	-5(3)	-4(3)	-10(3)

Table S-9 continued

Re(1A)	22(1)	10(1)	20(1)	-10(1)	-5(1)	0(1)
S(1A)	27(1)	16(1)	20(1)	-11(1)	-4(1)	3(1)
S(2A)	28(1)	15(1)	28(1)	-13(1)	-9(1)	-1(1)
P(1A)	22(1)	9(1)	20(1)	-7(1)	-4(1)	-1(1)
O(1A)	36(3)	27(3)	21(3)	-7(2)	-4(2)	-9(3)
C(1A)	50(6)	11(4)	34(5)	-14(3)	-9(4)	-2(4)
C(2A)	24(4)	24(5)	29(4)	-13(3)	-2(3)	0(3)
C(3A)	20(4)	23(4)	23(4)	-7(3)	-2(3)	-6(3)
C(4A)	29(4)	26(5)	27(4)	-2(3)	-1(3)	-1(4)
C(5A)	30(5)	32(5)	39(5)	-4(4)	-15(4)	5(4)
C(6A)	45(6)	39(6)	27(5)	-3(4)	-12(4)	-7(5)
C(7A)	35(5)	27(5)	26(4)	-15(3)	-6(4)	-6(4)
C(8A)	20(4)	15(4)	31(4)	-7(3)	-9(3)	-2(3)
C(9A)	26(4)	7(4)	32(4)	-12(3)	0(3)	-4(3)
C(10A)	35(5)	16(4)	35(5)	-4(4)	-1(4)	-3(4)
C(11A)	42(6)	29(5)	50(6)	-7(4)	13(5)	-9(4)
C(12A)	15(4)	24(5)	83(8)	-23(5)	2(5)	-9(4)
C(13A)	28(5)	27(5)	47(6)	-15(4)	-15(4)	-7(4)
C(14A)	31(5)	21(4)	31(4)	-16(3)	-10(4)	0(4)
C(15A)	17(4)	17(4)	35(4)	-12(3)	-4(3)	-4(3)
C(16A)	35(5)	10(4)	31(4)	-13(3)	-7(4)	-6(3)
C(17A)	43(6)	7(4)	63(6)	-5(4)	-5(5)	-5(4)
C(18A)	28(5)	26(5)	55(6)	-30(4)	-3(4)	-9(4)
C(19A)	36(5)	30(5)	40(5)	-21(4)	8(4)	-10(4)
C(20A)	35(5)	17(4)	26(4)	-12(3)	-5(4)	-10(4)
C(21A)	15(4)	14(4)	23(4)	-3(3)	-5(3)	-2(3)
C(22A)	37(5)	21(5)	29(4)	-6(3)	-4(4)	-3(4)
C(23A)	36(5)	14(4)	44(5)	4(4)	-18(4)	-7(4)
C(24A)	41(5)	27(5)	24(4)	7(4)	-12(4)	-15(4)
C(25A)	31(5)	24(5)	23(4)	-5(3)	-10(3)	-9(4)
C(26A)	21(4)	16(4)	23(4)	-5(3)	-1(3)	-2(3)

Table S–10. Hydrogen coordinates ($\times 10^4$) and isotropic displacement parameters ($\text{Å}^2 \times 10^3$) for M–L.

	x	y	z	U(eq)
H(1A)	1600	4522	613	62
H(1B)	2019	4533	-431	62
H(1C)	2920	4347	301	62
H(2A)	-524	2451	-785	27
H(2B)	-374	1336	-901	27
H(4A)	-1217	352	285	28
H(5A)	-2062	120	1750	36
H(6A)	-2034	1262	2786	40
H(7A)	-1016	2558	2351	33
H(10A)	4735	2586	675	25
H(11A)	6489	2876	1114	37
H(12B)	7760	3630	53	32
H(13B)	7273	4117	-1405	38
H(14A)	5543	3773	-1855	29
H(16B)	3742	730	-390	40
H(17A)	4599	-693	-971	58
H(18A)	5542	-681	-2415	51
H(19B)	5737	794	-3259	42
H(20B)	4979	2234	-2654	31
H(22A)	3700	4856	-1561	31
H(23B)	3056	5891	-2799	37
H(24A)	2237	5296	-3929	35
H(25A)	2036	3659	-3842	34
H(26A)	2585	2624	-2599	25
H(1AA)	-1893	421	4595	46
H(1AB)	-1731	472	5629	46
H(1AC)	-710	624	4881	46
H(2AA)	-5116	2607	5802	30
H(2AB)	-5345	3734	5862	30
H(4AA)	-6122	4664	4590	33
H(5AA)	-6564	4811	3107	40
H(6AA)	-5818	3605	2159	44

Table S-10 continued

H(7AA)	-4566	2307	2696	33
H(10B)	623	2303	4393	35
H(11B)	2575	1934	3972	49
H(12A)	3813	1282	5068	47
H(13A)	3091	913	6556	39
H(14B)	1150	1365	6995	32
H(16A)	-1166	4264	5344	29
H(17B)	-1025	5762	5833	45
H(18B)	-498	5844	7284	41
H(19A)	-112	4452	8241	41
H(20A)	-214	2946	7739	30
H(22B)	-267	222	6749	34
H(23A)	-989	-786	7970	37
H(24B)	-2409	-141	9015	36
H(25B)	-3090	1490	8871	30
H(26B)	-2403	2507	7668	24

CHAPTER III. SYNTHESIS AND STRUCTURAL CHARACTERIZATION OF NOVEL TERMINAL AND BRIDGING Re(V)SULFIDO COMPLEXES

Josemon Jacob, Ilia A. Guzei and James H. Espenson*

Abstract

New reactions of the dimeric rhenium(V) chelate, $[CH_3Re(O)(S_2L)]_2$ (D), where S_2L is a dithiolate chelate have been investigated. Treatment of D with PPh_3 and pyridine caused its monomerization, resulting in the green compounds $[CH_3Re(O)(S_2L)-L]$, L = PPh_3 or pyridine. The Re=O bond on the phosphine compound was converted to a Re=S bond by reaction with P_4S_{10}. The coordination sphere of rhenium resembles a distorted trigonal bipyramid, with apical S and P atoms. Treatment of D first with pyridine and then with P_4S_{10} gives rise to a new dinuclear compound, which was also characterized crystallographically. It has one terminal rhenium-oxo group and one asymmetric μ-S group bridging the two rhenium atoms at distances of 232.8 and 238.3 pm. The rhenium-rhenium distance is short, 277.7 pm, consistent with a bond order of two.

Introduction

Transition metal sulfur complexes are widely exploited in biology and industry.[1,2] Metal assisted cleavage of C-S bonds has been of particular interest since this process is believed to be involved in the catalytic hydrodesulfurization of fossil fuels. As part of our ongoing studies on catalytic sulfur atom transfer reactions, we had reported recently the synthesis of novel Re(V) complexes containing a bisthiolato ligand (complexes D and M-L in eqn 1).[3] We then

became interested in synthesizing the sulfur analogues of these complexes (Re=S in place of Re=O) since they form key catalytic intermediates. Many anionic terminal Re(V)sulfido complexes are known and some of them tend to oligomerize under suitable conditions.[4-6] Although H_2S has mostly been used in literature to effect metal-oxo to sulfido conversion,[2,7] the use of CS_2 has also been reported.[8] These reagents proved ineffective in our studies but the use of P_4S_{10} gave very promising results. Here, we report the synthesis of the first example of a neutral terminal Re(V)sulfido complex and a mixed oxo(sulfido)dimeric Re(V) complex (complexes M-L' and D').

Results and Discussion

When the green mononuclear complex, M-L (256mg, 0.4mmol) is treated with P_4S_{10} (143mg, 0.32mmol) in toluene at 25°C, a fast reaction follows with the color of the solution changing to red. The newly formed product, M-L' isolated

$$\text{D} \qquad \xrightarrow{2\ Ph_3P} \qquad 2 \quad \text{M-L} \tag{1}$$

$$\text{M-L} \qquad \xrightarrow[\text{Toluene, 25°C}]{P_4S_{10}} \qquad \text{M-L'} \tag{2}$$
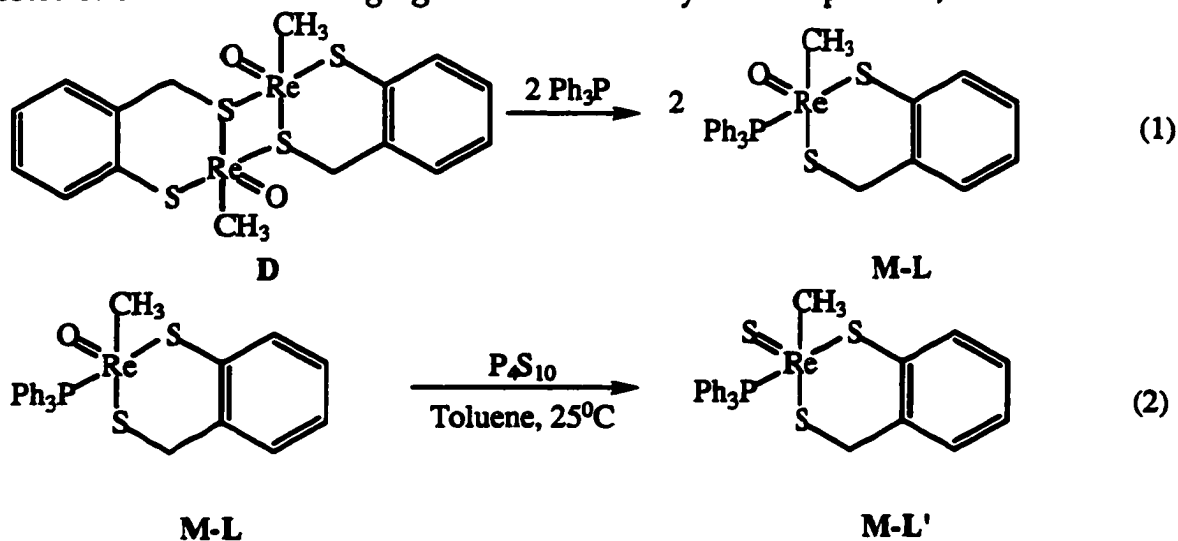
in 56% yield (column chromatography with 5%EtOAc in hexane as eluent), was characterized by X-ray crystallography, NMR and by elemental analysis.[9] An ORTEP of M-L' is shown in **Figure 1**.[10] Monomeric complex M-L' exhibits distorted trigonal bipyramidal geometry around the rhenium atom. Atoms C(1),

S(1), and S(2) define the equatorial plane while atoms S(3) and P occupy the apical positions. Angle S(3)-Re-P spans 156.78(3)° and differs significantly from the straight angle. As a result of the trans location of atoms P and S(3) the Re-S(3) distance (2.3135(10) Å) is somewhat longer than the Re-S(2) bond (2.2609(9) Å), however both bond lengths are well within the typical rhenium-sulfur distance range. The double rhenium-sulfur bond to the sulfide ligand is significantly shorter (2.0975(10) Å) and is consistent with similar Re=S distances found in anionic Re(V) complexes.[11] The rhenium-phosphorous and rhenium-carbon distances are in good agreement with corresponding bonds in similar compounds.

Numerous attempts to extend the same approach to synthesize a sulfur analogue directly from D using P_4S_{10} always lead to an insoluble material. We then adopted a different strategy towards the synthesis of a sulfur analogue of D (eqn 3). Our approach was to convert the dimer to the monomeric pyridine complex first and then treat this with P_4S_{10} to exchange the Re=O by sulfur. Finally, the bound pyridine can be removed from the complex by acidification to generate a sulfur analogue of D. When the yellow dimeric complex, D is treated with 2.2 equivalents of pyridine in toluene at 25°C, the green mononuclear pyridine complex is formed in a slow reaction. Further treatment of this
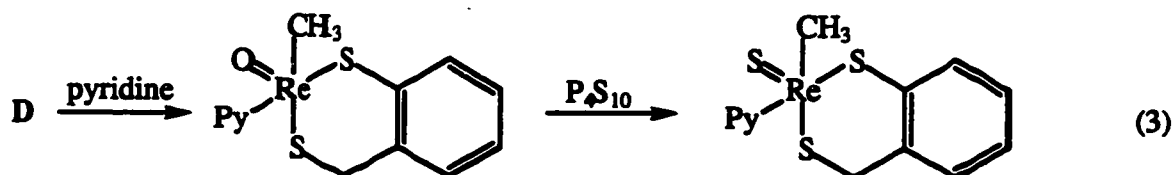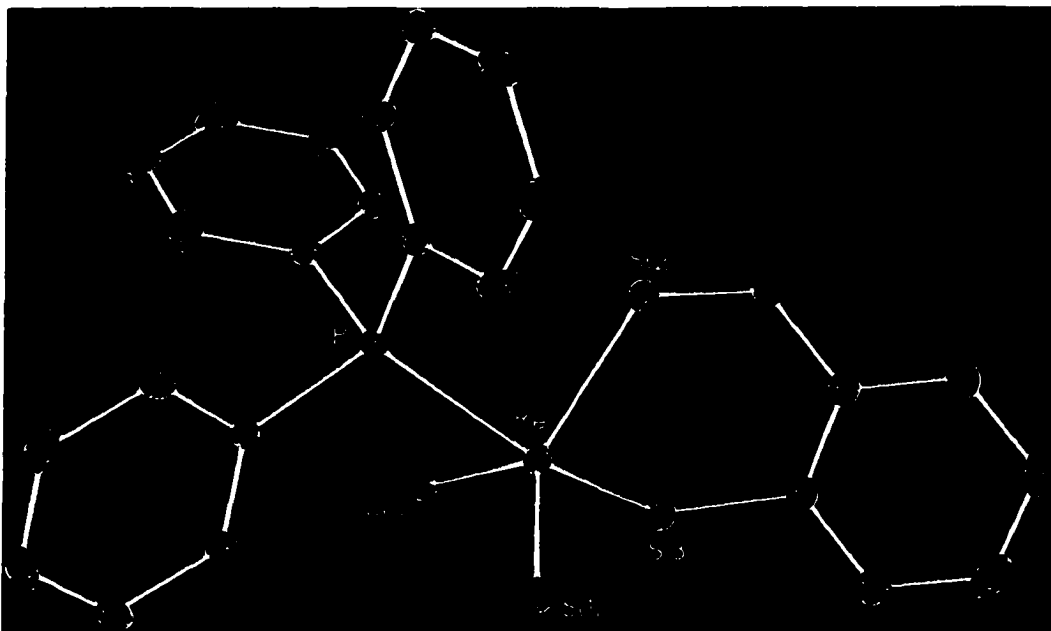

(3)

Figure 1. Perspective view of **M-L'** with thermal ellipsoids at the 30% probability level. Selected bond lengths(A°) and bond angles(°): Re-S(1) = 2.098(2); Re-S(2) = 2.261(2); Re-S(3) = 2.314(2); Re-P = 2.445(2); S(3)-Re-P = 156.8(1); S(3)-Re-S(1) = 107.4(1); S(3)-Re-C(1) = 79.5(2); S(3)-Re-S(2) = 90.9(1).

solution with P_4S_{10} results in the formation of a red complex which was isolated by column chromatography. NMR analysis of the isolated product suggested an asymmetric dimeric complex in which a pyridine is bound to one of the rhenium centers. We were able to grow single crystals of this complex which on X-ray structural analysis was found to be a mixed oxo(sulfido)dimeric Re(V) complex, D' devoid of any bound pyridine. The structure is shown in figure 2.[12]

The molecular structure drawing of D' is presented in **Figure 2.** The dimeric structure is held together by a bridging sulfide ligand, bridging sulfur atom of one bidentate ligand, and by a rhenium-rhenium bond. Each rhenium atom is therefore six-coordinate. An octahedral consideration of rhenium environments is inadequate for the rhenium-rhenium bond is not directed to one of the ideal octahedral apexes. If the rhenium-rhenium bond is ignored, the environment about atom Re(1) is best described as severely distorted square planar while the geometry about atom Re(2) is best represented as severely distorted trigonal bipyramidal. In the case of Re(1) atoms S(1), S(2), S(5), and C(1) form the basal plane with the least squares a 0.15 Å deviation from planarity and the Re(1)-O vector forms a 88.4° angle to this plane. The trigonal bipyramidal approach would put atoms S(1), C(1), and O in the equatorial plane and atoms S(2) and S(5) in the apical positions. The S(2)-Re(1)-S(5) angle measuring 134.16(5)° clearly cannot be attributed to this geometry. The Re(1)-S(1) distance (2.3828(11) Å) is slightly longer than the Re(1)-S(2) bond (2.3288(11) Å) due to the coordination of atom S(1) to the second rhenium atom. The Re(1)-S(5) separation (2.3072(13) Å) is unexpectedly shorter than the other rhenium(1)-sulfur distances and falls in the usual range of single rhenium-sulfur bonds. In the case of atom Re(2) the geometry is best characterized as trigonal bipyramidal with atoms S(3), S(5), and C(2) forming the equatorial plane and atoms S(1) and S(4) located at the

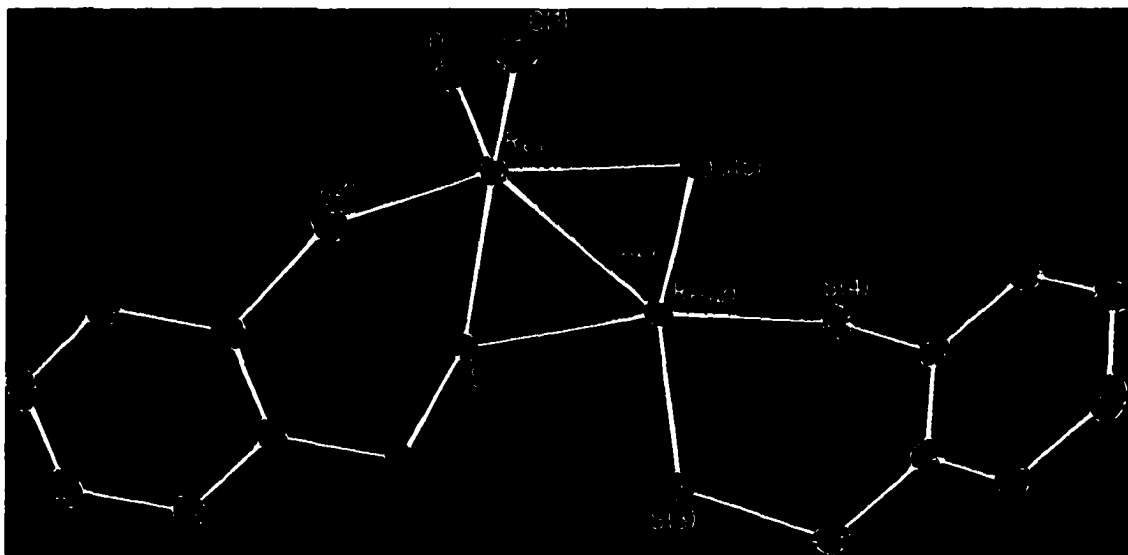**Figure 2.** Perspective view of **D'** with thermal ellipsoids at the 30% probability level. Selected bond lenths(A°) and bond angles(°): Re(1)-S(5) = 2.307(1); Re(1)-S(1) = 2.383(1); Re(1)-O = 1.675(3); Re(1)-Re(2) = 2.777(1); Re(2)-S(5) = 2.190(1); Re(2)-S(1) = 2.328(2); S(2)-Re(1)-S(5) = 134.2(1); S(4)-Re(2)-S(1) = 156.7(1); S(4)-Re(2)-S(5) = 94.0(1); S(4)-Re(2)-S(3) = 91.1(1); S(4)-Re(2)-C(2) = 81.5(2)

apexes. The geometry is distorted as illustrated by the S(1)-Re(2)-S(4) angle value of 156.71(4)° which is far from being linear. An alternative discussion of the Re(2) environment as square pyramidal would place atoms S(1), S(3), S(4), and C(2) in the basal plane with the least square deviation from planarity of 0.26 Å and atom S(5) in the apex. The Re(2)-S(5) vector comprises a 82.8° angle with the basal plane. The latter two numbers significantly deviate from the ideal values of 0 and 90°. The Re(2)-S(4) bond length (2.3118(12) Å) is somewhat longer than the Re(2)-S(3) distance of 2.2502(11) Å due to the *trans* positions of atoms S(4) and S(1). The Re(2)-S(5) bond measured 2.1901(10) Å which is indicative of the multiple character of the bond. The rhenium-rhenium bond was found to be 2.7773(3) Å, a value on the shorter end for reported single bonds and on the longer end for reported double bonds.[13-16]

The formation of **D'** is probably best explained as follows: unlike the phosphine terminal sulfido complex, **M-L'** which is stable by itself, the analogous pyridine complex is not stable and hence likely to dimerize under the reaction conditions. High oxidation state transition metal sulfidocomplexes are known to dimerize or oligomerize and has been well documented in literature. Hence it is likely that the pyridine bound terminal sulfidocomplex reacts with another pyridine oxo complex.to generate a dimeric complex. This complex can slowly

D'
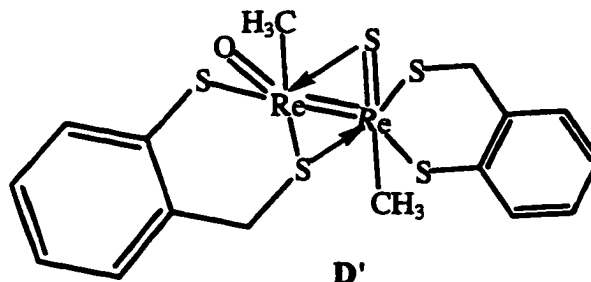
lose pyridine to form D' which slowly crystallizes out. Since the bridging sulfur is closer to Re(2) than Re(1) by 0.12A° and the Re-Re distance of 2.7773(3)Å, the structure of D' is probably best depicted as shown above.

Conclusions

In summary, we have reported here the synthesis and characterization of the first example of a neutral terminal Re(V)sulfido complex. Also we have shown that in suitable cases P_4S_{10} can be successfully used to effect metal-oxo to sulfido conversion. We are currently studying the extension of this approach to other Re=S complexes and further studying the reactivity of these complexes.

References

1) Stiefel, E. I.; Matsumoto, K. *Transition Metal Sulfur Chemistry: Biological and Industrial Significance*, ACS Symposium Series 653, **1996**, Washington D.C.

2) Weisser, O.; Landa, S. *Sulphide Catalysts, Their Properties and Applications*, Pergamon press, New York, **1973**.

3) Jacob, J.; Guzei, I. A.; Espenson, J. H. *Inorg. Chem.*, **1999**, *38*, 1040.

4) Goodman, J. T.; Rauchfuss, T. B. *Inorg. Chem.*, **1998**, *37*, 5040.

5) Goodman, J. T.; Rauchfuss, T. B. *Angew. Chem. Int. Ed. Engl.* **1997**, *36*, 2083.

6) Cotton, F. A.; Kibala, P. A.; Matusz, M. *Polyhedron*, **1988**, *7*, 83.

7) Broadbent, H. S.; Slaugh, L. H.; Jarvis, N. L. *J. Am. Chem. Soc.*, **1954**, *76*, 1519.

8) Herrmann, W. A.; Jung, K. A.; Herdtweek, E. *Chem. Ber.*, **1989**, *122*, 2041.

9) Spectroscopic data for M-L' are as follows: ^{1}H NMR: δ 7.73-7.41 (m, 15H) 7.29 (t, 1H, J = 7.6Hz) 7.25 (m, 2H) 7.15 (t,1H, J = 7.6Hz) 4.98 (d, 1H, J = 11.6Hz) 3.75(d, 3H, J =

8.4Hz) 2.63 (d, 1H, J = 11.6Hz) ppm. ^{13}C NMR: δ 146.74, 138.91, 134.58, 132.34, 131.61, 131.09, 128.83, 128.66, 128.41, 126.45, 49.66, 16.06 ppm. ^{31}P NMR: δ 23.42ppm

10) X-ray crystal data for $C_{29}H_{27}PReS_3.1/2C_6H_6$ (M-L'): monoclinic, $P21/n$, a = 9.2936(5) Å, b = 22.2088(12) Å, c = 13.0576(7) Å, β = 91.237(1)°, V = 2694.5(3) Å^3, Z = 4, T = 173(2) K, Dcacld = 1.698 Mg/m^3, $R(F)$ = 2.46% for 4280 independent observed ($I = 2\sigma(I)$) reflections (4=2=53°). X-ray crystal data for $C_{16}H_{18}ORe_2S_5$ (D'): monoclinic, $P21/c$, a = 11.2214(6) Å, b = 12.8234(7) Å, c = 13.7784(8) Å, β = 90.423(1)°, V = 1982.61(19) Å^3, Z = 4, T = 193(2) K, Dcacld = 2.543 Mg/m^3, $R(F)$ = 2.03% for 3334 independent observed ($I = 2\sigma(I)$) reflections (4=2=52°). All non-hydrogen atoms were refined with anisotropic displacement coefficients. All hydrogen atoms were included in the structure factor calculation at idealized positions and were allowed to ride on the neighboring atoms with relative isotropic displacement coefficients. In the case of M-L' the asymmetric unit also contains one half of a solvate benzene molecule. All software and sources of the scattering factors are contained in the SHELXTL (version 5.1) program library (G. Sheldrick, Bruker Analytical X-Ray Systems, Madison, WI).

11) Goodman, J. T.; Inomoto, S.; Rauchfuss, T. B. *J. Am. Chem. Soc.* **1996**, *118*, 11674.

12) ^1H NMR for D': δ 7.10 (m, 4H) 6.65 (m, 4H) 5.09 (d, 1H, J = 12.0Hz) 4.83 (d, 1H, J = 12.0Hz) 3.41 (s, 3H) 3.05 (d, 1H, J = 12.0Hz) 3.04 (d, 1H, J = 12.0Hz) 2.93(s, 3H) ppm.

13) Cotton, F. A.; Dunbar, K. R. *Inorg. Chem.* **1987**, *26*, 1305.

14) Cotton, F. A.; Davison, A.; Ilsley, W. H.; Trop, H. S. *Inorg. Chem.* **1979**, *18*, 2719.

15) Stiefel, E. I.; Wei, L.; Halbert, T. R.; Murray, H. H. *J. Am. Chem. Soc.* **1990**, *112*, 6431.

16) Ciani, G.; D'Alfonso, G.; Freni, M.; Romiti, P.; Sironi, A. *J. Organometallic. Chem.* **1977**, *136*, C49.

SUPPORTING INFORMATION

General Considerations

Spectroscopic procedures

The ^{1}H, ^{13}C and ^{31}P NMR spectra were recorded on either a Varian VXR-300 or Bruker DRX-400 spectrometers. C_6D_6 or $CDCl_3$ was used as the reference in the ^{1}H and ^{13}C NMR experiments and 85%H_3PO_4 for ^{31}P NMR. The ligand and the dimer were synthesized according to procedures reported earlier. All other chemicals were purchased from commercial sources.

Synthesis of the terminal sulfido complex, M-L':

150mg (0.2mmol) of dimer, D dissolved in 20mL of toluene is stirred with 121.8mg of Ph$_3$P (2.3 equiv.) at room temperature in an erlenmeyer flask. The formation of the monomeric phosphine complex is indicated by the color of the solution changing from yellow to green. After 8 hours, 143mg of P_4S_{10} is added and stirred for another 2 hours. The color of the solution changes to red in this period. The reaction mixture is concentrated at the pump to ~1mL and chromatographed on silica (5% EtOAc in hexane). Isolated yield = 147mg (56%). Single crystals were grown by slow diffusion of hexane into a benzene solution of M-L'.

Spectroscopic data for M-L':

^{1}H NMR: δ 7.73-7.41 (m, 15H) 7.29 (t, 1H, J = 7.6Hz) 7.25 (m, 2H) 7.15 (t,1H, J = 7.6Hz) 4.98 (d, 1H, J = 11.6Hz) 3.75(d, 3H, J = 8.4Hz) 2.63 (d, 1H, J = 11.6Hz) ppm.

^{13}C NMR: δ 146.74, 138.91, 134.58, 132.34, 131.61, 131.09, 128.83, 128.66, 128.41, 126.45, 49.66, 16.06 ppm.

^{31}P NMR: δ 23.42ppm

.

Synthesis of the dimeric complex, **D'**:

To 50mg of the complex, **D** (0.067mmol) in 10mL of toluene at 25°C, 12.0μL of pyridine is added and stirred for six hours. To this P4S10 (0.134mmol, 59mg) is added and the color of the solution slowly changes from green to red. After 30h, the reaction mixture is first filtered through silica and then concentrated at the pump to ~1mL. This is then chromatographed on silica (5-20% EtOAc in hexane as eluent) and the product so isolated is characterized by NMR. Single crystals of the product were grown by slow diffusion of hexane to a CH_2Cl_2 solution of **D'**.

Spectroscopic data for **D'**:

^{1}H NMR: δ 7.10 (m, 4H) 6.65 (m, 4H) 5.09 (d, 1H, J = 12.0Hz) 4.83 (d, 1H, J = 12.0Hz) 3.41 (s, 3H) 3.05 (d, 1H, J = 12.0Hz) 3.04 (d, 1H, J = 12.0Hz) 2.93(s, 3H) ppm.

Table 1. Crystal data and structure refinement for M-L'

Identification code	esp06
Empirical formula	C29H27PReS3
Formula weight	688.86
Temperature	173(2) K
Wavelength	0.71073 Å
Crystal system	Monoclinic
Space group	P21/n
Unit cell dimensions	a = 9.2936(5) Å α= 90°
	b = 22.2088(12) Å β= 91.237 (1)°
	c = 13.0576(7) Å γ = 90°
Volume	2694.5(3) Å^3
Z	4
Density (calculated)	1.698 Mg/m^3
Absorption coefficient	4.818 mm^{-1}
F(000)	1356
Crystal size	0.45 x 0.26 x 0.08 mm^3
Theta range for data collection	1.81 to 26.37°.
Index ranges	-11<=h<=11, 0<=k<=27, 0<=l<=16
Reflections collected	23674
Independent reflections	5496 [R(int) = 0.0406]
Completeness to theta = 26.37°	99.7 %
Absorption correction	Empirical with SADABS
Max. and min. transmission	0.6992 and 0.2204
Refinement method	Full-matrix least-squares on F^2
Data / restraints / parameters	5496 / 0 / 308
Goodness-of-fit on F^2	1.001
Final R indices [I>2sigma(I)]	R1 = 0.0246, wR2 = 0.0416
R indices (all data)	R1 = 0.0408, wR2 = 0.0436
Largest diff. peak and hole	0.958 and -0.612 e.Å^{-3}

Table 2. Atomic coordinates (x 10^4) and equivalent isotropic displacement parameters (Å^2x 10^3) for M-L'. U(eq) is defined as one third of the trace of the orthogonalized U^{ij} tensor.

	x	y	z	U(eq)
Re	4233(1)	6128(1)	7196(1)	22(1)
S(1)	5883(1)	6415(1)	6240(1)	32(1)
S(2)	2001(1)	6521(1)	6990(1)	27(1)
S(3)	3437(1)	5204(1)	6594(1)	31(1)
P	4517(1)	6958(1)	8416(1)	21(1)
C(1)	4914(4)	5554(2)	8442(3)	28(1)
C(2)	698(4)	5967(2)	6458(3)	31(1)
C(3)	1166(4)	5698(2)	5479(3)	26(1)
C(4)	388(4)	5790(2)	4563(3)	34(1)
C(5)	849(5)	5552(2)	3653(3)	40(1)
C(6)	2090(5)	5214(2)	3643(3)	46(1)
C(7)	2872(4)	5113(2)	4542(3)	36(1)
C(8)	2402(4)	5349(2)	5458(3)	28(1)
C(9)	6388(4)	7176(2)	8683(3)	22(1)
C(10)	7506(4)	6766(2)	8592(3)	29(1)
C(11)	8887(4)	6926(2)	8874(3)	35(1)
C(12)	9182(4)	7499(2)	9232(3)	37(1)
C(13)	8092(4)	7914(2)	9314(3)	33(1)
C(14)	6699(4)	7755(2)	9035(3)	28(1)
C(15)	3656(4)	7662(2)	8020(3)	21(1)
C(16)	3814(4)	7854(2)	7019(3)	30(1)
C(17)	3153(4)	8376(2)	6677(3)	35(1)
C(18)	2325(4)	8712(2)	7325(3)	35(1)
C(19)	2166(4)	8529(2)	8325(3)	32(1)
C(20)	2816(4)	8004(2)	8672(3)	26(1)
C(21)	3808(4)	6807(2)	9687(3)	23(1)
C(22)	4471(4)	7031(2)	10578(3)	41(1)
C(23)	3875(5)	6924(2)	11517(3)	50(1)
C(24)	2632(5)	6590(2)	11591(3)	45(1)

Table 2 continued

C(25)	1965(4)	6370(2)	10721(3)	38(1)
C(26)	2550(4)	6477(2)	9780(3)	30(1)
C(27)	9222(4)	4976(2)	10892(3)	35(1)
C(28)	8612(4)	5222(2)	10010(3)	38(1)
C(29)	9389(4)	5242(2)	9121(3)	36(1)

Table 3. Bond lengths [Å] and angles [°] for M-L'.

Re-S(1)	2.0975(10)
Re-C(1)	2.152(3)
Re-S(2)	2.2609(9)
Re-S(3)	2.3135(10)
Re-P	2.4451(9)
S(2)-C(2)	1.852(3)
S(3)-C(8)	1.780(4)
P-C(15)	1.827(3)
P-C(21)	1.830(3)
P-C(9)	1.831(3)
C(2)-C(3)	1.485(5)
C(3)-C(8)	1.385(5)
C(3)-C(4)	1.399(5)
C(4)-C(5)	1.376(5)
C(5)-C(6)	1.376(5)
C(6)-C(7)	1.385(5)
C(7)-C(8)	1.386(5)
C(9)-C(10)	1.388(5)
C(9)-C(14)	1.394(5)
C(10)-C(11)	1.374(5)
C(11)-C(12)	1.380(5)
C(12)-C(13)	1.376(5)
C(13)-C(14)	1.384(5)
C(15)-C(16)	1.387(5)
C(15)-C(20)	1.392(5)
C(16)-C(17)	1.381(5)
C(17)-C(18)	1.377(5)
C(18)-C(19)	1.379(5)
C(19)-C(20)	1.385(5)
C(21)-C(26)	1.387(5)
C(21)-C(22)	1.396(5)
C(22)-C(23)	1.377(5)
C(23)-C(24)	1.378(5)

Table 3 continued

C(24)-C(25)	1.372(5)
C(25)-C(26)	1.376(5)
C(27)-C(29)#1	1.379(5)
C(27)-C(28)	1.385(5)
C(28)-C(29)	1.381(5)
C(29)-C(27)#1	1.379(5)
S(1)-Re-C(1)	115.05(10)
S(1)-Re-S(2)	119.46(4)
C(1)-Re-S(2)	124.99(10)
S(1)-Re-S(3)	107.44(4)
C(1)-Re-S(3)	79.51(10)
S(2)-Re-S(3)	90.93(3)
S(1)-Re-P	95.06(4)
C(1)-Re-P	85.91(10)
S(2)-Re-P	82.69(3)
S(3)-Re-P	156.78(3)
C(2)-S(2)-Re	112.27(12)
C(8)-S(3)-Re	106.62(12)
C(15)-P-C(21)	104.38(16)
C(15)-P-C(9)	103.66(16)
C(21)-P-C(9)	103.56(16)
C(15)-P-Re	114.88(11)
C(21)-P-Re	114.63(12)
C(9)-P-Re	114.35(12)
C(3)-C(2)-S(2)	112.9(3)
C(8)-C(3)-C(4)	118.6(4)
C(8)-C(3)-C(2)	120.0(3)
C(4)-C(3)-C(2)	121.4(3)
C(5)-C(4)-C(3)	121.1(4)
C(4)-C(5)-C(6)	119.6(4)
C(5)-C(6)-C(7)	120.3(4)
C(6)-C(7)-C(8)	120.0(4)
C(3)-C(8)-C(7)	120.4(4)

Table 3 continued

C(3)-C(8)-S(3)	121.2(3)
C(7)-C(8)-S(3)	118.4(3)
C(10)-C(9)-C(14)	118.8(3)
C(10)-C(9)-P	121.3(3)
C(14)-C(9)-P	119.7(3)
C(11)-C(10)-C(9)	120.3(4)
C(10)-C(11)-C(12)	120.5(4)
C(13)-C(12)-C(11)	120.2(4)
C(12)-C(13)-C(14)	119.6(4)
C(13)-C(14)-C(9)	120.6(4)
C(16)-C(15)-C(20)	118.8(3)
C(16)-C(15)-P	118.4(3)
C(20)-C(15)-P	122.8(3)
C(17)-C(16)-C(15)	120.5(3)
C(18)-C(17)-C(16)	120.5(4)
C(17)-C(18)-C(19)	119.7(3)
C(18)-C(19)-C(20)	120.2(4)
C(19)-C(20)-C(15)	120.4(3)
C(26)-C(21)-C(22)	118.2(3)
C(26)-C(21)-P	119.8(3)
C(22)-C(21)-P	122.0(3)
C(23)-C(22)-C(21)	120.1(4)
C(22)-C(23)-C(24)	120.6(4)
C(25)-C(24)-C(23)	119.9(4)
C(24)-C(25)-C(26)	119.9(4)
C(25)-C(26)-C(21)	121.3(3)
C(29)#1-C(27)-C(28)	119.6(4)
C(29)-C(28)-C(27)	120.0(4)
C(27)#1-C(29)-C(28)	120.4(4)

Symmetry transformations used to generate equivalent atoms:
#1 -x+2,-y+1,-z+2

Table 4. Anisotropic displacement parameters $(\text{Å}^2 \times 10^3)$ for M-L'. The anisotropic displacement factor exponent takes the form: $-2\pi^2[\, h^2 a^{*2}U^{11} + ... + 2\, h\, k\, a^*\, b^*\, U^{12}\,]$

	U^{11}	U^{22}	U^{33}	U^{23}	U^{13}	U^{12}
Re	25(1)	20(1)	20(1)	-2(1)	-1(1)	2(1)
S(1)	33(1)	33(1)	29(1)	-2(1)	5(1)	-1(1)
S(2)	27(1)	28(1)	27(1)	-6(1)	-4(1)	3(1)
S(3)	37(1)	21(1)	34(1)	-2(1)	-6(1)	1(1)
P	20(1)	22(1)	19(1)	-2(1)	-1(1)	0(1)
C(1)	34(2)	28(2)	23(2)	1(2)	-3(2)	9(2)
C(2)	23(2)	35(3)	34(2)	-3(2)	-5(2)	-1(2)
C(3)	30(2)	20(2)	28(2)	-2(2)	-3(2)	-8(2)
C(4)	36(2)	25(2)	41(3)	2(2)	-11(2)	-4(2)
C(5)	53(3)	39(3)	27(2)	2(2)	-14(2)	-15(2)
C(6)	56(3)	50(3)	32(3)	-16(2)	6(2)	-12(2)
C(7)	36(2)	32(2)	40(3)	-13(2)	-2(2)	-5(2)
C(8)	34(2)	20(2)	30(2)	-2(2)	-2(2)	-5(2)
C(9)	19(2)	28(2)	18(2)	1(2)	0(2)	-2(2)
C(10)	24(2)	31(2)	31(2)	-4(2)	0(2)	-2(2)
C(11)	21(2)	44(3)	41(3)	0(2)	-1(2)	7(2)
C(12)	25(2)	55(3)	30(2)	5(2)	-5(2)	-15(2)
C(13)	36(3)	34(2)	28(2)	-5(2)	-1(2)	-12(2)
C(14)	24(2)	31(2)	28(2)	-2(2)	2(2)	-2(2)
C(15)	20(2)	19(2)	24(2)	-3(2)	-2(2)	-3(2)
C(16)	37(2)	24(2)	28(2)	-5(2)	4(2)	3(2)
C(17)	53(3)	27(2)	26(2)	2(2)	5(2)	1(2)
C(18)	35(2)	24(2)	45(3)	5(2)	-6(2)	5(2)
C(19)	29(2)	27(2)	39(2)	-6(2)	5(2)	5(2)
C(20)	24(2)	30(2)	25(2)	-1(2)	2(2)	-2(2)
C(21)	23(2)	24(2)	20(2)	0(2)	4(2)	6(2)
C(22)	35(3)	60(3)	27(2)	-1(2)	-1(2)	-13(2)
C(23)	52(3)	79(4)	20(2)	-4(2)	-3(2)	-12(3)
C(24)	55(3)	54(3)	25(2)	5(2)	13(2)	0(3)
C(25)	36(3)	42(3)	36(2)	-1(2)	13(2)	-10(2)

Table 4 continued

C(26)	30(2)	34(2)	25(2)	-7(2)	3(2)	-3(2)
C(27)	48(3)	33(2)	25(2)	0(2)	5(2)	-3(2)
C(28)	35(3)	37(3)	42(3)	-3(2)	-2(2)	4(2)
C(29)	44(3)	33(3)	29(2)	-1(2)	-7(2)	3(2)

Table 5. Hydrogen coordinates (x 10^4) and isotropic displacement parameters
($Å^2$x 10^3) for M-L'.

	x	y	z	U(eq)
H(1A)	5257	5170	8169	42
H(1B)	4102	5480	8892·	42
H(1C)	5695	5749	8834	42
H(2A)	563	5642	6965	37
H(2B)	-243	6168	6343	37
H(4)	-474	6020	4569	41
H(5)	314	5621	3036	48
H(6)	2412	5050	3017	55
H(7)	3730	4880	4530	43
H(10)	7317	6373	8334	35
H(11)	9643	6641	8822	42
H(12)	10140	7606	9423	44
H(13)	8295	8308	9560	39
H(14)	5947	8043	9083	33
H(16)	4383	7626	6564	35
H(17)	3270	8503	5989	42
H(18)	1865	9069	7085	42
H(19)	1609	8764	8778	38
H(20)	2689	7876	9359	31
H(22)	5336	7257	10536	49
H(23)	4325	7082	12119	60
H(24)	2237	6513	12243	54
H(25)	1101	6144	10769	46
H(26)	2084	6322	9181	36
H(27)	8687	4957	11503	43
H(28)	7659	5377	10017	45
H(29)	8964	5407	8515	43

Table 6. Crystal data and structure refinement for **D'**

Identification code	esp11tm
Empirical formula	C16 H18 O Re2 S5
Formula weight	759.00
Temperature	193(2) K
Wavelength	0.71073 Å
Crystal system	Monoclinic
Space group	P21/c
Unit cell dimensions	a = 11.2214(6) Å α= 90°
	b = 12.8234(7) Å β= 90.423(1)°
	c = 13.7784(8) Å γ = 90°
Volume	1982.61(19) Å^3
Z	4
Density (calculated)	2.543 Mg/m^3
Absorption coefficient	12.728 mm^{-1}
F(000)	1408
Crystal size	0.41 x 0.39 x 0.09 mm^3
Theta range for data collection	2.17 to 26.37°.
Index ranges	-13<=h<=14, 0<=k<=16, 0<=l<=17
Reflections collected	20105
Independent reflections	3839 [R(int) = 0.0433]
Completeness to theta = 26.37°	94.9 %
Absorption correction	Semi-empirical
Max. and min. transmission	0.625 and 0.179
Refinement method	Full-matrix least-squares on F^2
Data / restraints / parameters	3839 / 0 / 219
Goodness-of-fit on F^2	1.006
Final R indices [I>2sigma(I)]	R1 = 0.0203, wR2 = 0.0449
R indices (all data)	R1 = 0.0269, wR2 = 0.0466
Largest diff. peak and hole	0.965 and -0.863 e.Å^{-3}

Table 7. Atomic coordinates (x 10^4) and equivalent isotropic displacement parameters ($Å^2$x 10^3) for **D'**. U(eq) is defined as one third of the trace of the orthogonalized U^{ij} tensor.

	x	y	z	U(eq)
Re(1)	8030(1)	8462(1)	5048(1)	22(1)
Re(2)	9521(1)	7145(1)	6099(1)	20(1)
S(1)	7763(1)	7875(1)	6673(1)	22(1)
S(2)	7278(1)	10068(1)	5538(1)	30(1)
S(3)	10434(1)	7922(1)	7366(1)	26(1)
S(4)	11033(1)	5927(1)	5990(1)	27(1)
S(5)	9911(1)	7851(1)	4690(1)	28(1)
O	7029(3)	7775(2)	4406(2)	34(1)
C(1)	8651(5)	9589(4)	3975(3)	34(1)
C(2)	8457(5)	5762(3)	6127(3)	30(1)
C(3)	7893(5)	8997(3)	7507(3)	27(1)
C(4)	6742(4)	9568(3)	7468(3)	24(1)
C(5)	6003(5)	9633(3)	8274(3)	29(1)
C(6)	4944(5)	10180(3)	8223(3)	32(1)
C(7)	4590(5)	10657(4)	7367(4)	38(1)
C(8)	5303(5)	10574(3)	6554(3)	34(1)
C(9)	6380(5)	10037(3)	6604(3)	26(1)
C(10)	11924(5)	7371(4)	7572(3)	32(1)
C(11)	12698(5)	7323(3)	6697(3)	26(1)
C(12)	13721(5)	7902(4)	6615(3)	34(1)
C(13)	14438(5)	7827(4)	5797(4)	38(1)
C(14)	14115(5)	7157(3)	5055(3)	33(1)
C(15)	13094(5)	6584(3)	5119(3)	29(1)
C(16)	12364(4)	6664(3)	5932(3)	24(1)

Table 8. Bond lengths [Å] and angles [°] for D'

Re(1)-O	1.675(3)
Re(1)-C(1)	2.185(4)
Re(1)-S(5)	2.3072(13)
Re(1)-S(2)	2.3288(11)
Re(1)-S(1)	2.3828(10)
Re(1)-Re(2)	2.7773(3)
Re(2)-C(2)	2.138(4)
Re(2)-S(5)	2.1901(10)
Re(2)-S(3)	2.2502(11)
Re(2)-S(4)	2.3118(12)
Re(2)-S(1)	2.3276(12)
S(1)-C(3)	1.847(4)
S(2)-C(9)	1.787(5)
S(3)-C(10)	1.836(5)
S(4)-C(16)	1.769(5)
C(3)-C(4)	1.485(7)
C(4)-C(9)	1.392(6)
C(4)-C(5)	1.393(6)
C(5)-C(6)	1.382(7)
C(6)-C(7)	1.384(7)
C(7)-C(8)	1.385(7)
C(8)-C(9)	1.393(7)
C(10)-C(11)	1.492(6)
C(11)-C(12)	1.373(7)
C(11)-C(16)	1.400(6)
C(12)-C(13)	1.393(7)
C(13)-C(14)	1.381(7)
C(14)-C(15)	1.365(7)
C(15)-C(16)	1.397(6)
O-Re(1)-C(1)	101.95(17)
O-Re(1)-S(5)	108.65(12)
C(1)-Re(1)-S(5)	77.47(14)

Table 8 continued

O-Re(1)-S(2)	112.02(13)
C(1)-Re(1)-S(2)	74.31(13)
S(5)-Re(1)-S(2)	134.16(5)
O-Re(1)-S(1)	103.93(11)
C(1)-Re(1)-S(1)	152.56(13)
S(5)-Re(1)-S(1)	102.46(4)
S(2)-Re(1)-S(1)	87.60(4)
O-Re(1)-Re(2)	110.76(12)
C(1)-Re(1)-Re(2)	124.14(14)
S(5)-Re(1)-Re(2)	49.99(3)
S(2)-Re(1)-Re(2)	127.23(3)
S(1)-Re(1)-Re(2)	52.96(3)
C(2)-Re(2)-S(5)	118.30(13)
C(2)-Re(2)-S(3)	127.20(13)
S(5)-Re(2)-S(3)	114.33(4)
C(2)-Re(2)-S(4)	81.47(14)
S(5)-Re(2)-S(4)	94.02(4)
S(3)-Re(2)-S(4)	91.14(4)
C(2)-Re(2)-S(1)	81.52(13)
S(5)-Re(2)-S(1)	108.05(4)
S(3)-Re(2)-S(1)	86.58(4)
S(4)-Re(2)-S(1)	156.71(4)
C(2)-Re(2)-Re(1)	100.32(14)
S(5)-Re(2)-Re(1)	53.79(3)
S(3)-Re(2)-Re(1)	113.83(3)
S(4)-Re(2)-Re(1)	144.71(3)
S(1)-Re(2)-Re(1)	54.80(2)
C(3)-S(1)-Re(2)	117.49(18)
C(3)-S(1)-Re(1)	109.22(14)
Re(2)-S(1)-Re(1)	72.25(3)
C(9)-S(2)-Re(1)	115.25(14)
C(10)-S(3)-Re(2)	111.00(14)
C(16)-S(4)-Re(2)	105.20(14)

Table 8 continued

Re(2)-S(5)-Re(1)	76.22(4)
C(4)-C(3)-S(1)	107.2(3)
C(9)-C(4)-C(5)	119.0(5)
C(9)-C(4)-C(3)	119.5(4)
C(5)-C(4)-C(3)	121.5(4)
C(6)-C(5)-C(4)	120.4(4)
C(5)-C(6)-C(7)	120.6(5)
C(6)-C(7)-C(8)	119.4(5)
C(7)-C(8)-C(9)	120.3(5)
C(4)-C(9)-C(8)	120.2(4)
C(4)-C(9)-S(2)	123.4(4)
C(8)-C(9)-S(2)	116.3(3)
C(11)-C(10)-S(3)	115.2(3)
C(12)-C(11)-C(16)	119.0(4)
C(12)-C(11)-C(10)	122.4(4)
C(16)-C(11)-C(10)	118.6(4)
C(11)-C(12)-C(13)	121.1(5)
C(14)-C(13)-C(12)	119.5(5)
C(15)-C(14)-C(13)	120.2(5)
C(14)-C(15)-C(16)	120.7(4)
C(15)-C(16)-C(11)	119.5(4)
C(15)-C(16)-S(4)	119.8(3)
C(11)-C(16)-S(4)	120.7(4)

Symmetry transformations used to generate equivalent atoms:

Table 9. Anisotropic displacement parameters $(\text{Å}^2 \times 10^3)$ for **D'**. The anisotropic displacement factor exponent takes the form: $-2\pi^2[\, h^2 a^{*2} U^{11} + ... + 2 h k a^* b^* U^{12} \,]$

	U^{11}	U^{22}	U^{33}	U^{23}	U^{13}	U^{12}
Re(1)	22(1)	26(1)	19(1)	-2(1)	1(1)	-2(1)
Re(2)	20(1)	20(1)	19(1)	-3(1)	4(1)	-2(1)
S(1)	21(1)	23(1)	22(1)	-2(1)	5(1)	-1(1)
S(2)	33(1)	26(1)	30(1)	3(1)	7(1)	2(1)
S(3)	28(1)	30(1)	19(1)	-4(1)	0(1)	3(1)
S(4)	28(1)	21(1)	32(1)	-3(1)	6(1)	0(1)
S(5)	25(1)	40(1)	19(1)	1(1)	6(1)	0(1)
O	29(2)	43(2)	31(2)	-9(1)	0(2)	-6(2)
C(1)	34(4)	38(3)	29(2)	9(2)	1(2)	-2(2)
C(2)	28(3)	25(2)	38(2)	-8(2)	9(2)	-6(2)
C(3)	32(3)	26(2)	22(2)	-7(2)	4(2)	1(2)
C(4)	22(3)	21(2)	29(2)	-8(2)	0(2)	-3(2)
C(5)	26(3)	28(2)	31(2)	-5(2)	3(2)	-2(2)
C(6)	25(3)	34(2)	38(2)	-8(2)	9(2)	-1(2)
C(7)	22(3)	34(3)	58(3)	-11(2)	7(3)	6(2)
C(8)	33(4)	29(2)	40(3)	-2(2)	0(2)	2(2)
C(9)	27(3)	21(2)	31(2)	-6(2)	2(2)	-4(2)
C(10)	35(4)	37(3)	25(2)	-4(2)	-6(2)	7(2)
C(11)	26(3)	29(2)	24(2)	1(2)	-2(2)	4(2)
C(12)	30(4)	35(3)	38(3)	-5(2)	-7(2)	2(2)
C(13)	24(3)	37(3)	52(3)	2(2)	-1(3)	-3(2)
C(14)	34(4)	32(2)	32(2)	4(2)	5(2)	1(2)
C(15)	31(3)	25(2)	29(2)	0(2)	-1(2)	4(2)
C(16)	23(3)	22(2)	25(2)	5(2)	-4(2)	2(2)

Table 10. Hydrogen coordinates (x 10⁴) and isotropic displacement parameters (Å²x 10 ³) for D'

	x	y	z	U(eq)
H(1A)	8946	9217	3403	51
H(1B)	9296	10009	4257	51
H(1C)	7990	10046	3783	51
H(2A)	8043	5682	5503	46
H(2B)	7870	5816	6648	46
H(2C)	8970	5156	6243	46
H(3A)	8057	8753	8177	32
H(3B)	8552	9460	7305	32
H(5)	6230	9299	8862	34
H(6)	4454	10229	8781	39
H(7)	3865	11039	7338	45
H(8)	5055	10885	5960	40
H(10A)	12335	7793	8075	39
H(10B)	11834	6656	7833	39
H(12)	13944	8363	7126	41
H(13)	15143	8232	5750	45
H(14)	14605	7096	4498	39
H(15)	12878	6126	4605	34

CHAPTER IV. MONOMERIZATION OF A Re(V) DIMER BY LIGATION

Josemon Jacob, Gabor Lente, Ilia A. Guzei and James H. Espenson*

Abstract

New reactions of the dimeric rhenium(V) chelate, $[CH_3Re(O)(S_2L)]_2$ (D), where S_2L is a dithiolate chelate have been investigated. D is easily monomerized by various ligands to form $[CH_3Re(O)(S_2L)\text{-}L]$, where L = ligand. The kinetics of this monomerization reaction was studied for L=PPh3 and dmso. In the case of dmso, the first formed intermediate, an asymmetric dimeric rhenium(V)complex was isolated and characterized crystallographically. The geometry of this complex suggests that in solution there can be fast exchange of dmso between the two rhenium centers.

Introduction

Stoichiometric and catalytic oxygen atom transfer reactions involving Re(V) and Re(VII) oxides and their derivatives have received great attention in recent years.[1-3] Our recent work has focused on elucidating the mechanisms of these reactions, those involving methyltrioxorhenium(VII) (MTO) and its reduced forms in particular.[4-6] A yellow-colored dimeric dithiolato(oxo)rhenium(V) compound, designated D in Chart 1, has been prepared from MTO and the dithiolate, 1. The synthesis and characterization of D have been reported.[7] We have also found that reactions between D and prospective ligands (L) cause its monomerization. The resulting family of compounds is designated as M–L. The net reaction between them is represented in eq 1. The structural formulas of the participants are given in Chart 1.

$$D + 2L \rightarrow 2 M\text{-}L \tag{1}$$

Chart 1
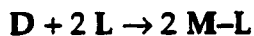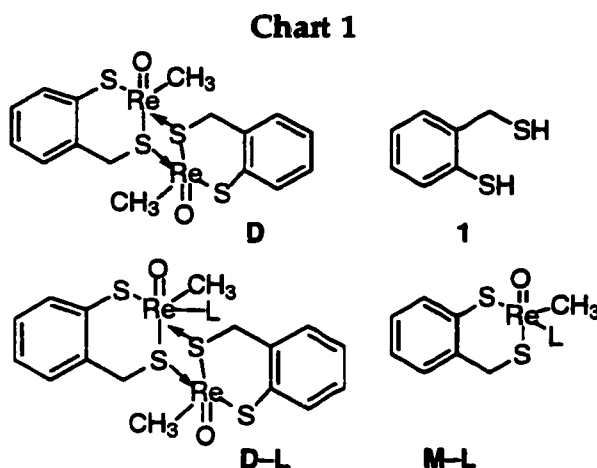
Results and Discussion

To learn about the mechanism of reaction 1, we have carried out experiments along several lines in toluene and benzene. Studies with L = PPh$_3$ and Me$_2$SO were used, in that each elucidates a separate facet of the mechanism. We were able to characterize the products and in the case of dmso, we were able to isolate the intermediate and characterize by X-ray crystallography. These results are presented below.

Figure 1 displays a series of repetitive scans for the reaction between D and PPh$_3$ in toluene. A few hours are needed to complete the formation of the green-colored complex M–PPh$_3$ (λ_{max} 606 nm, ϵ 190 L mol^{-1}cm^{-1}, δ = 2.97 ppm for ReCH_3), whose crystal structure we reported earlier.[7] The reaction rate is strictly

first-order with respect to [D]. The variation of the pseudo-first order rate-constant k_{obs} on [PPh$_3$] is shown in **Figure 2**. It confirms that the rate law is made up of two terms with first-order and second-order dependences on [PPh$_3$]:

$$\frac{d[M-PPh_3]}{dt} = 2\{k_a[PPh_3] + k_b[PPh_3]^2\} \cdot [D] \qquad (2)$$

These values at 25.0 °C were found in toluene by least-squares fitting: $k_a = (8.2 \pm 0.2) \times 10^{-3}$ L mol^{-1} s^{-1} and $k_b = (5.2 \pm 0.2) \times 10^{-2}$ L^2 mol^{-2} s^{-1}.

One possible reaction scheme features a **D** = 2 **M** interconversion, followed by the step **M** + **L** → **M–L**. Such a mechanism has been observed for the dimeric Re(V) oxo compound, $(Cp^*ReO)_2(\mu-O)_2$.[8] It can clearly be discarded in this instance, however, because the rate law would not have the correct form. The scheme given in reactions 3-5 does agree with kinetics. It features a dimeric intermediate, **D–L**, that is asymmetric with respect to its binding of **L**.

$$\mathbf{D+L} \underset{k_{-1}}{\overset{k_1}{\rightleftharpoons}} \mathbf{D-L} \qquad (3)$$

$$\mathbf{DL_2} \xrightarrow{k_4} 2\,\mathbf{M-L} \qquad (4)$$

$$\xrightarrow[\text{fast}]{+L} \mathbf{M-L}$$

$$\mathbf{M-L + M} \qquad (5)$$
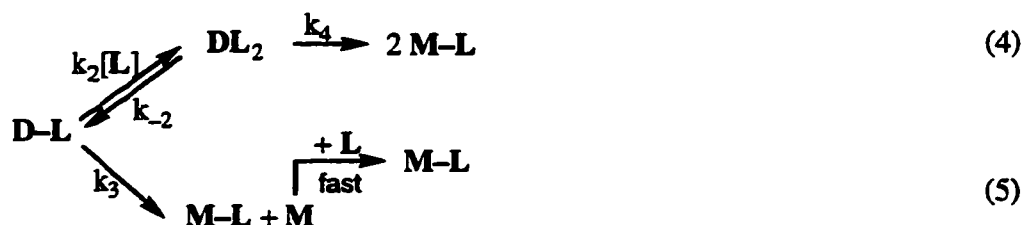
The equilibrium constants for coordination of PPh$_3$ are known to be small, since only **D** and **M–L** were detected during the time course. The rate law then agrees with eq 2, with $k_a = k_3 \cdot K_1$ and $k_b = k_4 \cdot K_1 \cdot K_2$. These composite constants cannot be resolved further.
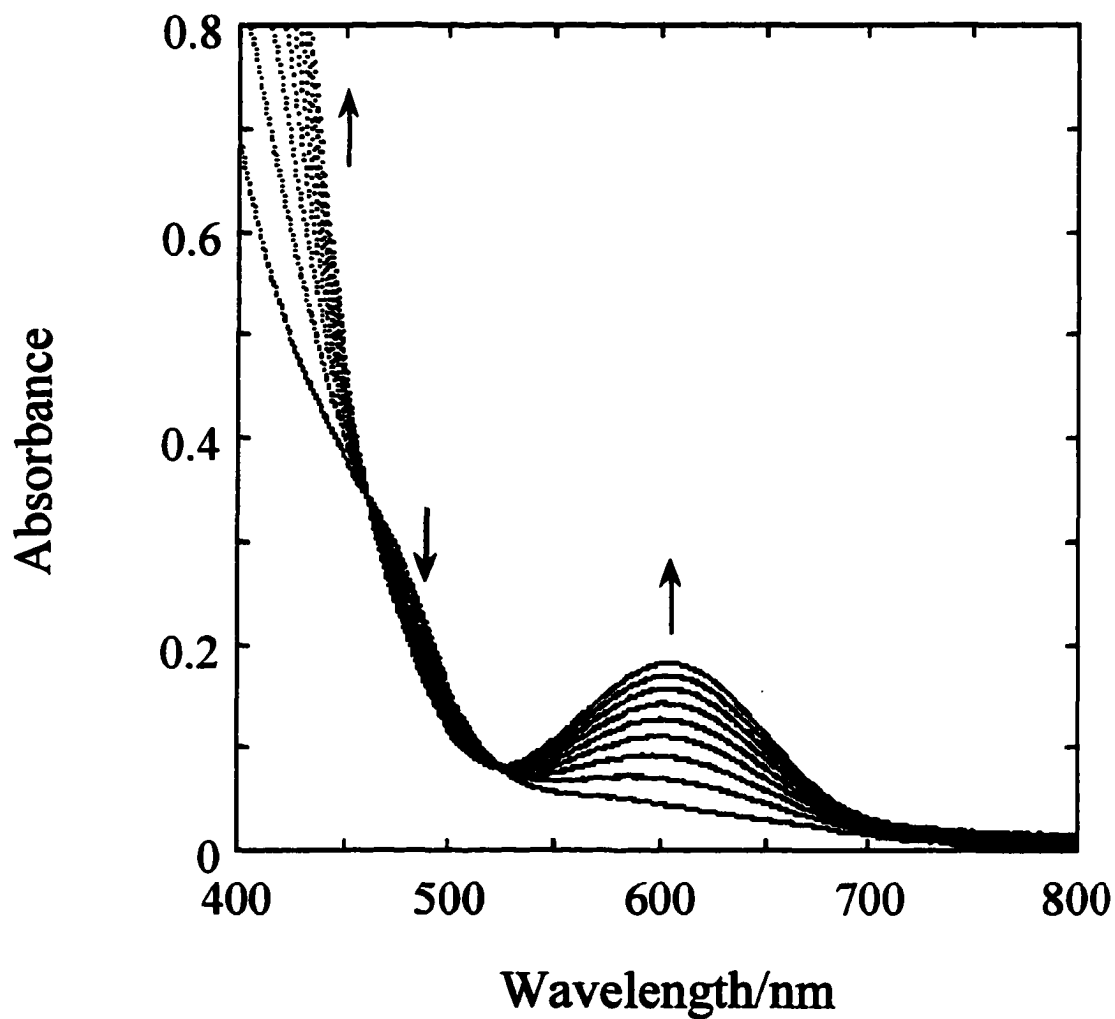
Figure 1: Changes in the UV-Visible spectra for the reaction of **D** (0.8 mM) with triphenylphosphine (16 mM) in toluene at 25.0 °C. Spectra were recorded at 10 min intervals.
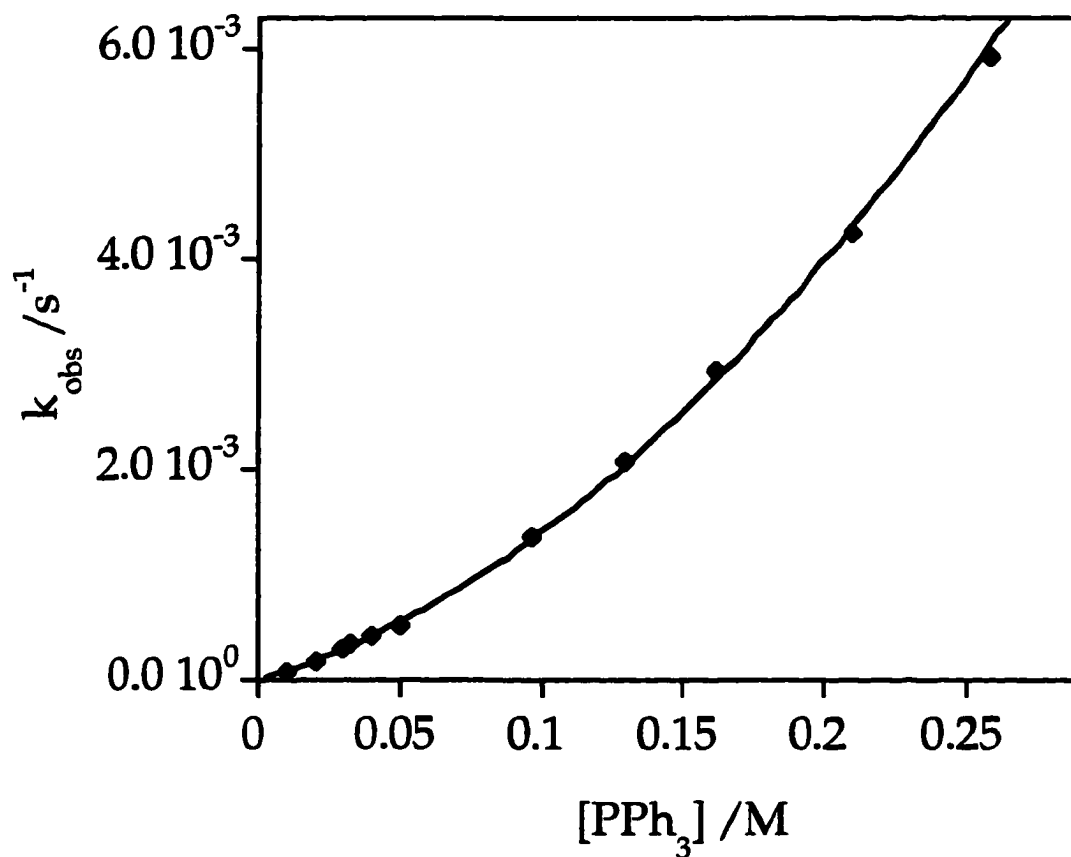
Figure 2: Dependence of the pseudo-first order rate constant k_{obs} on the concentration of triphenylphosphine in toluene at 25.0 °C. The solid line represents the least-squares fit based parallel paths with first-order and second-order dependences on phosphine concentration, as expressed by eq 2.

We next turned to the case of L = Me$_2$SO. The reaction between D and dmso is exceptionally rapid. The yellow color of D turned pink immediately upon addition of dmso. Stopped-flow determinations at the lowest allowable concentrations and temperature (1.0 mM D and 8.0 mM dmso in benzene at 280 K) gave evidence only for a completed reaction.[9] From that we set $k_1 > 3 \times 10^5$ L mol^{-1} s^{-1} Spectrophotometric and NMR determinations gave evidence of the equilibrium written in eq 2, with $K_1 = 120 \pm 6$ L mol^{-1} (298 K, benzene). Thermodynamic parameters for this reaction were determined from temperature-dependent values of K_1, giving $\Delta H_1° -35.6 \pm 0.8$ kJ mol^{-1} and $\Delta S_1°$ -80 ± 3 J mol^{-1} K^{-1}.

We were able to crystallize the 1:1 adduct of the D and dmso, D–dmso. Its molecular structure is shown in **Figure 3.**[10] The Re atoms are different, one being six-coordinate and the other five. A similar asymmetric dmso complex has been reported for a dimeric Re(III) complex.[11]

Weaker, very fast coordination of a second dmso to form D(dmso)$_2$ and subsequent monomerization of the dimeric complex were also noted from kinetic investigations with $K_2 \cong 0.6$ L mol^{-1} and $k_4 \cong 7 \times 10^{-5}$ s^{-1} (293 K, benzene). M–dmso was not detected, since subsequent fast redox reactions ensue including the breaking of the S–O bond. These events are unrelated to the present subject and will be reported separately.

Conclusions

In summary, we have shown that the monomerization of D by ligands goes through an initial 1:1 adduct, which was characterized by X-ray crystallography in the case of dmso. The kinetic role of the analogous adduct is clear in the reaction with PPh$_3$, but that adduct is not formed in significant
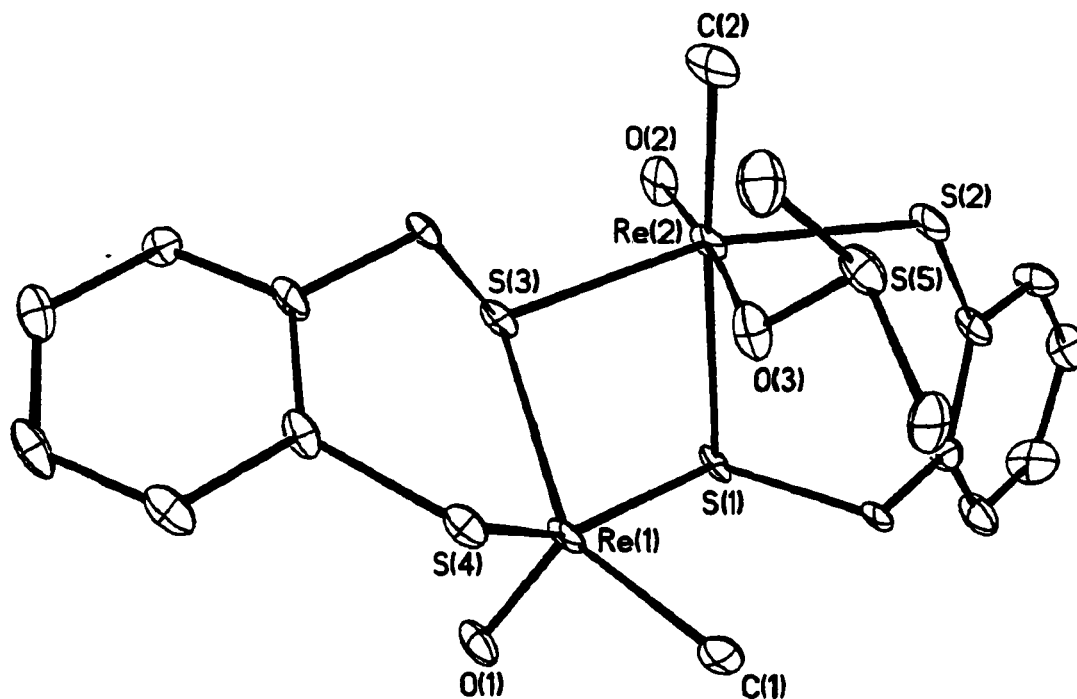
Figure 3: Perspective view of the asymmetric dinuclear dmso complex, D–L with thermal ellipsoids of 30% probability level. Selected bond lengths (pm) and angles(°): Re(2)–O(2) 169.4; Re(2)–C(2) 215.0; Re(2)–S(2) 233.0; Re(2)–O(3) 238.6; Re(2)–S(1) 238.8; Re(2)–S(3) 241.8; O(2)–Re(2)–C(2) 99.0; O(2)–Re(2)–S(2) 104.0; C(2)–Re(2)–S(2) 85.9; O(2)–Re(2)–O(3) 171.9; C(2)–Re(2)–O(3) 78.1; S(2)–Re(2)–O(3) 83.4; O(2)–Re(2)–S(1) 107.3; C(2)–Re(2)–S(1) 153.2; S(2)–Re(2)–S(1) 92.6; O(3)–Re(2)–S(1) 75.2; O(2)–Re(2)–S(3) 99.2; C(2)–Re(2)–S(3) 95.5; S(2)–Re(2)–S(3) 156.2; O(3)–Re(2)–S(3) 73.8; S(1)–Re(2)–S(3) 75.6.

concentrations. We are currently investigating the mechanism of monomerization with other neutral and anionic ligands.

References

1) Romão, C. C.; Kühn, F. E.; Herrmann, W. A. *Chem. Rev.* **1997**, *97*, 3197-3246.

2) Espenson, J. H.; Abu-Omar, M. M. *Adv. Chem. Ser.* **1997**, *253*, 99-134.

3) Conry, R. R.; Mayer, J. M. *Inorg. Chem.* **1990**, *29*, 4862-67.

4) Abu-Omar, M. M.; Appleman, E. H.; Espenson, J. H. *Inorg. Chem.* **1996**, *35*, 7751-57.

5) Espenson, J. H. *Chem. Comm.* **1999**, 479-88.

6) Abu-Omar, M. M.; Espenson, J. H. *Inorg. Chem.* **1995**, *34*, 6239-40.

7) Jacob, J.; Guzei, I. A.; Espenson, J. H. *Inorg. Chem.* **1999**, *38*, 1040-1041.

8) Gable, K. P.; Juliette, J. J. J.; Gartman, M. A. *Organometallics* **1995**, *14*, 3138-3140.

9) Under these conditions the complex formation reaction is not shifted to give the stoichiometric amount of D–L, but is still accompanied by a easily-detected absorbance change, ~0.2 absorbance units at 390 nm.

10) X-ray crystal data for $C_{25}H_{43}O_5Re_2S_7$: monoclinic, $P2_1/n$, a = 14.1515(12) Å, b = 10.8017(9) Å, c = 22.9054(19) Å, b = 101.503(2)°, V = 3431.0(5) Å^3, Z = 4, T = 193(2), D_{calc} = 1.975 Mg/m^3, R(F) = 6.7 for 4862 independently observed (I ≥ 2σ(I)) reflections (4° ≤ 2θ ≤ 53°). All atoms other than hydrogen were refined with anisotropic displacement coefficients. All hydrogen atoms were included in the structure factor calculation at idealized positions and were allowed to ride on the neighboring atoms with relative isotropic displacement coefficients. The software and sources of the scattering factors are contained in the SHELXTL

(version 5.1) program library (G. Sheldrick, Bruker Analytical X-Ray Systems, Madison, WI).

11) Hursthouse, M. B.; Malik, K. M. A. *J. Am. Chem. Soc.* **1962**, *84*, 2941-2944.

SUPPORTING INFORMATION

General Considerations

Materials and methods:

The dithiol and dimer were synthesized according to procedures reported earlier. All other chemicals were purchased from commercial sources. The ^{1}H NMR spectra were recorded using a Varian VXR 300 MHz spectrometer. The UV-Vis spectra were recorded using a Shimadzu UV-PC 2101 or a multispec 1501 spectrophotometer. In the kinetic experiments, spectrophotometric grade benzene purchased from Fisher was used.

Isolation of the dmso complex, D-L

To 2mL of 4mM toluene solution of dimer in a vial, dmso was added to give a concentration of 0.2M at room temperature. The color of the solution changed from yellow to pink immediately on mixing. The entire solution was transferred to a thin long tube and layered with hexane and left in the freezer overnight. Small needle like crystals that were formed at the interface were analyzed by X-ray crystallography.
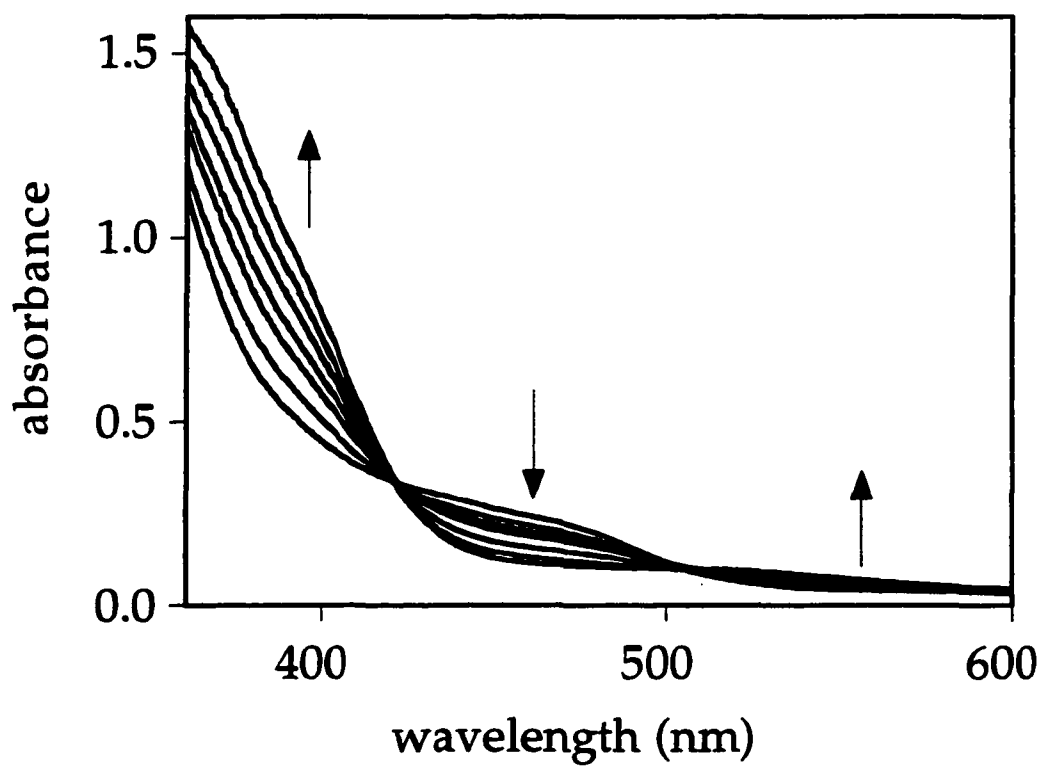
Figure 4. UV-VIS spectral changes accomponying the formation of D-L with dmso as a ligand. Arrows indicate the increase in the concentration of dmso. [D] = 0.488 mM for all spectra. [dmso] = 0, 1.58, 3.15, 6.30, 12.6, 25.2, 63.0 mM (benzene, 293 K).
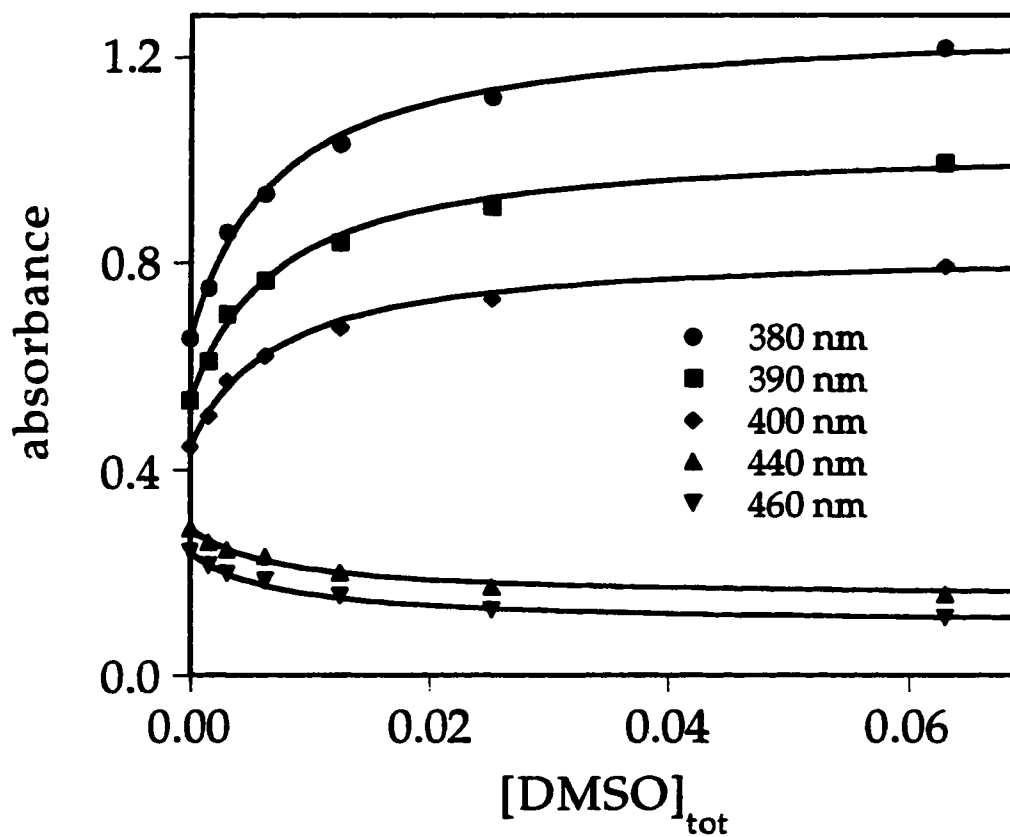
Figure 5. Absorbance as a function of dmso concentration for a selection of wavelengths. [D] = 0.488 mM for all points. Solid lines represent the best fit based on the D + L = D-L model (benzene, 293 K).
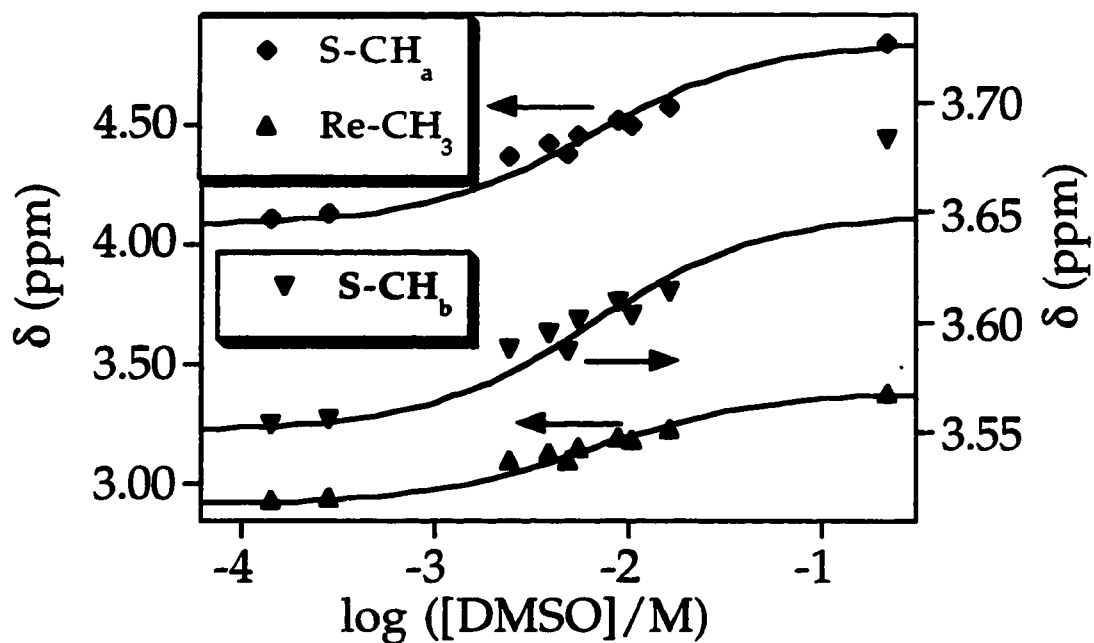
Figure 6. Change in the chemical shifts of signals during the gradual formation of the assymetric dmso complex D-L (C_6D_6, 298 K). Dimer concentrations from 1.5 to 3.0 mM were used. The logarithm of free (uncomplexed) dmso concentration is shown on the x axis. The actual values were calculated from the best fit and hence are prone to some error. Solid lines indicate the best fit to the data.
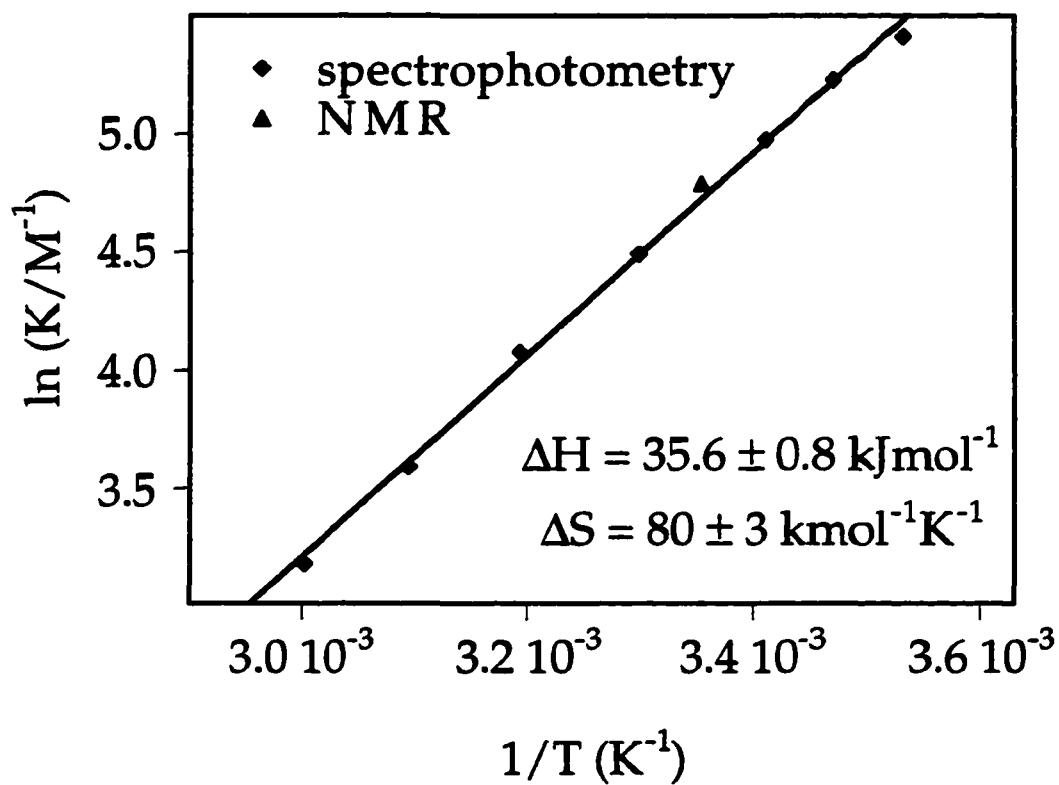
Figure 7. Temperature dependence of the equilibrium constant K_1 with dmso (benzene).

Table 1. Crystal data and structure refinement for **D-L**

Identification code	esp10
Empirical formula	$C_{25}H_{43}O_5Re_2S_7$
Formula weight	1020.41
Temperature	193(2) K
Wavelength	0.71073 Å
Crystal system	Monoclinic
Space group	P21/n
Unit cell dimensions	a = 14.1515(12) Å $\alpha= 90°$
	b = 10.8017(9) Å $\beta= 101.503(2)°$
	c = 22.9054(19) Å $\gamma= 90°$
Volume	3431.0(5) Å³
Z	4
Density (calculated)	1.975 Mg/m³
Absorption coefficient	7.508 mm⁻¹
F(000)	1980
Crystal size	0.45 x 0.10 x 0.08 mm³
Theta range for data collection	1.81 to 23.25°.
Index ranges	-15<=h<=15, 0<=k<=12, 0<=l<=25
Reflections collected	16873
Independent reflections	4862 [R(int) = 0.0873]
Completeness to theta = 23.25°	98.7 %
Absorption correction	Empirical with DIFABS
Max. and min. transmission	1.000 and 0.338
Refinement method	Full-matrix least-squares on F^2
Data / restraints / parameters	4862 / 112 / 346
Goodness-of-fit on F^2	0.997
Final R indices [I>2sigma(I)]	R1 = 0.0621, wR2 = 0.1352
R indices (all data)	R1 = 0.1012, wR2 = 0.1504
Largest diff. peak and hole	2.710 and -1.607 e.Å⁻³

Table 2. Atomic coordinates (x 10^4) and equivalent isotropic displacement parameters ($Å^2$x 10^3) for D-L. U(eq) is defined as one third of the trace of the orthogonalized U^{ij} tensor.

	x	y	z	U(eq)
Re(1)	4275(1)	3558(1)	1168(1)	24(1)
Re(2)	4847(1)	450(1)	1687(1)	23(1)
S(1)	4241(3)	1501(3)	771(2)	23(1)
S(2)	3636(3)	-1043(4)	1500(2)	28(1)
S(3)	5511(3)	2514(3)	1840(2)	23(1)
S(4)	4059(3)	4938(4)	1908(2)	27(1)
S(5)	2820(3)	1322(4)	2260(2)	31(1)
S(6)	479(4)	-434(5)	1042(2)	51(1)
S(7)	2794(5)	3594(6)	-809(3)	71(2)
O(1)	4720(9)	4368(10)	658(5)	33(3)
O(2)	5852(8)	-323(10)	1602(5)	35(3)
O(3)	3581(8)	1733(10)	1893(5)	32(3)
O(4)	921(9)	611(12)	761(6)	52(4)
O(5)	2067(13)	2666(15)	-1058(9)	100(6)
C(1)	2758(12)	3716(15)	893(8)	33(4)
C(2)	4897(15)	71(15)	2614(7)	40(4)
C(3)	3080(11)	852(13)	432(7)	22(3)
C(4)	3197(12)	-462(15)	282(7)	25(3)
C(5)	3119(13)	-859(16)	-315(8)	36(4)
C(6)	3230(15)	-2050(18)	-465(8)	43(5)
C(7)	3385(13)	-2957(16)	-23(8)	39(5)
C(8)	3505(12)	-2593(15)	569(7)	30(4)
C(9)	3444(12)	-1390(14)	730(7)	26(4)
C(10)	5607(12)	3112(13)	2591(7)	23(3)
C(11)	5901(12)	4448(14)	2628(7)	26(3)
C(12)	6777(12)	4848(14)	2902(7)	24(4)
C(13)	7021(13)	6058(16)	2921(8)	34(4)
C(14)	6385(14)	6964(16)	2635(8)	38(4)
C(15)	5487(13)	6577(15)	2336(8)	32(4)
C(16)	5219(12)	5313(14)	2326(7)	24(3)

Table 2 continued

C(17)	1776(11)	2218(18)	1973(8)	38(4)
C(18)	3149(13)	2085(18)	2957(8)	41(5)
C(19)	-784(16)	-270(20)	788(10)	70(6)
C(20)	590(20)	-1750(20)	619(12)	104(10)
C(21)	2808(19)	4730(20)	-1366(10)	73(7)
C(22)	3954(17)	2952(19)	-821(9)	59(5)
C(23)	-580(20)	3340(30)	891(14)	111(11)
C(24)	-20(40)	4380(40)	680(30)	260(30)
C(25)	-440(30)	5150(70)	130(20)	470(70)

Table 3. Bond lengths [Å] and angles [°] for **D-L**

Re(1)-O(1)	1.678(10)
Re(1)-C(1)	2.120(16)
Re(1)-S(4)	2.323(4)
Re(1)-S(3)	2.373(4)
Re(1)-S(1)	2.396(4)
Re(2)-O(2)	1.694(11)
Re(2)-C(2)	2.150(16)
Re(2)-S(2)	2.330(4)
Re(2)-O(3)	2.386(11)
Re(2)-S(1)	2.388(4)
Re(2)-S(3)	2.418(4)
S(1)-C(3)	1.812(15)
S(2)-C(9)	1.769(16)
S(3)-C(10)	1.815(16)
S(4)-C(16)	1.774(17)
S(5)-O(3)	1.557(11)
S(5)-C(18)	1.775(17)
S(5)-C(17)	1.780(17)
S(6)-O(4)	1.497(14)
S(6)-C(20)	1.75(2)
S(6)-C(19)	1.78(2)
S(7)-O(5)	1.468(16)
S(7)-C(21)	1.77(2)
S(7)-C(22)	1.79(2)
C(3)-C(4)	1.48(2)
C(4)-C(5)	1.42(2)
C(4)-C(9)	1.43(2)
C(5)-C(6)	1.35(2)
C(6)-C(7)	1.39(2)
C(7)-C(8)	1.39(2)
C(8)-C(9)	1.36(2)
C(10)-C(11)	1.50(2)
C(11)-C(12)	1.34(2)

Table 3 continued

C(11)-C(16)	1.42(2)
C(12)-C(13)	1.35(2)
C(13)-C(14)	1.40(2)
C(14)-C(15)	1.38(2)
C(15)-C(16)	1.42(2)
C(23)-C(24)	1.513(2)
C(24)-C(25)	1.524(2)
C(25)-C(25)#1	1.524(2)
O(1)-Re(1)-C(1)	104.5(6)
O(1)-Re(1)-S(4)	107.1(4)
C(1)-Re(1)-S(4)	83.8(5)
O(1)-Re(1)-S(3)	111.7(4)
C(1)-Re(1)-S(3)	143.4(5)
S(4)-Re(1)-S(3)	91.04(15)
O(1)-Re(1)-S(1)	101.7(4)
C(1)-Re(1)-S(1)	91.1(4)
S(4)-Re(1)-S(1)	151.12(14)
S(3)-Re(1)-S(1)	76.24(14)
O(2)-Re(2)-C(2)	99.0(7)
O(2)-Re(2)-S(2)	104.0(4)
C(2)-Re(2)-S(2)	85.9(5)
O(2)-Re(2)-O(3)	171.9(5)
C(2)-Re(2)-O(3)	78.1(6)
S(2)-Re(2)-O(3)	83.4(3)
O(2)-Re(2)-S(1)	107.3(4)
C(2)-Re(2)-S(1)	153.2(5)
S(2)-Re(2)-S(1)	92.60(14)
O(3)-Re(2)-S(1)	75.2(3)
O(2)-Re(2)-S(3)	99.2(4)
C(2)-Re(2)-S(3)	95.5(5)
S(2)-Re(2)-S(3)	156.23(15)
O(3)-Re(2)-S(3)	73.8(3)

Table 3 continued

S(1)-Re(2)-S(3)	75.55(14)
C(3)-S(1)-Re(2)	109.2(5)
C(3)-S(1)-Re(1)	118.0(5)
Re(2)-S(1)-Re(1)	97.57(15)
C(9)-S(2)-Re(2)	106.9(6)
C(10)-S(3)-Re(1)	110.6(5)
C(10)-S(3)-Re(2)	114.8(5)
Re(1)-S(3)-Re(2)	97.40(15)
C(16)-S(4)-Re(1)	107.3(5)
O(3)-S(5)-C(18)	105.5(8)
O(3)-S(5)-C(17)	104.9(8)
C(18)-S(5)-C(17)	97.4(9)
O(4)-S(6)-C(20)	106.4(11)
O(4)-S(6)-C(19)	105.1(9)
C(20)-S(6)-C(19)	95.7(14)
O(5)-S(7)-C(21)	107.4(12)
O(5)-S(7)-C(22)	107.7(11)
C(21)-S(7)-C(22)	96.6(11)
S(5)-O(3)-Re(2)	124.6(6)
C(4)-C(3)-S(1)	109.7(11)
C(5)-C(4)-C(9)	116.3(15)
C(5)-C(4)-C(3)	121.6(15)
C(9)-C(4)-C(3)	122.1(14)
C(6)-C(5)-C(4)	122.9(17)
C(5)-C(6)-C(7)	119.7(17)
C(8)-C(7)-C(6)	118.7(16)
C(9)-C(8)-C(7)	122.3(16)
C(8)-C(9)-C(4)	119.8(15)
C(8)-C(9)-S(2)	117.9(13)
C(4)-C(9)-S(2)	122.3(12)
C(11)-C(10)-S(3)	111.4(11)
C(12)-C(11)-C(16)	119.3(15)
C(12)-C(11)-C(10)	123.8(15)

Table 3 continued

C(16)-C(11)-C(10)	116.8(14)
C(11)-C(12)-C(13)	122.2(16)
C(12)-C(13)-C(14)	121.7(17)
C(15)-C(14)-C(13)	117.5(16)
C(14)-C(15)-C(16)	121.1(16)
C(15)-C(16)-C(11)	118.2(15)
C(15)-C(16)-S(4)	116.4(13)
C(11)-C(16)-S(4)	125.4(12)
C(23)-C(24)-C(25)	122(5)
C(24)-C(25)-C(25)#1	89(4)

Symmetry transformations used to generate equivalent atoms:

#1 -x,-y+1,-z

Table 4. Anisotropic displacement parameters (Å^2x 10^3) for **D-L**. The anisotropic displacement factor exponent takes the form: $-2\pi^2[\ h^2\ a^{*2}U^{11} + ... + 2\ h\ k\ a^*\ b^*\ U^{12}\ ]$

	U^{11}	U^{22}	U^{33}	U^{23}	U^{13}	U^{12}
Re(1)	38(1)	3(1)	30(1)	1(1)	7(1)	1(1)
Re(2)	36(1)	1(1)	32(1)	-1(1)	6(1)	1(1)
S(1)	33(2)	2(2)	34(2)	-1(2)	10(2)	-3(2)
S(2)	45(3)	6(2)	33(3)	1(2)	6(2)	-5(2)
S(3)	34(2)	3(2)	35(2)	0(2)	10(2)	3(2)
S(4)	38(3)	7(2)	37(3)	-4(2)	9(2)	5(2)
S(5)	46(3)	17(2)	35(3)	-4(2)	18(2)	-3(2)
S(6)	64(4)	41(3)	45(3)	7(3)	8(3)	-5(3)
S(7)	101(5)	48(4)	69(4)	1(3)	27(4)	-24(3)
O(1)	61(8)	18(6)	21(6)	-4(4)	11(5)	-15(6)
O(2)	37(6)	9(5)	58(8)	-13(5)	8(5)	2(4)
O(3)	30(6)	21(6)	51(7)	-12(5)	21(5)	-3(4)
O(4)	50(8)	39(8)	68(10)	10(7)	10(7)	-5(7)
O(5)	95(11)	47(10)	152(17)	-5(10)	7(12)	-31(9)
C(1)	42(6)	10(9)	41(10)	-2(7)	-3(6)	6(6)
C(2)	81(14)	9(8)	28(6)	-6(5)	10(6)	-2(7)
C(3)	22(8)	5(6)	38(9)	7(6)	4(6)	1(6)
C(4)	30(10)	11(6)	31(6)	-3(5)	-3(7)	-3(7)
C(5)	54(12)	20(7)	36(7)	-1(6)	11(9)	-12(9)
C(6)	65(14)	39(9)	25(8)	-14(6)	6(9)	5(10)
C(7)	53(13)	14(8)	48(9)	-15(6)	2(10)	-8(9)
C(8)	46(11)	10(6)	32(7)	2(6)	7(8)	6(8)
C(9)	43(10)	6(6)	32(6)	-3(5)	10(7)	-5(7)
C(10)	32(7)	5(5)	32(6)	3(5)	3(5)	-2(5)
C(11)	40(8)	5(6)	33(10)	-4(6)	10(6)	-2(6)
C(12)	35(8)	11(6)	23(9)	-9(7)	0(7)	8(6)
C(13)	39(10)	24(8)	41(12)	-10(8)	15(8)	-10(6)
C(14)	54(11)	10(8)	54(13)	-8(8)	24(9)	-5(6)
C(15)	46(9)	12(6)	41(11)	-3(7)	21(7)	7(6)
C(16)	30(7)	9(6)	38(9)	-7(6)	16(6)	1(5)

Table 4 continued

C(17)	17(8)	48(13)	52(11)	-3(9)	15(7)	-3(7)
C(18)	39(11)	43(13)	45(9)	-14(9)	18(7)	-11(9)
C(19)	68(8)	73(17)	66(16)	24(13)	4(11)	-28(10)
C(20)	190(30)	27(10)	89(19)	8(11)	30(20)	15(15)
C(21)	120(20)	46(13)	65(15)	1(9)	33(14)	-1(11)
C(22)	92(10)	35(12)	52(14)	-11(10)	17(11)	-22(9)

Table 5. Hydrogen coordinates (x 10^4) and isotropic displacement parameters (Å^2x 10 ^{3}) for **D-L**

	x	y	z	U(eq)
H(1A)	2592	3810	459	49
H(1B)	2533	4442	1083	49
H(1C)	2449	2970	1011	49
H(2A)	5467	-432	2772	60
H(2B)	4315	-382	2658	60
H(2C)	4932	852	2834	60
H(3A)	2631	920	711	27
H(3B)	2803	1319	66	27
H(5)	2981	-259	-624	44
H(6)	3202	-2270	-870	52
H(7)	3409	-3808	-125	47
H(8)	3635	-3206	872	36
H(10A)	4978	3023	2713	28
H(10B)	6089	2620	2869	28
H(12)	7240	4260	3088	28
H(13)	7639	6301	3134	40
H(14)	6564	7813	2647	45
H(15)	5043	7169	2134	38
H(17A)	1935	3100	2017	57
H(17B)	1267	2022	2193	57
H(17C)	1549	2025	1550	57
H(18A)	3759	1745	3177	61
H(18B)	2644	1959	3188	61
H(18C)	3225	2973	2891	61
H(19A)	-1011	458	979	106
H(19B)	-1113	-1009	889	106
H(19C)	-924	-151	355	106
H(20A)	233	-1634	211	156
H(20B)	335	-2473	796	156
H(20C)	1276	-1893	613	156

Table 5 continued

H(21A)	3001	4341	-1711	110
H(21B)	3268	5380	-1207	110
H(21C)	2162	5084	-1487	110
H(22A)	4071	2242	-550	89
H(22B)	4451	3581	-694	89
H(22C)	3976	2679	-1226	89
H(23A)	-1266	3426	709	167
H(23B)	-501	3387	1326	167
H(23C)	-342	2544	779	167
H(24A)	587	4010	600	313
H(24B)	168	4960	1013	313
H(25A)	-503	6045	218	562
H(25B)	-1052	4822	-104	562

CHAPTER V. 1,3-TRANSPOSITION OF ALLYLIC ALCOHOLS CATALYZED BY METHYLRHENIUM TRIOXIDE

A paper published in *Organometallics*[1]

Josemon Jacob, James H. Espenson*, Jan H. Jensen and Mark S. Gordon

Abstract

Methylrhenium trioxide (MTO) catalyzes the 1,3-transposition of allylic alcohols to generate the more stable isomer at equilibrium. The direction of the equilibrium is largely decided by the nature of the OH group, i.e., whether it is primary, secondary or tertiary. In the case of aliphatic allylic alcohols, tertiary is preferred to secondary to primary. For aromatic allyl alcohols, the more conjugated isomer predominates largely at equilibrium. Oxygen-18 labelling showed that the OH groups of parent and product are the same thus ruling out a chemical mechanism involving the oxygen atoms on MTO. The reaction is first order with respect to allyl alcohol and MTO, but strongly inhibited by traces of water. Theoretical calculations suggest the same in the case of aliphatic allyl alcohols though aromatic allyl alcohols do not follow the predictions. Studies of deuterium labelled substrates show a large *equilibrium isotope* effect (K= 1.20 ± 0.02). For isomeric allyl alcohols differing in the position of deuterium only, the isomer with the deuterium at sp^3 center predominates at equilibrium. The effect of conjugation from a phenyl group appears to be less important since calculations suggest that the phenyl group is forced out of plane of the allylic π system.

[1]. Jacob, J.; Espenson, J. H.; Jenson, J. J.; Gordon, M. S.; *Organometallics*, **1998**, *17*, 1835-40.

Introduction

Functional group transpositions[1,2] contribute an important technique to supplement the formation of carbon–carbon bonds and the interconversion of functional groups, which constitute the substance of much synthetic work. We shall address here a rearrangement of allylic alcohols that converts one isomer to another, related to the first by a 1,3-transposition of the OH group. The conversion can be complete or partial, depending on the spontaneity of the reaction. Such rearrangements do not occur on their own, however, and the role played by a particular catalyst is of considerable fundamental interest. The utility of this transposition arises when the more readily accessible allylic alcohol is not the desired one. A chemical equation for the general case, ignoring issues of regioselectivity to be addressed later, is:

$$R^3 \underset{R^4}{\overset{R^5}{\diagdown}} \underset{OH}{\overset{R^1}{\diagup R^2}} \quad \underset{\longleftarrow}{\overset{cat. \ MTO}{\longrightarrow}} \quad R^3 \underset{R^4}{\overset{R^5}{\diagdown}} \underset{OH}{\overset{}{\diagup}} \overset{}{\underset{R^2}{\diagdown}} R^1$$

(1)
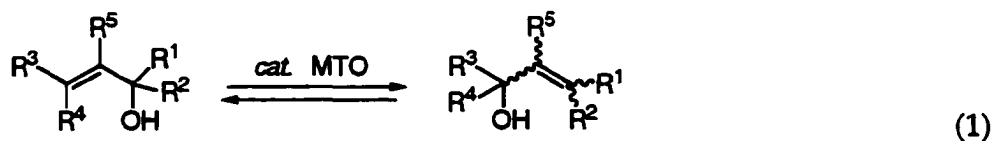
Early studies of the synthesis of vitamin A represent pioneering investigations of the use of allylic rearrangements in the natural products area. The sulfuric acid-catalyzed rearrangement of one allylic alcohol to its more conjugated isomer was used in the original C_{14}–aldehyde route to Vitamin A.[3,4] Multiple allylic rearrangements are characteristic features of Vitamin A synthesis.[5,6] Allylic transpositions of oxygen functionality have found wide applications in many other natural product areas.[7-10]

The classical method for equilibrating an allylic alcohol or ester is with a strong protic or Lewis acid catalyst.[6,9-18] In favorable cases, this method succeeds splendidly, and near quantitative yields have been obtained.[6] More typically, however, the yields are only moderate, the allyl cation intermediates being

diverted in part along other reaction pathways.[11] Side reactions typically encountered are elimination to yield dienes,[12] skeletal rearrangements,[13] cyclization[14] and the formation of resinous materials.[11,15] Herein we report the use of the Lewis acid methylrhenium trioxide (CH_3ReO_3, abbreviated as MTO) to effect allylic transpositions in a single step.

In recent years MTO has received much attention as a versatile homogeneous catalyst for various transformations. The ability of MTO to activate hydrogen peroxide has made it a very useful catalyst for olefin epoxidation and other oxidations.[16-23] Non-oxidative transformations catalyzed by MTO include its use to activate diazo reagents,[24] oligomerize aldehydes,[25] convert epoxides and carbonyl compounds to 1,3-dioxolanes,[25] olefinate aldehydes[26] and metathesize alkenes.[27]

Results and Discussion

Benzene was chosen as the solvent primarily because MTO is especially stable in it. Indeed, in all of the transpositions described in this work, many of which required reaction times of the order of days, no decomposition of the catalyst was noted. Acetonitrile was used in a few instances, and led to a mild prolongation of the reaction. Most data were obtained in benzene for the aforementioned reason.

In a generic sense, all the reactions are the same, resulting in the transformation of one allylic alcohol to another, the consequence of a 1,3 shift of the OH group with accompanying migration of the double bond. These are the features represented in eq 1.

The major results refer to 14 primary, secondary and tertiary allylic alcohols. Both aromatic and aliphatic allylic alcohols were investigated to understand the nature of these isomerizations. The products formed, their

yields, and the reaction times required are presented in **Table 1**. Several of the reactions were nearly quantitative: see entries 2-5. The other cases gave lesser yields, which might be attributed to decomposition/deactivation of the catalyst, to an insufficient reaction time, to side reactions consuming the catalyst, or to the attainment of chemical equilibrium. A proper understanding of this system required that each possibility be explored.

In all cases, MTO was detected by ^{1}H–NMR at the end of the allotted time: it remained intact at essentially the initial concentration, clearly ruling out catalyst decomposition/deactivation. Also any deactivation by polymerisation of MTO can be ruled out since low concentrations of catalyst (5mM) were used.[34] To check this further, additional MTO was added after the allowed time in one experiment, entry 10, but no additional product was formed. Had sufficient time been allowed? These reactions were checked intermittently by NMR, prior to the reported reaction time and after. The buildup of product to a certain level (only) was seen, but waiting longer gave no increase in yield.

We thus turned to the remaining explanations. In certain cases (see entries 6, 7, and 11) the irreversible formation of by-products occurred. Once they were allowed for, mass balance was satisfactory; little starting material remained. The reactions responsible are well known and also require MTO as a catalyst. These reactions consist of condensation (entry 7, eq 2) and dehydration of the product (entries 6, shown in eq 3 and 11).

$$2ROH \xrightarrow{\text{cat. MTO}} ROR + H_2O \qquad (2)$$

$$(3)$$
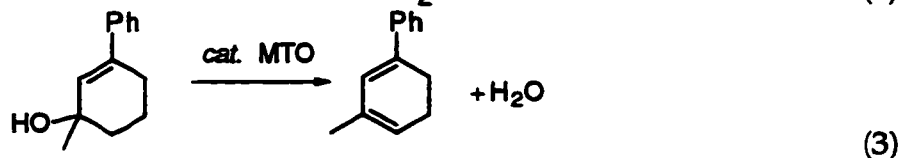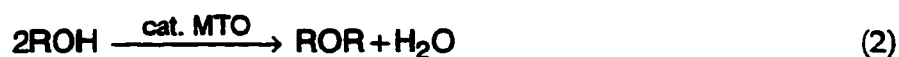
The attainment of chemical equilibrium can also account for lower yields. This is best illustrated by the same direction carried out independently in each reaction, entries 9 and 10, with 1-octene-3-ol and 3-octene-1-ol. They come to essentially the same point, and the mass balance is satisfactory (94%). The equilibrium constant for reaction 4 from these data is K_4 = 1.7 ± 0.2 in benzene at ~23 °C.

$$\overset{HO}{\diagdown}\diagup\!\!\diagdown\diagup\text{-}C_5H_{11} \; \rightleftharpoons \; \diagup\!\!\diagdown\diagup\underset{OH}{\diagdown}\text{-}C_5H_{11}$$

(4)
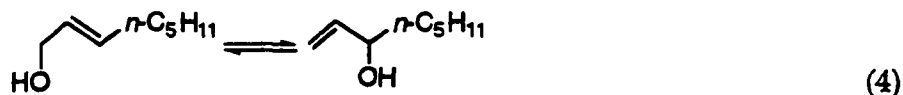
An independent examination of the attainment of equilibrium was sought, with a compound for which the 1,3-transposed pair would be the same. These experiments were carried out with 2-cyclohexen-1-deutero-1-ol. They are interconverted by a degenerate reaction, as shown:

$$\rightleftharpoons$$

(5)

The equilibrium was approached starting from 2-cyclohexen-1-deutero-1-ol and can be easily followed by NMR for the growing alcohol CH proton. Several independent investigations gave the same result. The amounts of the two species at equilibrium are similar but not identical. This can be expressed as an equilibrium constant, K_5 = 1.20 ± 0.02 in benzene at ~23 °C. In other words, this equilibration shows an appreciable *equilibrium isotope effect*; we shall return to discuss this among the theoretical results.

The reaction is found to be very sensitive to the presence of water. Deliberate addition of water (0.25 mol%) to entry 9 showed that the isomerization was largely inhibited in the presence of water (the control reaction

gave 25% of rearranged isomer in 16 h whereas in the presence of added water there was only 5% of rearranged isomer at the same time). The reaction times needed to attain equilibrium from each direction were different: 1 d and 3 d (entries 9 and 10). This, on face value, poses a formidable problem, in that the lifetime for the attainment of equilibrium should be the same starting from either side: $\tau = (k_f + k_r)^{-1}$. The difference in this case arises from a trivial source, because of the sensitivity of the reaction rate to traces of water, which were not rigorously controlled.

We also checked to see whether the catalyst is still active after the equilibration is reached. In a kinetic experiment which was followed by ^{1}H NMR, the isomerization of 3-methyl-2-buten-1-ol(50mM) with 25mM MTO was monitered. After the attainment of equlibrium betweeen the two isomeric allylic alcohols, a second batch of 3-methyl-2-buten-1-ol(50mM) was added. The experimental trace is shown in **figure 1**. In fact, the rate constants agree very well for the two stages of the reaction.

Reaction kinetics

To define the mechanism, we carried out a series of kinetic studies, using 3-methyl-2-buten-1-ol as the test substrate. The reaction was monitored by ^{1}H NMR under varying concentration conditions. In every case, the reaction followed exact first order kinetics. One series of kinetic experiments in C_6D_6 at room temperature was carried out at a constant concentration, 50mM, of allyl alcohol. These are the rate constants obtained at various catalyst concentrations:

[MTO]/mM:	25	40	75	100
$k/10^{-3}$ s^{-1}:	1.53	2.40	4.58	5.94

The plot of k vs [MTO] defines a straight line that passes through the origin, as shown in **Figure 2**. The slope of this line, 0.06 $Lmol^{-1}s^{-1}$, is the second-order rate constant for the reaction between 3-methyl-2-buten-1-ol and MTO.

There is however, an alarming effect of changing the concentration of the allyl alcohol substrate. The following data for 3-methyl-2-buten-1-ol, taken at 25.0 mM MTO, illustrate the situation.

[AA]/mM:	50	100	200	300
$k/10^{-3}s^{-1}$:	1.53	2.72	1.29	0.55

That is, the rate constant decreases with increasing substrate concentration despite the excellent fit to first-order kinetics in each separate experiment. We could identify no kinetic scheme, plausible or otherwise, to account for this set of facts. We also examined the reproducibility of the kinetic data, which was satisfactory among experiments carried out any one day. On other days, variations of the rate constants by factors of 2-4 were not uncommon. Again, the effect of uncontrollable amounts of water seem to be the limiting factor, just as it was in the previously described equilibration studies for entries 9 and 10.

Despite the limitations, the data are nonetheless important to defining the reaction orders in the system. The data present are internally consistent; they are also indicative of the approximate rate constants, within the factors cited.

Attempts to detect two catalyst species, free and bound, by NMR in acetonitrile at low temperature did not succeed. Only allylic alcohols undergo this isomerization with MTO. When a bishomoallylic alcohol (entry 13) was used, no transposition of the OH group was observed. Also allylic ethers (entry 14) do not undergo any isomerization.
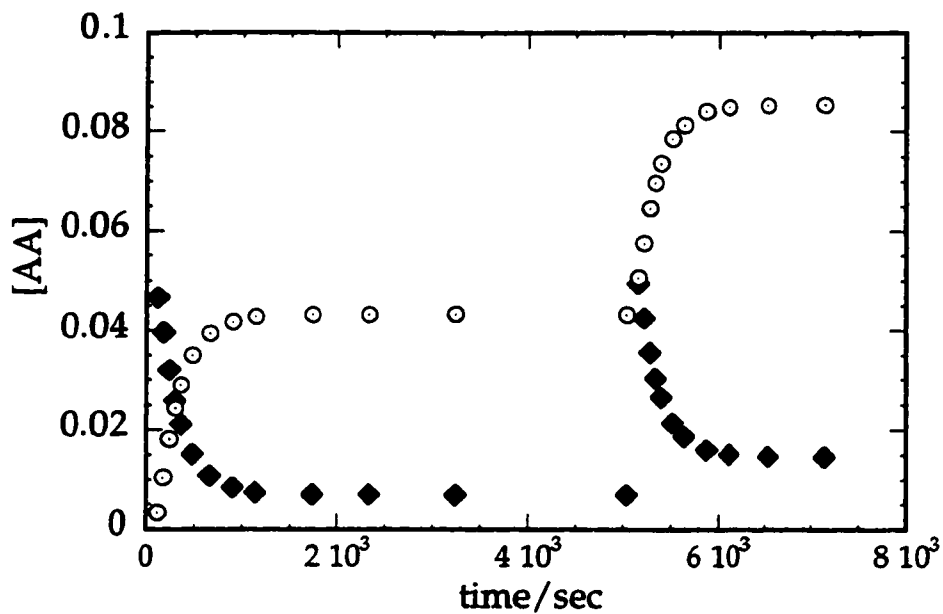
Figure 1. Kinetic trace obtained by NMR spectroscopy for the isomerization of 3-methyl-2-buten-1-ol (decreasing with time) to 2-methyl-3-buten-2-ol (increasing with time). [MTO] = 25mM, [AA] = allyl alcohol = 50mM. The second stage of the reaction indicates a second addition of 3-methyl-2-buten-1-ol.
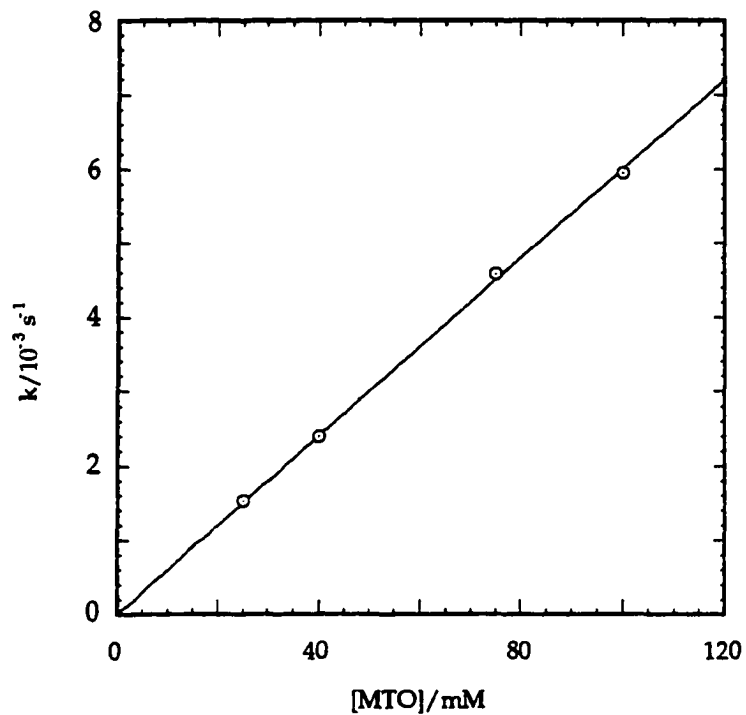
Figure 2. Kinetics of the rearrangement reaction of 3-methyl-2-buten-1-ol at varying concentrations of MTO and a fixed concentration of allyl alcohol, 50mM. The data are displayed as a plot of k vs [MTO], which defines a straight line through the origin.

18O Labelling experiment. Experiments were carried out to trace the origin of the oxygen atom of the rearranged allyl alcohol, in particular to learn whether it comes from MTO. To test this mechanism, ^{18}O-labeled MTO was prepared by allowing $MeRe(^{16}O)_3$ to equilibrate in 95% $H_2^{18}O$ at room temperature for 4 hours. The MTO was then extracted into dichloromethane. GC-MS analysis showed a high level of ^{18}O incorporation in MTO. A stoichiometric reaction between 3-methyl-2-buten-1-ol (entry 15 on Table 1) and $MeRe(^{18}O)_3$ (both at 25mM) was run in C_6D_6. These particular conditions were adopted to minimize exchange that might result after numerous catalytic turnovers. After equilibration, the reaction was analyzed by GC-MS by both CI and EI ionization methods. No ^{18}O incorporation into the rearranged allyl alcohol was observed; 2-methyl-3-buten-2-ol showed only m/z 86 and no m/z 88.

Theoretical Results. Three factors need to be considered to understand the direction of equilibrium in these reactions-a) the position of the OH group, b) the nature of the double bond i.e., more substituted or less substituted and, c) the effect of conjugation. To clarify these points, we adopted a theoretical approach to study these effects. The results are discussed below.

For the isotope substitution studies, we predict a ΔG_{298} difference of about 0.1 kcal/mol for the structures favoring substitution at the longest C–H bond (sp^3 vs sp^2). Calculations relating to the thermodynamics of different isotopic substitution on different substrates are shown in **Schemes 1 and 2.** Calculations on all four of these substrates suggested a ΔG difference of 0.1 kcal/mol in favor of deuterium at the sp^3 center. This agrees with the experimental observation for the substrates shown in **Scheme 1** for which the equilibrium constant was found to be 1.20, corresponding to a ΔG value of 0.11 kcal/mol.

Scheme 1

$$\Delta G_{298}$$

RHF/DZP: 0.12 kcal/mol   0.0 kcal/mol

Scheme 2. ΔG_{298} relative to D_B

RHF/DZP: 0.10   0.09   0.11 kcal/mol
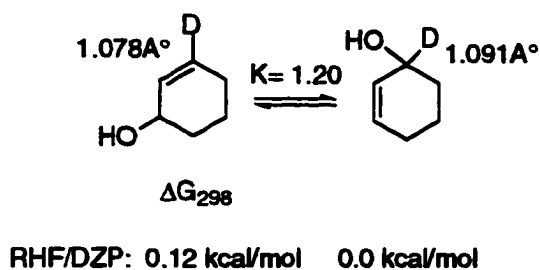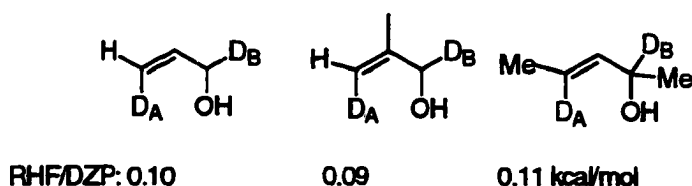
We chose entries 2 and 15 on **Table 1** to study the effect of various factors mentioned above on the direction of equilibrium. The results are summarized in **Scheme 3**. The parent equilibrium between 1 and 2 lies towards the more substituted olefin by 3.3 kcal/mol. This value seems converged with respect to correlation and basis set: MP2/DZP+ = 3.3 kcal/mol, MP2/aug-cc-p VDZ = 2.9 kcal/mol and MP4/DZP = 3.0 kcal/mol. The addition of the OH group reverses the equilibrium (between 5 and 6), while addition of the phenyl group favors substitution at the olefin. The calculations suggest two interesting things about 8: 1) the Z form is lower in energy than the E form by 1.0 kcal/mol, and 2) the two π systems are not in the same plane and the planar structure is a transition state to rotation about the C-Ph bond ($\Delta G^{\ddagger}_{298}$= 7.8 and 2.8 kcal/mol for the cis and trans form of 8 respectively).

The calculations suggest that the two isomers in entry 2 are essentially isoenergetic, whereas experiment predicts a 1.3 kcal/mol energy difference, favoring 8. Currently no level of theory can consistently guarantee a <1 kcal/mol

deviation from experiment for these relatively large systems. However the main conclusion to be drawn from **Scheme 3** regarding the entries in **Table 1** is that

Scheme 3. ΔG_{298} (kcal/mol) values obtained using MP2/DZP+//RHF/DZP
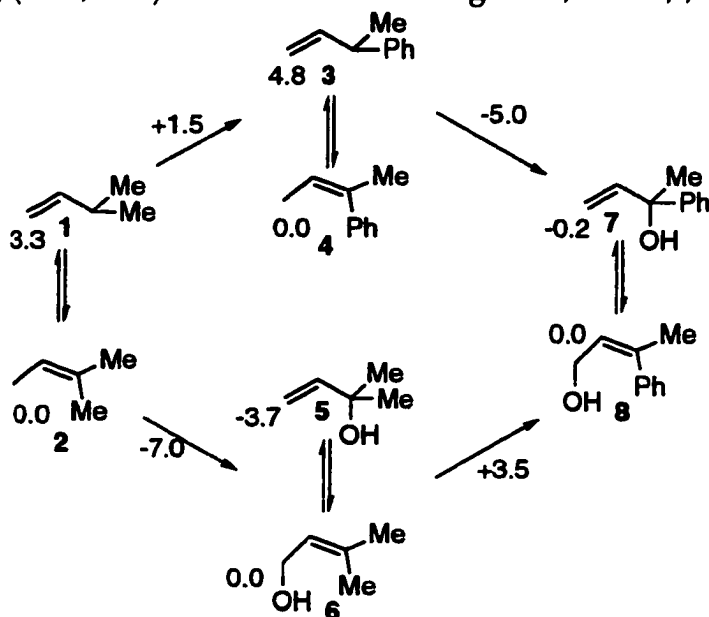
they represent the balance of two competing substituent effects: substitution at the alcohol or olefin site. In the case of alkyl substituents, the effect of substitution at the OH site dominates the effect of substitution at the olefin site (see entries 9-12). According to Scheme 3 this dominance at the OH site is almost, but not quite cancelled when one alkyl substituent is replaced by a phenyl substituent, while experiment suggests that this replacement does shift the dominance to the olefin site (see entries 1-8). It is the shift in dominance between two competing effects on going alkyl to phenyl substituents that predicts a simple explanation of Table 1 in terms of 1°, 2° and 3° alcohols.

Reaction Mechanism. Previous work has shown that MTO readily forms complexes with alcohols and diols.[28] Many stable complexes have been isolated and reported in the literature.[29,30] The -OH group adds across a Re=O bond, just

as it does the reaction between MTO and hydrogen peroxide. This seems a reasonable place to begin the consideration of mechanism. **Scheme 4** presents one plausible mechanism. Similar mechanisms using oxometalcomplexes have been suggested in literature.[31,32] Hence in the first step, MTO most likely forms a monoalkoxy complex with the allylic alcohol. The rearranged isomer can be envisaged as readily obtained from this initially-formed complex by a suitable migration of bonds, **Scheme 4**.

Scheme 4. Suggested mechanism
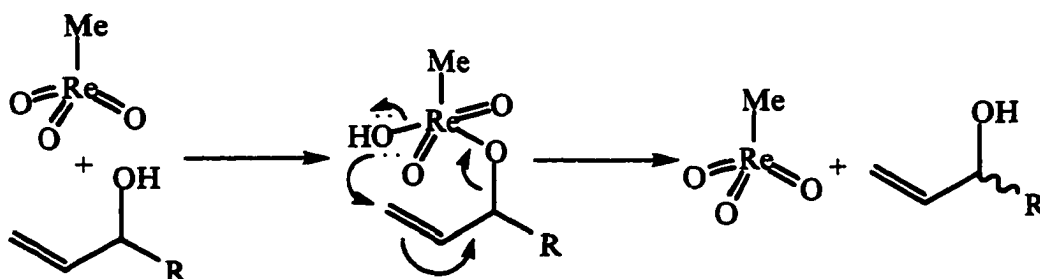
To our surprise, and in contradiction to **Scheme 4**, no ^{18}O incorporation was observed in the rearranged allyl alcohol. We thus suggest an alternative mechansim as depicted in **Scheme 5**. The transformation shown in Scheme 5 accounts for the labelling experiment and for the finding of second-order kinetics. A second allyl alcohol is not invoved in the scheme. We speculate that the inhibiting role of water is to compete with the allyl alcohol in the first step, producing a dead end species $MeRe(O)_2(OH)_2$. The reversible formation of this species accounts for the rapid O-18 exchange between MTO and water, and it parallels the peroxocomplexes formed in reaction between MTO and H_2O_2. Evidently it interferes with the allyl alcohol by reducing the active form of the catalyst.

Conclusions. MTO catalyzes the 1,3-transposition of allylic alcohols in a single step. For benzylic alcohols, the more conjugated isomer predominates at equilibrium. Quantum mechanical calculations suggest that the direction of

Scheme 5. Alternative mechanism
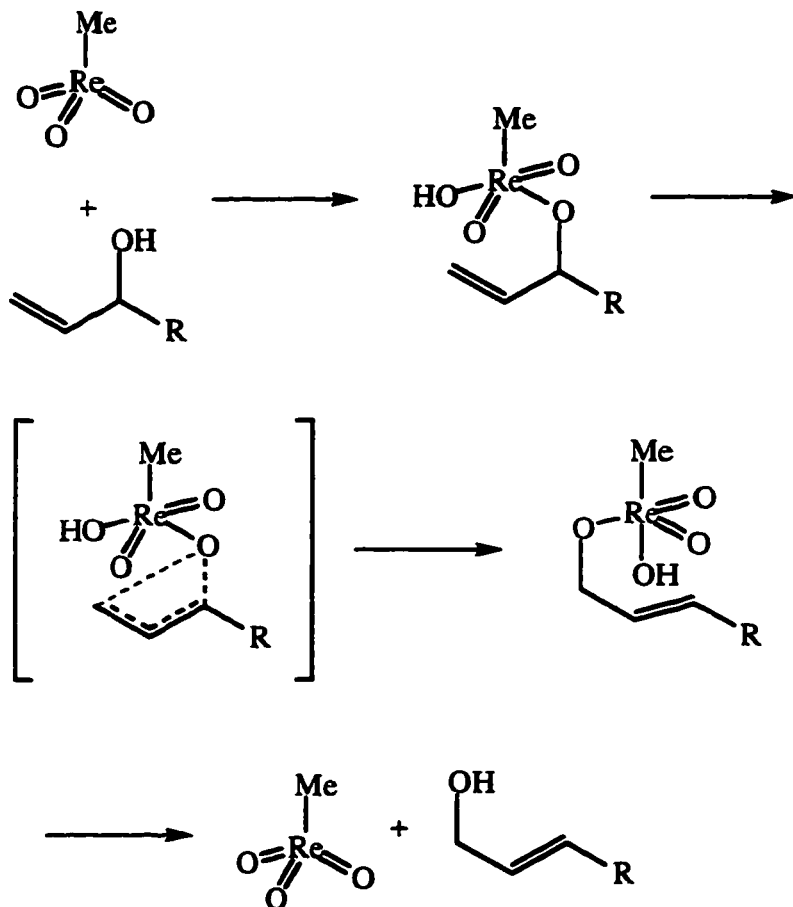
equilibrium is determined by a competition for substitution at the alcohol or olefin site. For alkyl substituents, the more heavily substituted alcohol is favored (entries 9-12, 15). For phenyl substituents, the more conjugated structure is favored. The effect of conjugation appears to be less significant than expected since the phenyl group is forced out of the plane of the allylic π bond.

Experimental Section

Materials. The allyl alcohols used in this study were obtained from commercial sources or synthesized according to literature procedures.[33-37] Their

purities were checked by ^{1}H– and ^{13}C–NMR and by GC–MS. Benzene-d$_6$ obtained commercially was dried by distillation over CaH$_2$ prior to use. The NMR spectra were measured at 300 MHz for protons with Me$_4$Si as an internal standard.

General Procedure. All experiments were done in benzene-d$_6$ with 50 mM substrate concentration and 5 mM catalyst at room temperature. The reactions were followed by NMR and analyzed by GC-MS on attaining equilibrium. The yields were determined by proton integration relative to solvent or Me$_4$Si. The spectral data are in good agreement with accepted values.[38,39]

Computational Methodology. All structures were optimized at the RHF level of theory using the Dunning-Hay polarized double-zeta (DZP) basis set.[40] All structures were shown to be minima (transition states) by analytically computing vibrational frequencies and verifying that none were (only one was) imaginary. Relative energies were computed using second order Moller-Plesset (MP2)[41,42] perturbation theory using the DZP basis set augmented with a diffuse sp shell on each non-hydrogen atom (denoted DZP+).[43] Selected relative energies were also calculated using MP2 with Dunning's augmented correlation-consistent polarized valence double zeta (aug-cc-p VDZ)[44] basis set, and using fourth-order MP theory (MP4)[45] with the DZP basis set. The free energies were computed within the rigid rotor- harmonic oscillator approximation. All calculations were done with the program GAMESS,[46] with the exception of the MP4 calculations which were done with GAUSSIAN92.[47]

Professors V. J. Shiner and G. A. Russell for assistance with considerations relating to the equilibrium isotope effect.

References

1) Buchi, G.; Vederas, J. C. *J. Am. Chem. Soc.* **1972,** *94,* 9128.

2) Overman, L. E.; Campbell, C. B.; Knoll, F. M. *J. Am. Chem. Soc.* **1978,** *100,* 4822.

3) Isler, O.; Ranco, A.; Guex, W.; Hindley, N. C.; Huber, W.; Digler, K.; Kofler, M. *ibid* **1949,** *32,* 489.

4) Isler, O.; Huber, W.; Ranco, A.; Kofler, M. *Helv. Chim. Acta* **1947,** *30,* 1911.

5) Attenburrow, J.; Cameron, A. F. B.; Chapman, J. H.; Evans, R. M.; Hems, B. A.; Jansen, A. B. A.; Walker, T. *J. Chem. Soc* . **1952,** 1094.

6) Olson, G. L.; Cheung, H. C.; Morgan, K. D.; Boren, R.; Saucy, G. *Helv. Chim. Acta.* **1976,** *59,* 567.

7) Woodward, R. B.; Cava, M. P.; Ollis, W. D.; Hunger, A.; Daeniker, H. U.; Schenker, R. *J. Am. Chem. Soc.* **1954,** *76,* 4749.

8) Fehr, T.; Stadler, P. A. *Helv. Chim. Acta* **1975,** *58,* 2484.

9) Babler, H. J.; Olsen, D. O.; Arnold, W. H. *J. Org. Chem.* **1974,** 1656.

10) Babler, J. H. *Tetrahedron Lett.* **1975,** 2045.

11) Murray, A. W. *Organic Reaction Mechanisms;* Interscience: New York, 1975, pp 445.

12) Letourneux, Y.; Lee, M. M.; Choudhari, N.; Gut, M. *J. Org. Chem.* **1975,** *40,* 516.

13) Morrow, D. F.; Culbertson, T. P.; Hofer, R. M. *J. Org. Chem* . **1967,** *32,* 361.

14) Babler, J. H.; Olsen, D. O. *Tetrahedron Lett.* **1974,** 351.

15) de la Mare, P. B. O. *Molecular Rearrangements;* New York, 1963; Vol. 1.

16) Abu-Omar, M. M.; Espenson, J. H. *J. Am. Chem. Soc.* **1995,** *117,* 272.

17) Abu-Omar, M. M.; Hansen, P. J.; Espenson, J. H. *J. Am. Chem. Soc.* **1996,** *118,* 4966.

18) Al-Ajlouni, A.; Espenson, J. H. *J. Am. Chem. Soc.* **1995**, *117*, 9243.

19) Brown, K. N.; Espenson, J. H. *Inorg. Chem.* **1996**, *35*, 7211.

20) Herrmann, W. A.; Fischer, R. W.; Rauch, M. U.; Scherer, W. *J. Mol. Cat* . **1994**, *86*, 243.

21) Murray, R. W.; Iyanar, K.; Chen, J.; Waring, J. T. *Tetrahedron Lett.* **1996**, *37*, 805.

22) Vassell, K. A.; Espenson, J. H. *Inorg. Chem.* **1994**, *33*, 5491.

23) Zhu, Z.; Espenson, J. H. *J. Org. Chem.* **1995**, *60*, 1326.

24) Zhu, Z.; Espenson, J. H. *J. Am. Chem. Soc.* **1996**, *118*, 9901.

25) Zhu, Z.; Espenson, J. H. *submitted for publication*

26) Herrmann, W. A.; Wang, M. *Angew. Chem. Int. Ed. Engl.* **1991**, *103*, 1709.

27) Herrmann, W. A.; Wagner, W.; Flessner, U. N.; Volkhart, U.; Komber, H. *Angew. Chem.Int. Ed. Engl.* **1991**, *103*, 1704.

28) Zhu, Z.; Espenson, J. H. *J. Org. Chem.* **1996**, *61*, 324.

29) Zhu, Z.; Al-Ajlouni, A. M.; Espenson, J. H. **1996**, *35*, 1408.

30) Takacs, J.; Cook, M. R.; Kiprof, P.; Kuchler, J. G.; Herrmann, W. A. *Organomet.* **1991**, *10*, 316.

31) Bellemin-Lopez, S.; Giese, H.; Ny, J. P. L.; Osborn, J. A. *Angew. Chem. Int. Ed. Engl.* **1997**, *36*, 976.

32) Belgacem, J.; Kress, J.; Osborn, J. A. *J. Am. Chem. Soc.* **1992**, *114*, 1501.

33) Johnson, M. R.; Rickborn, B. *J. Org. Chem.* **1969**, *35*, 1041.

34) Luche, J.-L. *J. Am. Chem. Soc.* **1978**, *100*, 2226.

35) Rossi, R.; Carpita, A. *Synthesis* **1977**, 561.

36) Grant, B.; Djerrassi, C. *J. Org. Chem.* **1973**, *39*, 968.

37) Larock, R. C. *Comprehensive Organic Transformations*; VCH Publishers. Inc.: New York, 1989.

38) Silverstein, R. M.; Bassler, G. C.; Morril, T. C. *Spectrometric Identification of Organic Compounds*; 5th ed.; 1991.

39) Pouchert, J. C.; Behnke, J. *The Aldrich Library of* ^{13}C *and* ^1H *FT NMR Spectra*; 1993; Vol. 1.

40) Dunning Jr, T. H. *J. Chem. Phys* . **1989**, *90*, 1007.

41) Moller, C.; Plesset, M. S. *Phys. Rev* . **1934**, *46*, 618.

42) Pople, J. A.; Binkley, J. S.; Beeger, R. *Int. J. Quantum Chem.; Quantum Chem. Symp.* **1976**, *10*, 1.

43) Clark, T.; Chandrasekhar, J.; Spitznagel, G. W.; Schleyer, P. *J. Comp. Chem.* **1983**, *4*, 294.

44) Kendall, R. A.; Jr, T. H. D.; Harrison, R. J. *J. Chem. Phys* . **1992**, *96*, 6796.

45) Krishnan, R.; Frisch, M. J.; Pople, J. A. *J. Chem. Phys* . **1980**, *72*, 4244.

46) Schmidt, M. W.; Baldridge, K. K.; Boatz, J. A.; Elbert, S. T.; Gordon, M. S.; Jenson, J. H.; Koseki, S.; Matsunaga, N.; Nguyen, K. A.; Su, S.; Windus, T. L.; Dupius, M.; Jr, J. A. M. *J. Comp. Chem* . **1993**, *14*, 1347.

47) Frisch, M. J.; Trucks, G. W.; Gordon, M.; Gill, P. M. W.; Wong, M. W.; Foresman, J. B.; Johnson, B. G.; Schlegel, H. B.; Robb, M. A.; Replogle, E. S.; Gomperts, R.; Andres, J. L.; Raghavachari, K.; Binkley, J. S.; Gonzalez, C.; Martin, R. L.; Fox, D. J.; Defrees, D. J.; Baker, J.; Stewart, J. J. P.; Pople, J. A. *Gaussian 92*; A ed.; Gaussian Inc: Pittsburgh PA, 1992.

Table 1. Yields obtained for MTO-catalyzed isomerizations of allylic alcohols [a]
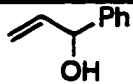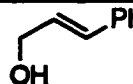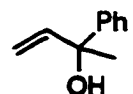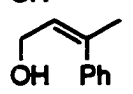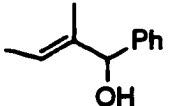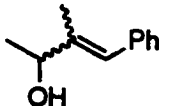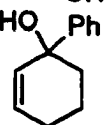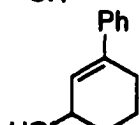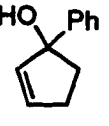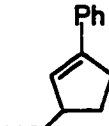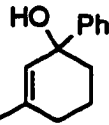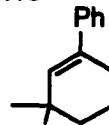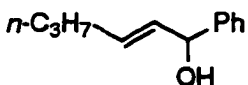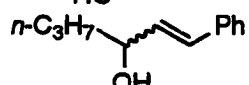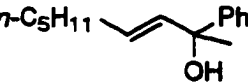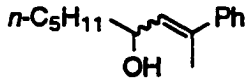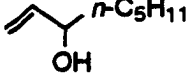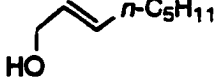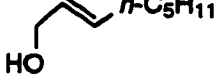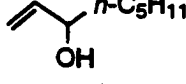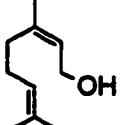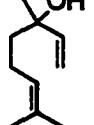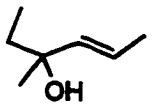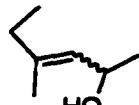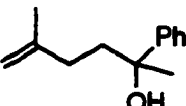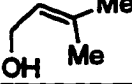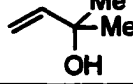
Entry	Substrate	Product	Time	% Yield
1			5 d	63
2			4 d	90[b]

Table 1 continued

Entry	Substrate	Product	Time	Yield
3	(Me)C=CH–CH(OH)–Ph	Me–CH(OH)–CH=CH–Ph	12 h	93
4	1-Ph-1-OH-cyclohex-2-ene	3-Ph-5-HO-cyclohexene	10 h	98
5	1-Ph-1-OH-cyclopent-2-ene	3-Ph-4-HO-cyclopentene	1 d	98
6	1-Ph-1-OH-4-Me-cyclohex-2-ene	3-Ph-1-Me-1-HO-cyclohexene	2 d	65[c]
7	n-C$_3$H$_7$–CH=CH–CH(OH)–Ph	n-C$_3$H$_7$–CH(OH)–CH=CH–Ph	2 d	67[d]
8	n-C$_5$H$_{11}$–CH=CH–C(Me)(OH)–Ph	n-C$_5$H$_{11}$–C(OH)(Me)–CH=CH–Ph	3 d	52
9	CH$_2$=CH–CH(OH)–n-C$_5$H$_{11}$	HO–CH$_2$–CH=CH–n-C$_5$H$_{11}$	1 d	33
10	HO–CH$_2$–CH=CH–n-C$_5$H$_{11}$	CH$_2$=CH–CH(OH)–n-C$_5$H$_{11}$	3 d	61
11	geraniol	linalool	2.5 d	86[e]
12			2 d	30
13	2-Me-5-Ph-5-OH-hex-1-ene	No rxn		
14	C$_5$H$_{11}$–CH=CH–C(Ph)(OEt)–	No rxn		
15	3-Me-but-2-ene-1-ol,3-Me	2-Me-3-Me-but-1-en-3-ol	2.5	87

[a] Reactions carried out in benzene with 5% MTO catalyst; [b] 4:1 ratio of Z and E isomers were obtained. [c] 35% of the dehydration product was also observed, eq 3; [d] ~30% of the ether product was also observed, eq 2; [e] 7% of the dehydration product also observed. {entries 1-8, 13 and 14 were synthesized by direct addition of phenyl lithium to the corresponding aldehyde or ketone.[37] All the remaining substrates were purchased from comercial sources.}

Supporting Information

¹H and ¹³C NMR data for the different allylic alcohols

Product	¹H NMR	¹³C NMR
trans-3-phenyl-2-propen-1-ol	7.74-7.03 (m, 5H)6.41 (dt, 1H, J=15.9Hz, 1.5Hz)6.08 (dt, 1H, J=15.9Hz, 5.4 Hz) 3.92 (dd, 2H, J= 5.4Hz, 1.5Hz)ppm	137.37, 130.52, 129.31, 128.79, 126.73, 115.70, 63.35 ppm
3-phenyl-2-buten-1-ol (Z- isomer)	7.46-7.01 (m, 5H) 5.85 (tq, 1H, J= 6.3 Hz, 1.2 Hz) 4.0 (dq, 2H, J= 6.3Hz, 1.2Hz) 1.76 (d, 3H, J= 1.2 Hz) ppm	145.48, 129.75, 128.99, 127.45, 126.96, 125.56, 59.47, 29.48 ppm
3-phenyl-2-buten-1-ol (E- isomer)	7.46-7.01 (m, 5H) 5.56 (tq, 1H, J= 6.9Hz, 0.9Hz) 3.90 (dq, 2H, J= 6.9Hz, 0.9Hz) 1.74 (d, 3H, J= 0.9Hz) ppm	141.68, 129.34, 128.49, 127.34, 126.57, 126.05, 59.80, 30.51 ppm
3-methyl-4-phenyl-3-buten-2-ol	7.54-7.01(m, 5H) 5.54 (q, 1H, J= 6.8Hz) 4.89 (s, 1H) 1.46 (d, 3H, J=6.8Hz) 1.39 (s, 3H) ppm	138.44, 128.99, 127.45, 127.20, 126.52, 120.85, 79.34, 13.06, 11.48 ppm
3-phenyl-2-cyclohexen-1-ol	7.3-7.11(m, 5H) 6.31 (m, 1H) 4.14 (m, 1H) 2.26-1.46 (m, 6H) ppm	141.68, 139.37, 128.74, 127.85, 125.43, 65.93, 31.66, 29.35, 27.33, 19.48 ppm

3-phenyl-2-cyclopenten-1-ol	7.46-7.40 (m, 2H) 7.20-7.14 (m, 2H) 7.05 (m, 1H) 5.68 (d, 1H) 3.90 (m, 1H) 2.27-2.00(m, 4H) ppm	147.67, 137.17, 133.74, 128.74, 126.59, 125.05, 62.55, 42.20, 31.34 ppm
1-methyl-3-phenyl-2-cyclohexen-1-ol	7.57 (dd, 2H, J= 8.4 Hz, 1.2Hz) 7.22-7.09 (m, 3H) 5.37 (s, 3H) 1.91-1.86 (m, 2H) 1.70-1.25 (m, 4H) 1.54 (s, 3H) ppm	149.34, 137.62, 128.99, 128.16, 126.79, 125.99, 72.45, 39.78, 30.06, 23.71, 19.71 ppm
1-phenyl-1-hexen-3-ol (trans)	7.65-7.20 (m, 5H) 5.54 (d, 1H, J=15.9Hz) 5.08 (dd, 1H, J=15.9, 6.3Hz) 4.15 (m, 1H) 1.62-1.41 (m, 4H) 0.92 (t, 3H) ppm	146.57, 135.44, 132.84, 130.17, 128.91, 128.01, 62.54, 35.83, 24.08, 14.90 ppm
2-phenyl-3-nonen-2-ol (trans)	7.48-7.45 (m, 2H) 7.19-7.04 (m, 3H) 5.70-5.31(m, 2H) 1.36 (s, 3H) 1.92-1.16 (m, 8H) 0.82 (t, 3H) ppm	148.17, 137.93, 126.84, 125.68, 129.02, 128.47, 74.09, 32.53, 31.77, 30.26, 29.33, 22.86, 14.27 ppm
1- Octen-3-ol	5.79-5.68 (ddd, 1H, J= 17.4Hz, 10.5Hz, 6Hz) 5.1 (dt, 1h, J= 17.4Hz, 1.5Hz) 4.94 (ddd, 1H, J= 10.5, 1.5, 1.5Hz) 3.85 (m, 1H) 1.41-1.19 (m, 8H)0.85 (t, 3H, J= 7.2Hz) ppm	142.20, 113.65, 72.95, 37.48, 32.13, 25.38, 22.99, 14.24 ppm

2-Octen-1-ol	5.5(m, 5H) 3.90 (m, 2H) 1.94 (m, 2H) 1.44 (br, 1H) 1.33- 1.17 (m, 6H) 0.89 (t, 3H) ppm	132.07, 129.97, 63.50, 32.53, 31.67, 29.25, 22.87, 14.21ppm
geraniol	5.40 (m, 1H) 5.06 (m, 1H) 4.11(d, 1H, J= 6.9 Hz) 2.03 (m, 4H) 1.64 (s, 3H) 1.59 (s, 3H) 1.57 (d, 3H, J= 1.8Hz) ppm	139.63, 131.68, 123.85, 122.87, 59.30, 39.49, 26.33, 25.62, 17.63, 16.20 ppm
linalool	5.80 (dd, 1H, J= 7.8 Hz, 12.9Hz) 5.10 (d, 1H, J= 12.9 Hz, 0.9Hz) 5.0 (t, 1H) 4.94 (dd, 1H, J= 8.9 Hz, 0.9Hz) 1.90 (t, 2H) 1.56 (s, 3H) 1.49 (d, 3H, J= 0.9Hz) 1.45 (m, 2H) 1.16 (s, 3H) ppm	144.99, 131.92, 124.28, 111.65, 73.44, 42.00, 27.84, 25.67, 22.76, 17.66 ppm
3-methyl4-hexen-3-ol	5.60-5.40 (m, 2H) 1.65 (d, 3H, J= 6Hz) 1.42 (q, 2H, J= 7.6Hz) 1.37 (s, 3H) 0.80 (t, 3H, J= 7.6Hz) ppm	137.79, 122.61, 72.87, 35.16, 30.21, 27.11, 17.60 ppm
2-Cyclohexen-1-deutero-1-ol	5.70 (d, 1H, J= 10.20 Hz) 5.60 (dt, 1H, J= 10.2Hz, 3.3 Hz)1.74-1.37 (m, 6H) ppm	130.97, 129.55, 64.90(t), 32.19, 25.76, 19.33 ppm

2-Cyclohexen-3-deutero-1-ol	5.70 (d, 1H) 4.03 (m, 1H) 1.74-1.29 (m, 6H) ppm	
5-methyl-5-hexen-2-phenyl-2-ol	7.36-7.01 (m, 5H) 4.72 (m, 2H) 2.04-1.79 (m, 4H) 1.54 (s, 3H) 1.31 (s, 3H) ppm	148.10, 145.93, 128.74, 126.34, 124.90, 109.63, 73.95, 42.15, 32.18, 30.51, 22.45 ppm
3-methyl-2-buten-1-ol	5.35 (tq, 1H, J= 6.8Hz, 1.2Hz) 4.07 (d, 2H, J= 6.8Hz) 1.69 (s, 3H) 1.63 (s, 3H) ppm	136.15, 123. 56, 59.17, 25.65, 17.72 ppm
2-methyl-3-buten-2-ol	5.80 (dd, 1H, J= 15.0, 10.8 Hz) 5.20 (dd, 1H, J= 15.0, 1.5Hz) 4.93 (dd, J= 10.8, 1.5Hz) 1.18 (s, 6H) ppm	146.07, 110.79, 71.06, 29.34 ppm

CHAPTER VI. ISOMERIZATION OF PROPARGYLIC ALCOHOLS TO ENONES AND ENALS CATALYZED BY METHYLRHENIUM TRIOXIDE

Introduction

The oxophilicity of rhenium in the highly electrophilic and organic-soluble compound methylrhenium trioxide (CH_3ReO_3, abbreviated as MTO) affords any number of possibilities for organic transformations. The potential of MTO as a catalyst for selective oxidations was considerably advanced by a synthesis of MTO[1] more convenient than the original.[2]

Selective oxidations comprise one major area first recognized for MTO.[3-12] Other, non-oxidative transformations have also been discovered: alcohols are catalytically dehydrated to ethers,[13] aldehydes oligomerized to 1,3,5-trioxanes,[14] epoxides and carbonyl compounds converted 1,3-dioxolanes;[14] also, epoxides and sulfoxides are deoxygenated with triphenyl phosphine as the oxygen acceptor and MTO as the catalyst,[15,16] etc. Epoxides are catalytically converted to 1,2-diols with MTO, and much more rapidly with MTO/H_2O_2.[17,18]

With these points in mind, the possibility of using easily-synthesized propargylic alcohols as synthetic precursors in catalytic reactions was examined. These alcohols afford rearrangement products, α,β-unsaturated carbonyl compounds.[19] They are valuable intermediates in organic synthesis, finding application for fragrances, carotenoids, etc.[20] Certain transition metal complexes are known to mediate the isomerization of propargylic alcohols by a 1,3 transposition of oxygen, as given in eq 1, referred to as a Meyer-Schuster rearrangement,[21-25] or by hydride migration, a Rupe rearrangement.[21,26-29]

$$R^2 \overset{R^1}{\underset{HO}{\overset{|}{\underset{|}{C}}}} - C \equiv C - R(H) \quad \xrightarrow[\text{C}_6\text{H}_6, \text{ RT}]{\text{MTO (10 mol\%)}} \quad H - \overset{O}{\underset{C}{\underset{\|}{\overset{\|}{C}}}} \overset{\overset{\|}{C}}{R(H)} \overset{R^1}{\underset{R^2}{}}$$

(1)
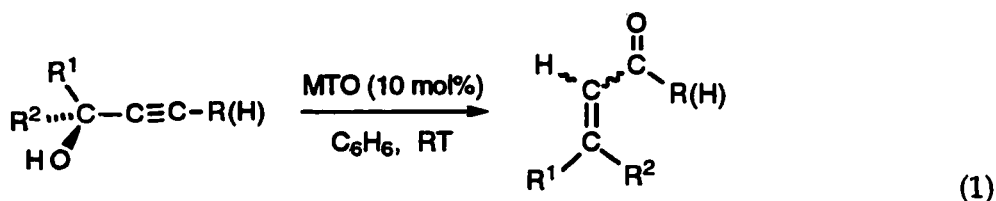
Owing to the potential synthetic economy of such isomerizations, both of these rearrangements have been the focus of prior effort, as cited previously. During our studies of the catalytic functionalization of alcohols and related oxygen-containing substances[13,16] we found that MTO could catalyze several rearrangement reactions of oxygenates. Consequently we examined its effect on propargylic alcohols, and report here MTO catalyzes the rearrangement of propargylic alcohols into α,β-unsaturated aldehydes and ketones with a 1,3- shift of OH group.

Results and Discussion

A considerable number and variety of secondary and tertiary α-acetylenic alcohols were examined. The findings are summarized in **Table 1**. Most of the catalytic reactions with MTO produced good yields of the rearranged enals and enones. Those propargylic alcohols that are benzylic (R^1 = arene, eq 1) gave the rearranged carbonyl compounds in good yield. Both internal and terminal alkynes underwent efficient catalytic conversion to the rearranged product.

Several aliphatic propargylic alcohols (R = alkyl) were also investigated. They gave low yields; two examples are presented in entries 10 and 12; seven others, not tabulated, were equally unsatisfactory. Two silyl-substituted acetylenes, entries 6 and 11, underwent a previously-reported[13] condensation reaction to an ether (eq 2) rather than rearrangement, and a third bearing a strongly electron-attracting group, entry 5, underwent neither reaction.

$$2 \, R^1R^2C(OH)C{\equiv}CSiMe_3 \rightarrow [Me_3SiC{\equiv}CCR^1R^2]_2O + H_2O \qquad (2)$$

Water has been shown to inhibit ether formation.[13] When 1 eq of water was also added was added at the start of one of the reactions (repeating entry 11 in table 1), no ether formed within 3 days. This is probably due to the preferential coordination of water to the catalyst. The starting material remain unchanged during this period.

Several days were required for these reactions to reach completion. This delay is the result of a long induction period, often 2-4 days, more than an inherently slow process. Once that time had elapsed, product buildup occurred usually within 10-24 hours and could be observed in the ^1H NMR spectra.

Our attempts to use ^1H NMR to determine the origin of the induction period were not successful. Neither MTO alone nor the reaction mixture gave signals for species other than those for the separate species themselves. Variation of the catalyst to substrate ratio doesn't seem to have any significant effect on the induction period. The phenomenon of an induction period is not unique to this one MTO catalytic system, as it has been observed elsewhere. The reactions between alcohols and ethyl diazoacetate[30,31] experienced long and unaccountable delays before the onset of reaction. Neither exceptionally dry materials nor deliberately moist ones altered the situation.[32] When 1 eq of water and propargyl alcohol were added, only 30% conversion was found; otherwise it was 98% (entry 1).

Further NMR studies were carried out for 1-phenyl-2-propyne-1-ol, entry 1. After 18 h, the ^1H spectrum showed two new olefinic doublets at δ 5.80 and 5.35 ppm with a coupling constant of 2.1 Hz, probably indicating an allene type intermediate. This intermediate was detected in no more than 10% yield. The

concentration of the intermediate was too low for a reliable ^{13}C NMR signal. When $TiCl_4$ was added, its concentration was considerably enhanced and the ^{13}C spectrum showed a new signal at 202.17 ppm, which comes in the region expected for the central carbon of an allene. The carbonyl carbons of the products have chemical shifts of δ 189 (Z) and 190 (E) ppm.[33]The effect of titanium(IV) is to stabilize the intermediate; we suggest the species formed in this interaction is:
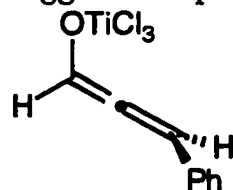

In our efforts to find a co-catalyst to accelerate the rearrangement, we tried both $TiCl_4$ and $Sn(OTf)_2$, but neither were effective. Instead, each of them led to the formation of a more intense NMR signal for the intermediate, increasing its concentration as depicted.

The reaction was also carried out by adding PhCH(OH)C≡CH (cf. entry 1) in three successive portions to a given MTO-solvent mixture. The first portion (0.072 mmol) was, after 3.5 d, converted to product in 82% yield. The second portiom (0.06 mmol) gave 83% conversion (overall) after 1.5 days, and the third (0.06 mmol) 73% conversion in 1.5 d. The fact that the second two increments cut the reaction time more than two-fold suggests that a more active form of MTO is produced during the induction period. Clearly the catalyst is not deactivated as a result of having participated in a large number of turnovers.

Mechanism

Scheme 1 presents a plausible mechanism. We were guided in our thinking by the results obtained for MTO-catalyzed reactions of alcohols, where it was shown that the initial step is an association between MTO and the alcohol;

actually, addition of RO–H across Re=O, reaction I.[13] Within the alkoxyrhenium complex so formed, it appears the bonds reorganize either as in Reactions II or III, which represent polar and ionic alternatives. Reaction II would give rise to an allenol-type intermediate that goes on to give the α,β-unsaturated aldehyde or ketone. Evidence for such came from the NMR data for the detected intermediate, presented in the preceding section. **Scheme 1. Scheme 1. Suggested Mechanism**
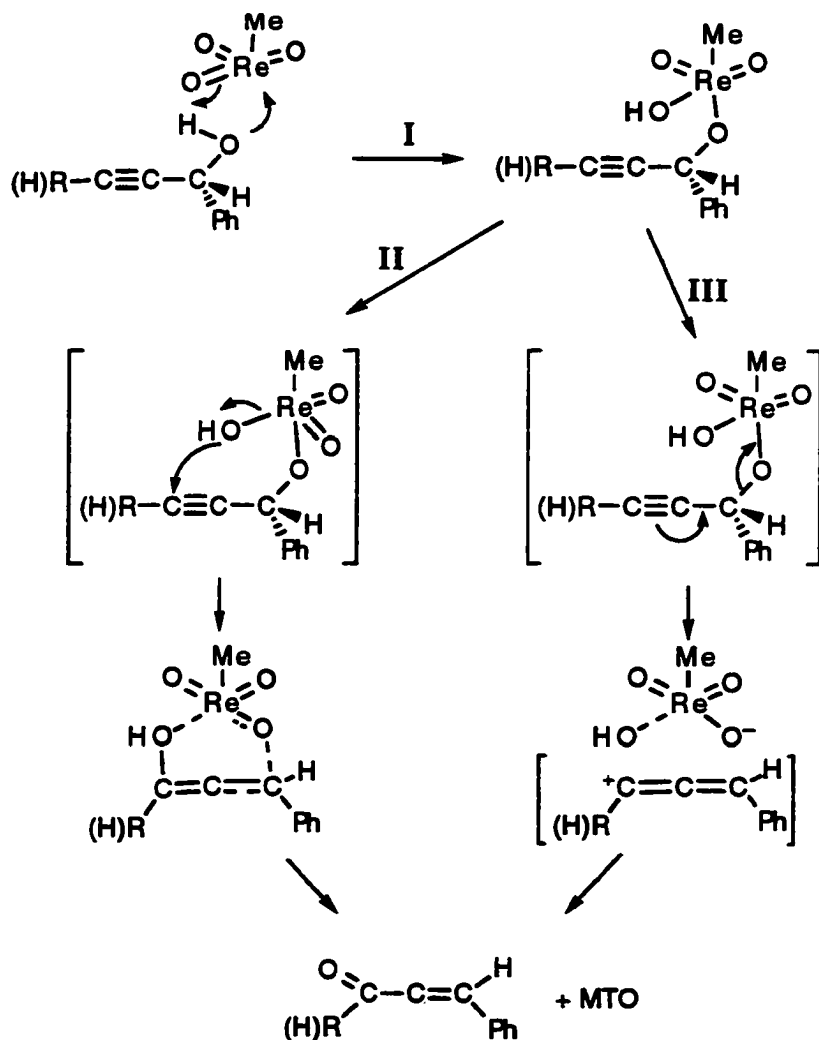
The intermediate amounts to, at most, 10% of the substrate taken; the MTO catalyst was used at the 10% level. This coincidence hints that the allenol intermediate may be bound to rhenium.

That fact that the p-nitro compound did not rearrange at all is indicative of a powerful electronic effect. An ionic mechanism, Reaction III of Scheme 1, can be considered. On this basis a higher rate would have been expected for entries 7 and 9, whereas they take a longer time, perhaps owing to steric factors. Changing the solvent to the more polar solvent acetonitrile did not increase the rate, but this is very likely just another manifestation of the long induction period. The catalyst is very stable in benzene.

Conclusions. The Meyer-Schuster rearrangement of propargylic alcohols to α,β-unsaturated ketones and aldehydes proceeds in good-to-excellent yields with the MTO catalyst. The rearranged products are valuable Michael acceptors widely used in organic synthesis. The variable induction period which is poorly understood poses a serious limitation to this otherwise interesting reaction.

EXPERIMENTAL SECTION

Materials. The propargylic alcohols were prepared according to literature procedures.[34,35] Their purities were checked by ^{1}H and ^{13}C NMR and by GC-MS. Methylrhenium trioxide was synthesized according to a literature procedure.[1] Anhydrous benzene was obtained commercially, and used as such, avoiding exposure to atmospheric moisture. The NMR spectra were measured at 300 MHz for protons with Me_4Si as an internal standard.

General procedure. In a typical experiment, the propargylic alcohol (1.25 mmol) and MTO (0.125 mmol) were added to 10 mL anhydrous benzene in a round-bottomed flask and stirred at room temperature. The reaction was

monitored intermittently by TLC. After the reaction was complete, the solvent was evaporated under vacuum and the products isolated by column chromatography, if necesssary. The products were characterized by ^1H and ^{13}C NMR and by GC-MS. The spectral data are in good agreement with accepted values.[36,37]

Table 1. Products and yields of catalytic rearrangement of propargylic alcohols to ketones and aldehydes

Entry	Substrate R	R^1	R^2	Product yield	Time/d	E/Z
1	H	Ph	H	98%	4	9:1
2	H	Ph	Me	95	7	2:1
3	Ph	p-MeOC$_6$H$_4$	H	>99	2	1:4
4	H	p-MeOC$_6$H$_4$	H	83	4	5:2
5	SiMe$_3$	p-O$_2$NC$_6$H$_4$	H	nr		
6^a	SiMe$_3$	p-MeOC$_6$H$_4$	H	98	3	
7	H	p-MeOC$_6$H$_4$	p-MeOC$_6$H$_4$	96	7	
8	n-C$_6$H$_{13}$	Ph	H	43	5	2:1
9	n-C$_6$H$_{13}$	Ph	Ph	95	7	
10	H	n-C$_5$H$_{11}$	H	5	4	

| 11[a] | SiMe$_3$ | p-MeOC$_6$H$_4$ | p-MeOC$_6$H$_4$ | 98 | 3 | |
| 12 | Me | Me | Et | 30 | 5 | 2:1 |

[a] The ether formed by condensation of two substrate molecules, as shown in eq 2, was the major product.

References

1) Herrmann, W. A.; Kühn, F. E.; Fischer, R. W.; Thiel, W. R.; Romao, C. C. *Inorg. Chem.* **1992,** *31,* 4431.

2) Beattie, I. R.; Jones, P. J. *Inorg. Chem.* **1979,** *18,* 2318.

3) Herrmann, W. A.; Fischer, R. W.; Marz, D. W. *Angew. Chem. Int. Ed. Engl.* **1991,** *30,* 1638.

4) Herrmann, W. A.; Fischer, R. W.; Scherer, W.; Rauch, M. H. *Angew. Chem. Int. Ed. Engl.* **1993,** *32,* 1157.

5) Thiel, W. R.; Fischer, R. W.; Herrmann, W. A. *J Organomet. Chem.* **1993,** *459,* C9-C11.

6) Huston, P.; Espenson, J. H.; Bakac, A. *Inorg. Chem.* **1993,** *32,* 4517.

7) Vassell, K. A.; Espenson, J. H. *Inorg. Chem.* **1994,** *33,* 5491.

8) Espenson, J. H.; Pestovsky, O.; Huston, P.; Staudt, S. *J. Am. Chem. Soc.* **1994,** *116,* 2869.

9) Abu-Omar, M. M.; Espenson, J. H. *J. Am. Chem. Soc.* **1995,** *117,* 272.

10) Hansen, P. J.; Espenson, J. H. *Inorg. Chem.* **1995,** *34,* 5389.

11) Zhu, Z.; Espenson, J. H. *J. Org. Chem.* **1995,** *60,* 1326.

12) Zhu, Z.; Espenson, J. H. *J. Org. Chem.* **1995,** *60,* 7727.

13) Zhu, Z.; Espenson, J. H. *J. Org. Chem.* **1996,** *61,* 324.

14) Zhu, Z.; Espenson, J. H. , submitted for publication.

15) Herrmann, W. A.; Wang, M. *Angew. Chem. Int. Ed. Engl.* **1991,** *30,* 1641.

16) Zhu, Z.; Espenson, J. H. *J. Mol. Catal.* **1995,** *103,* 87.

17) Herrmann, W. A.; Fischer, R. W.; Rauch, M. U.; Scherer, W. *J. Mol. Catal.* **1994,** *86,* 243.

18) Jacob, J.; Espenson, J. H. , submitted for publication.

19) Corey, E. J.; Terashima, S. *Tetrahedron Letters* . **1972,** *18,* 1815-16.

20) Meyer, H.; Isler, O. *Carotenoids*; Birkhaeuser Verlag, Basle:, 1971.

21) Swaminathan, S.; Narayanan, K. V. *Chem. Rev.* **1971**, *71*, 429.

22) Choudary, B. M.; Prassad, A. D.; Valli, V. L. K. *Tetrahedron Letters* **1990**, *31*, 7521.

23) Pauling, H.; Andrews, D. A.; Hindley, N. C. *Helv. Chim. Acta* **1976**, *59*, 1233.

24) Narasaka, K.; Kusuma, H.; Hayashi, Y. *Tetrahedron* **1992**, *48*, 2059.

25) Chabardes, P. *Tetrahedron Letters* **1988**, *29*, 6523.

26) Trost, B. M.; Livingston, R. C. *J. Am. Chem. Soc.* **1995**, *117*, 9586-87.

27) Lu, X.; Ji, J.; Guo, C.; Shen, W. *J . Organomet. Chem.* **1992**, *428*, 259.

28) Ma, D.; Lu, X. *Tetrahedron Letters* . **1989**, *30*, 2109.

29) Minn, K. *Synlett* **1991**, 115.

30) Zhu, Z.; Espenson, J. H. *J. Org. Chem.* **1995**, *60*, 7090.

31) Zhu, Z.; Espenson, J. H. submitted for publication.

32) Stankovic´, S. unpublished information.

33) Landor, S. R. *The Chemistry of the Allenes*; Academic Press: New York, 1982; Vol. 3.

34) Larock, R. C. *Comprehensive Organic Transformations*; VCH Publishers. Inc.: New York, 1989.

35) Brandsma, L.; Verkruijsse, H. D. *Synthesis of Acetylenes, Allenes and Cumulenes*; Elsevier Scientific Publishing Company: New York, 1981.

36) Pouchert, C. J.; Behnke, J. *The Aldrich Library of ^{13}C and ^{1}H FT-NMR Spectra*, 1993.

37) Silverstein, R. M.; Bassler, G. C.; Morrill, T. C. *Spectrometric Identification of Organic Compounds.*; John Wiley & Sons,Inc: New York, 1991.

SUPPORTING INFORMATION

Table 2: NMR data in $CDCl_3$ (rel to Me_4Si) for the less common products

Product	^1H NMR	^{13}C NMR
Ph(Me)C=CH-CHO (Z-isomer)	9.46 (d, 1H, J 8.1 Hz), 7.67-7.32 (m, 5H), 6.13(dq, 1H, J 8.1,1.5 Hz), 2.3 (d, 3H, J 1.5 Hz)	193.40, 162.12, 138.37, 129.68, 128.28, 127.21, 125.92, 26.38
Ph(Me)C=CH-CHO (E-isomer)	10.17 (d, 1H, J 7.8 Hz), 7.67-7.32 (m, 5H), 6.4 (dq, 1H, J 1.2, 7.8 Hz) 2.56 (d, 3H, J 1.2Hz)	191.21, 157.60, 136.56, 129.11, 128.35, 126.21, 122.17, 16.32
Ph-CO-CH=CH-Ar (Z-isomer)	7.99 (dd, 2H, J 8.4,1.5 Hz), 7.79-7.48 (m, 5H), 7.42 (d, 1H, J 11.4 Hz), 7.34 (d, 1H, J 11.4 Hz), 6.9 (dd, 2H, J 8.4, 1.5 Hz), 3.79 (s, 3H)	190.34, 161.55, 144.54, 138.34, 132.43, 130.11, 128.43, 128.27, 127.43, 119.55, 114.28, 55.22
Ph-CH=CH-CO-(CH2)5-CH3 (E-isomer)	7.63 (d, 2H), 7.56 (d, 1H, J 16 Hz), 7.15 (m, 3H), 6.65 (d, 1H, J 16 Hz), 2.38 (t, 3H), 1.73-1.68 (m, 2H), 1.45-1.14 (m, 8H), 0.94 (3H, t, J 7.2 Hz)	201.82, 135.91, 130.14, 130.09, 129.11, 128.40, 126.70, 41.08, 32.02, 31.54, 29.32, 24.21, 22.80, 14.25

Ph-CH=CH-CO-(CH$_2$)$_5$- CH$_3$ (Z-isomer)	7.63 (d, 2H), 7.15 (m, 3H), 6.48 (1H, d, J 12 Hz), 5.94 (d, 1H, J 12 Hz), 2.24 (t, 2H), 1.62 (m, 2H), 1.45-1.14 (m, 8H), 0.89 (3H, t, J 7.2 Hz)	198.80, 142.43, 138.93, 135.16, 129.22, 128.97, 128.13, 43.63, 31.89, 29.08, 24.36, 22.80, 14.25
Ar$_2$C=CH-CHO	9.77 (d, 1H, J 8.4Hz), 7.19 (d, 2H, J 8.8 Hz), 6.95 (d, 2H, J 8.8 Hz), 6.64-6.60 (overlapping doublets, 5H, J= 8.4, 8.8 Hz)	192.21, 161.85, 160.95, 160.83, 132.59, 130.66, 129.58, 127.92, 126.23, 114.29, 113.19, 54.83, 54.74
Ph$_2$C=CH-CO-(CH$_2$)$_5$- CH$_3$	7.18-6.99 (m, 10H), 6.53 (s, 1H), 2.06 (t, 2H, J 6.6 Hz), 1.58-1.48 (m, 2H), 1.24-1.06 (m, 6H), 0.82 (t, 3H, J 7.2 Hz)	200.73, 152.02, 141.70, 139.65, 130.05, 129.17, 128.65, 128.57, 128.50, 128.39, 127.82, 43.16, 31.89, 29.19, 24.57, 22.82, 14.22

Ar = p-methoxyphenyl

CHAPTER VII. SELECTIVE C-H BOND ACTIVATION OF ARENES CATALYZED BY METHYLRHENIUM TRIOXIDE

Josemon Jacob and James H. Espenson*

Abstract

Arenes, in glacial acetic acid, are oxidized to para-benzoquinones by hydrogen peroxide in high yields when methylrhenium trioxide (CH_3ReO_3 or MTO) is used as a catalyst. In some cases an intermediate hydroquinone was also obtained in lower yield. Oxidation of the methyl side chains of various methylbenzenes did not occur. The active catalyst species are the previously-characterized η^2-peroxorhenium complexes, $CH_3Re(O)_2(\eta^2-O_2)$ and $CH_3Re(O)(\eta^2-O_2)_2(H_2O)$. Separate tests showed that hydroquinones and phenols are oxidized by H_2O_2–MTO more rapidly than the simple arenes; in the proposed mechanism they are intermediate products. Higher conversions were found for the more highly-substituted arenes, consistent with their being the most reactive species toward the electrophillically-active peroxide bound to rhenium. Failure to achieve high conversions in the less substituted members of the series reflects concurrent deactivation of MTO-peroxide, a process of greater import for the more slowly-reacting substrates.

Introduction

The oxidation of methyl-substituted arenes can occur either at the side chains or at the ring; see **Scheme 1**. Both processes are important, in that hydroquinones and quinones are valuable intermediates; finding even greater

---

1. Jacob, J.; Espenson, J. H. *Inorg. Chim. Acta*, **270**, **1998**, 55–59.

application are the benzene polycarboxylic acids, which give rise to useful polymers. Polycarboxylic acids are produced on a commercial scale by oxidation of methyl side chains. [1] Ring oxidation, as ordinarily carried out, is less satisfactory; the existing methods are insufficiently selective, in that some side-chain oxidation occurs as well. [2-7]
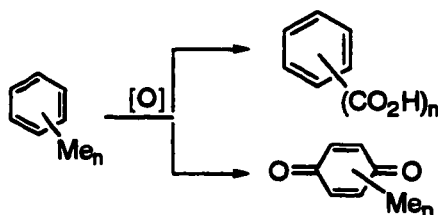
Scheme 1 – competing oxidation of ring and side chain

A catalyst is needed whichever mode of oxidation is the desired one in given circumstances, since these oxidations are invariably sluggish under ordinary conditions and even at higher temperatures. It is also essential that the desired oxidation be made to occur with high selectivity.

To address these issues, we have explored the use of hydrogen peroxide in reactions catalyzed by methylrhenium trioxide (CH_3ReO_3, abbreviated as MTO). Herrmann and co-workers recognized the potential of MTO in catalytic oxidations, [8-11] The operative mechanisms have been explored not only for oxidations [12-17] but for other organic transformations. [18-22]

Certain background information pertaining to MTO-catalyzed reactions of hydrogen peroxide should be noted. The reactions occur by oxygen atom transfer from either of the two η^2-peroxorhenium species that exist in equilibrium with MTO and hydrogen peroxide solutions. The peroxides will be referred to as **A**, the monoperoxo complex, and **B**, the diperoxo complex. The reversible reactions by which they are formed and consumed are given in **Scheme 2**. [23, 24]

$$\text{CH}_3\text{ReO}_3 \overset{K_1 \ \text{H}_2\text{O}_2}{\underset{\text{H}_2\text{O}}{\rightleftharpoons}} \left[\text{A} \right] \overset{K_2 \ \text{H}_2\text{O}_2}{\rightleftharpoons} \left[\text{B} \right]$$
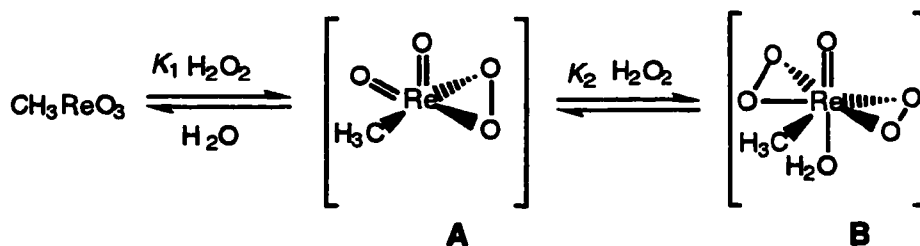
Scheme 2: Equilibrium formation of peroxorhenium complexes

Isotopic labeling [13] and kinetic data have shown that the oxygen atom which is transferred to a given substrate (the substrate used for labeling was PhSMe) is an oxygen atom of hydrogen peroxide, not one from water or from an oxo-rhenium group. In particular, the transferred atom is from a peroxo-oxygen present in **A** or **B**. [10, 23] The group of successful oxidation reactions consists entirely of those in which an oxygen-atom is transferred in the initial step.

Oxidation processes that require C–H bond addition are much less well known to this point, although some results have appeared. [21] As a part of a larger effort to define MTO-catalyzed selective oxidations, we turned to the family of methyl benzenes: p-xylene, durene, etc., along with certain polynuclear aromatic hydrocarbons (PAH's). We have found that ring oxidation readily occurs with H_2O_2–MTO, yielding para-benzoquinones without perceptible conversion of the methyl groups to carboxylates. One exception aside, the reactions proceed to a single product, without oxidation of the methyl side chains in high yields. These are the results that we report in this investigation.

Results and Discussion

The reactions were carried out in glacial acetic acid. In a typical experiment, the arene (relative amount 5), peroxide (100), and catalyst (0.4) were maintained at ~57 °C, for several hours. **Table 1** lists the products, conversions,

and yields obtained with this procedure. As shown, the only important product is the quinone; oxidation of the methyl side chains is unimportant. Thus the general equation for this transformation in the case of methyl benzenes is

$$\text{(structure) } + 3\,H_2O_2 \xrightarrow[\text{HOAc, 57 °C}]{\text{MTO (8 mol\%)}} \text{(structure) } + 4\,H_2O \tag{1}$$
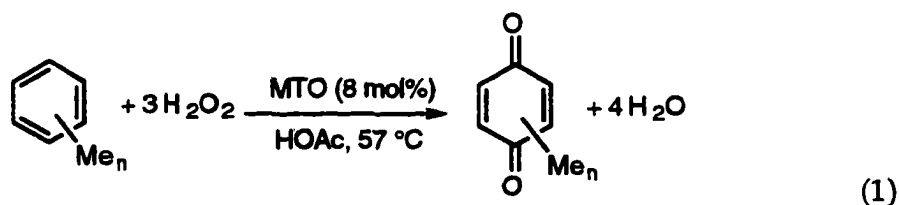
The MTO-catalyzed oxidations are specific for the ring; none of the substrates investigated underwent side chain oxidation. It can be seen from **Table 1** that the yields of quinones were greater, the greater the number of methyl groups substituted on the ring. These findings can be taken to indicate that the more highly substituted substrates are faster reacting because they are more electron rich. Given the established pattern for H_2O_2–MTO reactions of, for example, alkenes, [14, 25] this trend is consistent with the view that such substrates attack the electrophilically-activated peroxide oxygens of A and B.

In a few cases, hydroquinones were found as by-products. These data are also cited in **Table 1**. These hydroquinones are presumably intermediates along the pathway from hydrocarbon to quinone. When subjected again to the reaction conditions, they were converted to quinone. Indeed, this secondary stage of the overall oxidation occurred considerably more rapidly than the initial reaction of the hydrocarbon.

Another test was run with a phenol (Table 1, entry 9), the logical first product of hydroxylation of the hydrocarbon. The oxidation of 2-methylphenol occurred more rapidly than that of methyl benzene, itself a slow and unsatisfactory substrate. Both phenols and hydroquinones were converted to benzoquinones more rapidly than the methyl benzenes were under the reaction

conditions. These results are as expected and are consistent with a recent report. [26]

In view of our finding that the intermediates (hydroquinone, phenol) are oxidized more rapidly than the arenes, we must inquire why such intermediates can sometimes be found among the products. Incomplete conversion of the arene to its quinone in certain cases signals the deactivation of the MTO-peroxide catalyst. This subject is one we have explored previously. [27] Allowing a longer reaction time or adding a second portion of peroxide did not lead to further substrate conversion. In the case of durene, after the initial stage that proceeded in 75% yield in 3.5 h, entry 5, an additional 2% of MTO was added. In a further 1.5 h, the yield rose to 88%. This supports our premise that decomposition of the peroxorhenium intermediates occurs during the reaction time. Of course, the only deactivation processes that matter are those which are irreversible, by virtue of cleavage of the methyl–rhenium bond. If it remains intact in an inactive form, addition of hydrogen peroxide will restore A and B.

Although specific investigations of catalyst deactivation have not been reported in glacial acetic acid, information is available from studies in aqueous and semi-aqueous solutions. It is presumably applicable here as well, with suitable extrapolations. [27] The reactions are:

$$CH_3ReO_3 + OH^- \rightarrow CH_4 + ReO_4^- \tag{2}$$

$$CH_3ReO_3 + HO_2^- \rightarrow CH_3OH + ReO_4^- \tag{3}$$
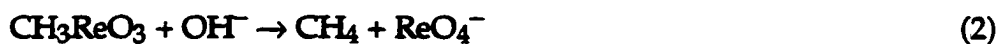
Both reactions have rate constants in excess of 10^8 L mol^{-1} s^{-1}, and proceed at measurable rates in solutions as acidic as pH 2~3, in water. [27] In solutions containing hydrogen peroxide, the first of these is more important.

In the present study there is another manifestation of the irreversible decomposition of MTO under the reaction conditions. In several instances, very

low conversions of the starting material were obtained: Table 1, entries 1-3 and 6. The conversions of these substrates are so low, in fact, that these reactions would not be of much use in practice unless one were willing to add successive portions of MTO, an expensive practice.

Other means were therefore sought to improve the conversions. p-Xylene was used as the test case. In each instance the concentrations and conditions were the same as reported, except for the changes and additions specified. These alterations were made: (1) Trifluoromethanesulfonic acid (2 M) was added in an attempt to stabilize the catalyst, since a high acid concentration stabilized aqueous rhenium peroxides. [27] (2) The MTO–H_2O_2 solution was added dropwise to p-xylene in HOAc over a period of one hour. (3) MTO was added in three equal portions, but in the same total amount. (4) The reaction flask was positioned in a soniccator (a cleaning bath) at room temperature for 10 h; <5% of the substrate was converted. In none of these cases did the specified alteration of procedure improve the conversion of p-xylene probably due to the faster decomposition of MTO at higher temperatures.

Despite the low conversions of certain of the substrates, for most this new method offers an attractive reaction.

The importance of quinones in biological systems has been established in numerous studies. [28-30] Various reports have also appeared in the literature on the oxidation of arenes and phenols to benzoquinones. [2-7] Different materials were shown to oxidize arenes directly to benzoquinones. Some of these oxidations involved the use of hydrogen peroxide–palladium supported on sulfonated polystyrene resins, [31] of I_2 and HI [32], and of $RuCl_3$. [7] The oxidation of substituted naphthalenes to naphthoquinones by MTO and hydrogen peroxide was recently reported. [33]

Most of the existing methods for the direct oxidation of arenes to quinones suffer from the disadvantage that the alkyl side chains undergo competitive oxidation leading to a complex mixture of products. The MTO-catalyzed oxidations, on the other hand, are specific for the ring; for none of the substrates investigated was side chain oxidation observed. Partial oxidation products were occasionally observed, as tabulated.

To understand the new reactions, it is helpful to consider the species recognized previously as intermediates in MTO-catalyzed peroxide reactions. In solutions of MTO and hydrogen peroxide, two η^2-peroxorhenium intermediates have been characterized. [10, 23, 24] They are the monoperoxo species **A** and the diperoxo species **B** in **Scheme 2**.

The peroxorhenium complexes definitely feature η^2-peroxide groups. In the course of their formation, an intermediate with the group Re(OH)(OOH) is believed to intervene. [34] Coordination of the peroxide dianion to rhenium(VII) activates the peroxide electrophilically, allowing nucleophilic attack of the arene on the oxygen atom. This will generate a phenol, possibly (as a referee pointed out) following an NIH shift in an arene epoxide. Karasevich et.al. have studied the oxidation of anisole with the same catalytic system and found that ortho and para methoxyphenols were formed as products. We have not detected any epoxide, but have tested this premise by showing that a phenol was rapidly converted to the benzoquinone under the reaction conditions, Table 1, entry 9. The same is true of hydroquinones.

The phenols, being more electron-rich than arenes, are more reactive with the peroxorhenium compounds and hence the subsequent steps in the oxidation occur more rapidly than the first. [26, 35] On the basis of a considerable body of MTO-H_2O_2 chemistry, in which **A** and **B** are catalysts of comparable reactivity, it

seems plausible to assume the same holds here as well. Thus either **A** or **B** could be used in diagrams; the representation of the first step, based on previously established studies of MTO–H_2O_2 reactions, is the following, depicted for **B** in **Scheme 3**:

Consistent with this proposal, the less-substituted arenes are the more difficult to oxidize. The first-formed intermediate results from nucleophilic attack on one of the peroxide oxygen atoms of **B**.
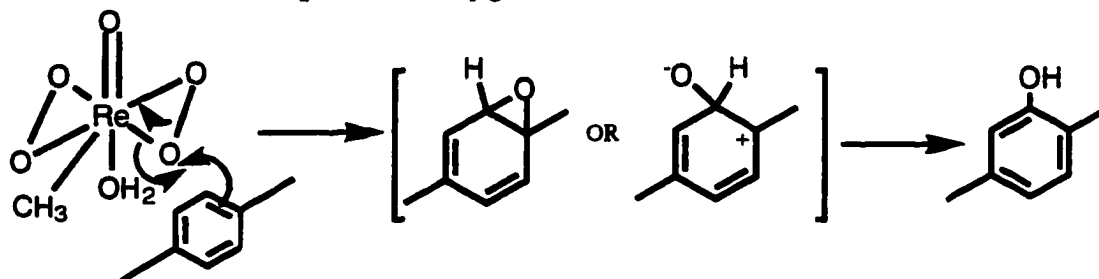
Scheme 3: Mechanism for arene oxidation

In summary, the MTO–catalyzed direct oxidation of arenes to benzoquinones constitutes a convenient and novel route for the synthesis of quinones: 30% peroxide is safe, inexpensive, and convenient. The uniqueness in this instance is that the MTO-catalyzed reaction leads to only a single oxidation product. Moreover, the reaction by-product is water, which makes this method free of salts and other by-products formed in some of the more traditional oxidants; acetic acid is in addition a relatively benign solvent. The heavy metal catalyst is used in small quantity, and in any event rhenium is believed to be considered nontoxic. [36]

Experimental section

Materials

The methyl benzenes were obtained from commercial sources and the purity of each was verified by GC–MS before use. Hydrogen peroxide (30%,

Fisher) was used without further treatment. Methylrhenium trioxide was prepared from Re_2O_7 and $Sn(CH_3)_4$ according to a literature procedure. [9]

General procedures

In a typical experiment, 1.25 mmol of p-xylene was added to 10 mL of glacial acetic acid in a single-necked flask sealed with a rubber stopper, followed by 0.1 mmol MTO, and a ~20-fold excess of 30% hydrogen peroxide. The reaction was maintained at 57 ± 2 °C in a water bath. The product was isolated by extraction into ether and the unreacted p-xylene removed under vacuum. This procedure left the pure benzoquinone as a yellow solid in excellent purity. The products were characterized by GC–MS, ^1H– and ^{13}C–NMR. The mass spectra and chemical shifts agreed well with the literature. [2-7, 37] The yields reported are based on peak integrations from GC.
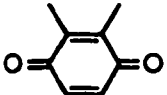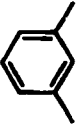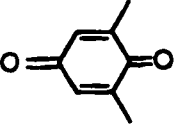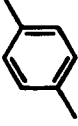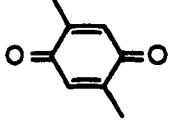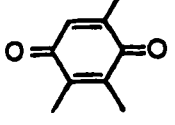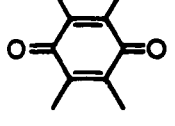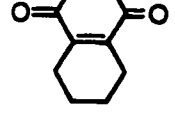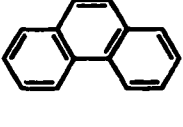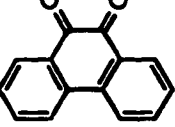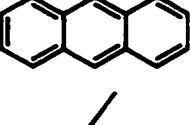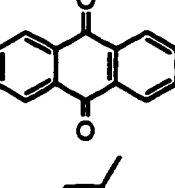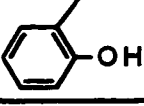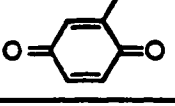
References

1) W. Partenheimer, *Catalysis Today*, **1995**, *23* 69.

2) Y. Asakawa, R. Matsuda, M. Tori and M. Sono, *J. Org. Chem.*, **1988** *53*, 5453.

3) H. Orito, M. Shimizu, T. Hayakawa and K. Takehira, *Bull. Chem. Soc. Jpn*, **1989**, *62*, 1652

4) S. Yamaguchi, M. Inoue and S. Enomoto, *Chem. Lett.*, **1985**, 827.

5) D. Liotta, J. Arbiser, J. W. Short and M. Siandane, *J. Org. Chem.*, **1983**, *48*, 2932.

6) M. Matsumoto and H. Kobayashi, *J. Org. Chem.*, **1985**, *50* , 1766.

7) S. Ito, K. Aihara and M. Matsumoto, *Tetrahedron Lett.*, **1983**, *24*, 5249.

8) W. A. Herrmann, W. Wagner, U. N. Flessner, U. Volkhardt and H. Komber, *Angew. Chem. Int. Ed. Engl.*, **1991**, *30*, 1636.

9) W. A. Herrmann, F. E. Kühn, R. W. Fischer, W. R. Thiel and C. C. Romão, *Inorg. Chem.*, **1992**, *31*, 4431.

10) W. A. Herrmann, R. W. Fischer, W. Scherer and M. U. Rauch, *Angew. Chem., Int. Ed. Engl.*, **1993**, *32*, 1157.

11) W. A. Herrmann, R. W. Fischer and J. D. G. Correia, *J. Mol. Catal.*, **1994**, *94*, 213.

12) P. Huston, J. H. Espenson and A. Bakac, *Inorg. Chem.*, **1993**, 32, 4517.

13) K. A. Vassell and J. H. Espenson, *Inorg. Chem.*, **1994**, 33, 5491.

14) A. Al-Ajlouni and J. H. Espenson, *J. Am. Chem. Soc.*, **1995**, *117*, 9243.

15) C. K. Chang, B. Ward, R. Young and M. P. Kondylis, *J. Macromol. Sci. Chem.*, **1988**, *A25*, 1307.

16) B. A. Moyer and T. J. Meyer, *J. Am. Chem. Soc.*, **1979**, *101*, 1326.

17) Z. Zhu and J. H. Espenson, *J. Org. Chem.*, **1995**, *60*, 1326.

18) R. Buffon, A. Choplin, M. Leconte, J.-M. Basset, R. Touroude and W. A. Herrmann, *J. Mol. Catal.*, **1992**, *72*, L7.

19) W. A. Herrmann, P. W. Roesky, M. Wang and W. Scherer, *Organometallics*, **1994**, *13*, 4531.

20) Z. Zhu and J. H. Espenson, *J. Org. Chem.*, **1995**, *60* 7090.

21) R. W. Murray, K. Iyanar, J. Chen and J. T. Wearing, *Tetrahedron Lett.*, **1995**, *36*, 6415.

22) Z. Zhu and J. H. Espenson, *J. Org. Chem.*, **1996**, *61*, 324.

23) S. Yamazaki, J. H. Espenson and P. Huston, *Inorg. Chem.*, **1993**, *32*, 4683.

24) P. J. Hansen and J. H. Espenson, *Inorg. Chem.*, **1995**, *34*, 5839.

25) A. Al-Ajlouni and J. H. Espenson, *J. Org. Chem.*, **1996**, *61*, 3969.

26) W. Adam, W. A. Herrmann, J. Lin and C. R. Saha-Möller, *J. Org. Chem.*, **1994**, *59*, 8281.

27) M. M. Abu-Omar, P. J. Hansen and J. H. Espenson, *J. Am. Chem. Soc.*, **1996**, *118*, 4966.

28) J. Rodriguez, E. Quinoa, R. Riguera, B. M. Peters, L. M. Abrell and P. Crews, *Tetrahedron*, **1992**, *48*, 6667.

29) A. S. Triolo, L. A. Carpino and R. A. Berglund, *J. Org. Chem.*, **1989**, *54*, 3303.

30) B. L. Trumpower, *Function of Quinones in Energy Conserving Systems*, Academic Press, New York, **1982** .

31) S. Yamaguchi, M. Inoue and S. Enomoto, *Bull. Chem. Soc. Jpn*, **1986**, *59*, 2881.

32) F. Minisci, A. Citterio, E. Vismara, F. Fontana and S. DeBernardinis, *J. Org. Chem.*, **1989**, *54*, 728.

33) W. Adam, W. A. Herrmann, J. Lin, C. H. Saha-Möller, R. W. Fischer and J. D. G. Correia, *Angew. Chem., Int. Ed. Engl.*, **1994**, *33*, 2475.

34) O. Pestovsky, R. van Eldik, P. Huston and J. H. Espenson, *J. Chem. Soc., Dalton Trans.*, **1995**, 133.

35) J. D. McClure, *J. Org. Chem.*, **1963**, *28*, 69.

36) *Dictionary of Organometallic Compounds*, 2nd Ed., Chapman & Hall, New York, **1995**, p. 3136.

37) C. J. Pouchert and J. Behnke, *The Aldrich Library of ^{13}C and ^{1}H FT-NMR Spectra*, Aldrich Chemical Co., Milwaukee, **1993**.

Table 1. Conversions and yields in the MTO–catalyzed oxidation of arenes by hydrogen peroxide in glacial acetic acid

Entry	Substrate	Product	Time/h	% Conversion	% Yield[c]
1			3.5	15	100
2			3.5	12	100
3			3.5	14	100
4[a]			4	75	67
5[b]			5	99	88
6			3	7	100
7			1.5	94	93
8			1.5	100	80
9			2.5	75	100

[a] 33% of the corresponding hydroquinone was also obtained. [b] These data reflect the use of 10 mol% MTO; 12% of the corresponding hydroquinone was also obtained. With 8% MTO, the yield was 75% in 3.5 hours, after which the reaction stopped until another 2% MTO was added. [c] conversion based on amount of starting material consumed and yield based on distribution of products.

GENERAL CONCLUSIONS

MTO catalyzes the desulfurization of thiiranes by triphenylphosphine. Enormous enhancement in rate is observed when MTO is pretreated with hydrogen sulfide prior to the reaction. The reaction is stereospecific and very tolerant to functional groups. Using 2-mercaptomethylthiophenyl as a ligand in model systems based on MTO, it was shown that the active form of the catalyst is a Re(V) species. Seven new complexes were synthesized and crystallographically characterized. The synthesis of the first examples of neutral terminal and bridging Re(V)sulfido complexes is particularly noteworthy. A new approach using P_4S_{10} for the conversion of M=O to M=S was developed. Some of these complexes undergo fast oxygen atom transfer reactions with organic and inorganic oxidants. We were able to trap the first formed complex in these reactions when DMSO is used as the ligand. These studies led us to the discovery that MTO catalyzes the selective oxidation of thiols to disulfides.

1,3-transposition of the hydroxyl group in a propargyl alcohol leads to an enone or an enal. MTO was shown to catalyze this reaction in good to excellent yields when the propargyl alcohol is benzylic. The same chemistry was extended to allylic systems where the more stable isomer at equilibrium is generated. The direction of the equilibrium is largely decided by the nature of the OH group, i.e., whether it is primary, secondary or tertiary. In the case of aliphatic allylic alcohols, 3° is preferred to 2° to 1°. For aromatic allyl alcohols, the more conjugated isomer predominates largely at equilibrium. Oxygen-18 labelling showed that the OH groups of parent and product are the same. The reaction is first order with respect to allyl alcohol and MTO, but strongly inhibited by traces of water. Theoretical calculations suggest the same in the case of aliphatic allyl alcohols though aromatic allyl alcohols do not follow the predictions. Studies of

deuterium labelled substrates show a large *equilibrium isotope* effect (K= 1.20 ± 0.02). For isomeric allyl alcohols differing in the position of deuterium only, the isomer with the deuterium at sp^3 centre predominates at equilibrium. The effect of conjugation from a phenyl group appears to be less important since calculations suggest that the phenyl group is forced out of plane of the allylic π system.

Arenes are oxidized to *p*-quinone by hydrogen peroxide in presence of catalytic amounts of MTO. In some cases, the intermediate hydroquinones were detected in small amounts. The active catalyst species are the previously-characterized η^2-peroxorhenium complexes, $CH_3Re(O)_2(\eta^2-O_2)$ and $CH_3Re(O)(\eta^2-O_2)_2(H_2O)$. Separate tests showed that hydroquinones and phenols are oxidized by H_2O_2–MTO more rapidly than the simple arenes; in the proposed mechanism they are intermediate products.

ACKNOWLEDGMENTS